

University of New Mexico  
**UNM Digital Repository**

---

Civil Engineering ETDs

Engineering ETDs

---

Summer 7-15-2024

**3D PRINTING OF LOCAL NEW MEXICAN SOIL MATERIAL:  
IMPROVING DURABILITY PROPERTIES BY ASSESSING  
TRADITIONAL METHODS TOWARDS ALTERNATIVE SUSTAINABLE  
CONSTRUCTION**

Daiquiri Devon Zozaya  
*University of New Mexico*

Follow this and additional works at: [https://digitalrepository.unm.edu/ce\\_etds](https://digitalrepository.unm.edu/ce_etds)

 Part of the Civil Engineering Commons, Construction Engineering and Management Commons, and the Structural Engineering Commons

---

**Recommended Citation**

Zozaya, Daiquiri Devon. "3D PRINTING OF LOCAL NEW MEXICAN SOIL MATERIAL: IMPROVING DURABILITY PROPERTIES BY ASSESSING TRADITIONAL METHODS TOWARDS ALTERNATIVE SUSTAINABLE CONSTRUCTION." (2024). [https://digitalrepository.unm.edu/ce\\_etds/330](https://digitalrepository.unm.edu/ce_etds/330)

---

This Thesis is brought to you for free and open access by the Engineering ETDs at UNM Digital Repository. It has been accepted for inclusion in Civil Engineering ETDs by an authorized administrator of UNM Digital Repository. For more information, please contact [disc@unm.edu](mailto:disc@unm.edu).

**Daiquiri Zozaya**

---

*Candidate*

**Gerald May Department of Civil, Construction, and Environmental Engineering**

---

*Department*

This thesis is approved, and it is acceptable in quality and form for publication:

*Approved by the Thesis Committee:*

**Dr. Maryam Hojati (Chairperson)**

---

**Dr. Anjali Mulchandani**

---

**Francisco Uviña-Contreras**

---

**3D PRINTING OF LOCAL NEW MEXICAN SOIL MATERIAL:  
IMPROVING DURABILITY PROPERTIES BY ASSESSING  
TRADITIONAL METHODS TOWARDS ALTERNATIVE  
SUSTAINABLE CONSTRUCTION**

**By  
DAIQUIRI ZOZAYA**

**BS IN CONSTRUCTION ENGINEERING  
THE UNIVERSITY OF NEW MÉXICO, ALBUQUERQUE, NEW MÉXICO (2011)**

**THESIS**

Submitted in Partial Fulfillment of the Requirements for the Degree of

**Master of Science**

**Civil Engineering**

The University of New México

Albuquerque, New México

July 2024

## **Dedication**

*To my precious daughter, Hazel Grace: May your faith, hope, and most importantly the love in your heart continue to guide you and stay ignited (1 Cor. 13). Always remember that you can do all things through Christ who strengthens us (Phil 4:13). I pray you continue to follow your dreams no matter how big or steep the mountain may seem (Matthew 17:20). I encourage you to nurture and remain close to those who are genuinely happy for you, believe in you, encourage you, inspire you, make you laugh, and see that beautiful sparkle in your eyes and heart; the fuel they provide to propel you is far stronger than the turbulence of your adversaries. If a bird is flying for pleasure, it flies with the wind, but if it meets danger it turns and faces the wind, so that it may rise higher (Corrie Ten Boom). So, shine your beautiful light, rise above, and fly like a butterfly my love, I love you with all my heart. This is for you, and all the generations to come, and all the generations that have passed - who remain within us.*

## ACKNOWLEDGEMENTS

First and foremost, I would like to thank God and my savior Jesus Christ for giving me the strength, faith, hope, and love to accomplish my dreams, goals, and purpose in this life. You are so good to me, and I am beyond thankful, grateful, and truly blessed for every opportunity I have been given.

I thank the National Science Foundation and the Transformation Network for the grant that allowed me to pursue this research. The connections I have made from this Network have enabled me to pursue my passion for sustainable construction engineering. It has also allowed me the opportunity to have a deeper connection with my community – a priceless gift that will remain for a lifetime. I really do feel transformed in such a positive way. I am excited about what is to come.

I thank my thesis committee: Dr. Maryam Hojati for guiding, pushing, and directing me throughout this rigorous journey. Your vast experience, advice, and knowledge have allowed me to complete this mission - even when it seemed impossible. Professor Francisco Uviña-Contreras for his invaluable traditional wisdom, hands-on expertise, and knowledgeable feedback - given so freely and wholeheartedly - muchísimas gracias por todo. Dr. Anjali Mulchandani for her encouragement and support, and also for being such a kind and effective instructor (your teaching style should be studied and adopted by everyone). Your valuable input and feedback are appreciated beyond measure.

I express my most sincere gratitude and appreciation to my mentor, advisor, big brother, and beer connoisseur/consumer partner Mark Stone for never forgetting about me, seeing the spark of light in me, and providing this South Valley mama with an opportunity to express my full potential. You are the guiding torch that led one more duckling across the road, I will ensure the light stays lit for others. I am immensely thankful to Asa Stone for being such a nurturing encourager, supportive editing expert, and master of what I am trying to spit out (but make it sound understandable) go-to person. The comfort in your praise, kindness, spiciness, and reassuring words reverberate in my soul. I am forever changed because of you two, and I thank you both from the bottom of my heart.

I humbly want to thank NACA who are more than community partners, they have become family: Chuck Charleston, Whisper C.K., Alice Tsoodle, Victoria Martine, and Maya Kwon. The grounding support they have provided for my emotional and mental self-wellness are priceless gifts I will carry forever. The encouragement to tell my story, and be my authentic true self is a self-empowerment realization I could never explain in words. I am so thankful for our relationship.

I would like to thank my colleagues for their time, assistance, and support: Reza Sedghi, Muhammad Saeed Zafar, Chris Vreeland, Leah Buechley, Lisair Servilla, Camila Friedman-Gerlicz,, Alyshia Bustos, and Fiona Bell for their support, expertise, encouragement, and

manual labor assistance in the lab and throughout the 3DSP printing process. A shoutout to Robin Elkin for providing the initial rice hull fibers. You all are amazing.

Thank you to my best friend (and lifesaver) Irenne Moreno, and her entire family for all their support, free parking, fashion expertise, counseling, and understanding during this challenging process. Thank you to Paul Gallegos for always being there for me, mentoring and advising me (in the field, and LIFE!), listening, and feeding me all my favorite foods. I love you all.

Thank you to my amazing boyfriend Clifford Miles (and Matthew too!) for buzzing into my life unexpectedly and supporting me during this demanding chapter. Your love, patience, understanding, and grace during my countless panic attacks, overthinking episodes, unavailability, and spicey bouts deserve the ultimate award. I am so blessed to have you by my side. I love you.

I would like to thank my entire family for all their cariño, prayers, support, inspiration, and encouragement they have provided throughout my life. It truly does take a village. Thank you to my siblings: Jerry, Destiny, and Mikela. I would name everyone, but it would probably be longer than my thesis. I love you all.

Thank you Diddy for being the best Father a daughter could ever ask for, no words can convey my gratitude for your unwavering support and for being my rock, in any storm I encounter, so I can be the best Chettis I can be. Mom, thank you for bringing me into this world, always being there at a moment's notice to help me with anything I need, and being the best cheerleader (and workout partner) anyone could ever ask for. To my Uncle Lindel, who went to heaven during the writing of this thesis, thank you for taking the time, and extreme patience, to introduce me to science and the engineering world at such a young age, the importance of education, and instilling the belief there was nothing I could not accomplish - even if what I was interested in was male-dominated (Oorah!), I will continue to carry the torch. To my Auntie Honey, thank you for infecting me with your overflowing love and laughter, you are my spirit animal, I LAVA you. Gracias a Dios for my Abuelita and Gpa for creating the opportunity for our family to grow and succeed in this land of opportunity. Finally, I would like to thank my Nana, in heaven, for raising and guiding me to be a strong, respectful, independent, classy yet sassy, and resilient woman. I know you have been with me every step of the way. I love you all from the bottom of my heart.

## Table of Contents

Dedication .....	iii
ACKNOWLEDGEMENTS .....	iv
Table of Contents .....	vi
List of Figures: .....	x
List of Tables: .....	xvi
List of Equations: .....	xviii
List of Abbreviations and Acronyms .....	xix
ABSTRACT.....	1
1. Introduction.....	3
1.1 Preface .....	3
1.2 Motivation and Background.....	8
1.3 Community Partnership With NACA .....	9
1.4 Research Objective.....	15
1.5 Research Approach .....	16
1.6 Thesis Outline .....	17
2. Literature Review.....	18
2.1 Human History of Earthen Material.....	18
2.1.1 Adobe.....	20
2.1.2 Limits in Adobe .....	24

2.1.3 Puddled Adobe/Mud/Cob .....	25
2.1.4 Rammed Earth/Pise De Terre .....	26
2.1.5 Compressed Earth Block (CEB).....	28
2.1.6 Pak Lum/Wattle and Daub/Jacál .....	28
2.1.7 Terrón .....	29
2.2 Earthen Building Codes and Standards .....	29
2.3 Sustainability in Construction .....	30
2.4 The 4 <sup>th</sup> Industrial Revolution: Digital Manufacturing.....	31
2.5 Digital Manufacturing with Earth .....	33
2.6 3DP Requirements.....	35
2.7 Previous Work.....	36
3. Evaluating Grain Size Distribution of Local Soils for 3D Printing in Sustainable Construction.....	37
3.1 Abstract .....	37
3.2 Introduction .....	38
3.3 Significance of Soil Particle Size Distribution in 3DSP .....	39
3.4 Collecting Soil from Belén, NM and Initial Soil Preparation .....	40
3.5 Lab Tests for Particle Size Distribution of Soil .....	42
3.6 Test 1. Conventional ASTM C136 Dry Sieve Test.....	43
3.7 Test 2. Modified ASTM C136 Dry Sieve Test .....	44

3.8 Test 3. Modified ASTM C117 Wet Sieve Test .....	45
3.9 Field Test for Particle Size Distribution of Soil: Test 4. Shake Jar Test.....	47
3.10 Comparing the Particle Size Distribution Results.....	48
3.11 Conclusion.....	50
3.12 X-Ray Diffraction Analysis .....	51
3.13 XRD Results.....	51
3.14 XRD Discussion.....	52
4. Addition of Xanthan Gum to Plain Belén Soil .....	55
4.1 Soil and Xanthan Gum - Mix Design.....	55
4.2 Soil and Xanthan Gum - Compressive Strength Preparation .....	57
4.3 Xanthan Gum and Soil - Compressive Strength Results and Discussion .....	60
5. Improving the Durability Performance of Local Soil Mix for 3D Printing .....	62
5.1 Abstract .....	62
5.2 Introduction .....	63
5.3 Materials and Methods .....	67
5.3.1 Soil Characterization .....	68
5.3.2 Soil Mix Design.....	70
5.3.3 Optimizing Soil Mix Design: Substituting Local Soil with Concrete Sand .....	71
5.3.4 Optimizing Soil Mix Design: Including Natural Fibers .....	76
5.3.5 Mixing procedure for soil mixes .....	78

5.3.6 Test Methods .....	80
5.3.7 Measurement of Compressive Strength in Cast Soil Cubes .....	80
5.3.8 Measurement of Shrinkage in Cast Soil Samples.....	82
5.3.9 3D Printability Tests and Mechanical Properties of 3D-Printed Soil Samples .....	83
5.3.10 3D Printability of Soil Samples on a Larger Scale .....	89
5.4 Results and Discussion.....	97
5.4.1 Traditional Consistency Examination of Mixes .....	97
5.4.2 Soil Mix Design.....	100
5.4.3 Optimizing Soil Mix Design: Including Natural Rice Hull Fibers.....	104
5.4.4 Printability Test Results.....	107
5.4.5 Large Scale 3D printing.....	111
6. Conclusions and Future Work .....	118
6.1 Summary .....	118
6.2 Major Findings .....	119
6.3 Future Research.....	120
7. References.....	122

## **List of Figures:**

Figure 1-1: (left) Chi-chi-Zoni in her hipil, and Abuelita (Family Photo circa 1970's) .....	6
Figure 1-2: (right) From left: Martha Zozaya (Auntie Honey), Abuelita, my father David Zozaya, and Catalino Zozaya (Uncle Cat) in front of the pak-lum hut they grew up in Tekal de Venegas (Family Photo 1986) .....	6
Figure 1-3: Nana posing by the Majestic wood stove on her 90th birthday (Nov. 2015) – Photo by Daiquiri Zozaya .....	7
Figure 1-4: BRC class at NACA's East Mountain property (Spring 2022), photo by Daiquiri Zozaya.....	11
Figure 1-5: NACA's Land-Based Healing & Learning Keepers [5].....	12
Figure 1-6: NACA's Wellness Wheel [6] .....	13
Figure 1-7: Jimmy Paywa (Zuni Pueblo) takes the cover off his traditional horno, considered the largest in NM [8].....	15
Figure 2-1: Timeline of Indian period, Adobe Conservation, A Preservation Handbook, pg. 20 [13].....	19
Figure 2-2: Interior view of Pueblo Bonito at Chaco Canyon, NM, constructed from the 9th to 12th century CE Photo Credit: Benjamin Oswald (2018) [15] .....	19
Figure 2-3 Bricks from Jericho, Pre-Pottery Neolithic A period, ca 9000 BC, Ashmolean Museum [17].....	20
Figure 2-4: Hazel Zozaya assisting in making adobes at Valle de Oro workshop (Sept. 2023). Photographed by Daiquiri Zozaya .....	24
Figure 2-5: Taos Pueblo, New México, 1880. Photo by John Hillers .....	26
Figure 2-6: Traditional Mayan wattle and daub (pak lum) home with translations in Mayan/Spanish/English [32].....	29

Figure 2-7: Examples of digital manufacturing methods – 1) Additive, 2) Subtractive, 3) Formative, 4) Assembly [44] .....	32
Figure 2-8: Solar sintering of sand by Markus Kayser (2011) [44].....	33
Figure 2-9: (left) Earth house prototype by WASP <sup>®</sup> in Italy, (right) Crane WASP <sup>®</sup> 3DP system, 2018.....	34
Figure 2-10: TECLA project WASP <sup>®</sup> and MCA, 2021.....	35
Figure 3-1: Google map of Belén, NM located South of UNM campus .....	41
Figure 3-2: (a) collecting local soil from family property located in Belén, NM; (b), (c) field examining soil material; (d), (e) crushing soil with a hand tamper into a fine powder .....	42
Figure 3-3: Test 2 – Belén soil soaked (left), dried (center), and re-tamped (right).....	45
Figure 3-4: Test 3. Wet sieve test .....	46
Figure 3-5: Test 4. Shake jar test .....	48
Figure 3-6: USDA Soil Textural Classification Chart [72] .....	48
Figure 3-7: The grain-size distribution curve of plain Belén soil .....	49
Figure 3-8: USGS Clay Mineral Identification Flow Diagram (XRD) .....	52
Figure 3-9: Random-oriented scan results for Belén soil samples .....	52
Figure 3-10: Particle-size and clay-size-mineralogy analyses of NM adobe producers [10, p. 50] .....	54
Figure 4-1: Plain (Belén) Soil Mix .....	57
Figure 4-2: SX1 Soil Mix .....	58
Figure 4-3: SX2 Soil Mix .....	58
Figure 4-4: 3 Day Results - Left: S Mix, Center: SX1 Mix, Right: SX2 Mix .....	59

Figure 4-5: 3 Day results after removing lids and scraping excess material off – Left: S Mix, Center: SX1 Mix, Right: SX2 Mix .....	59
Figure 4-6: 7 Day Results - Left: Plain Soil Mix, Center: SX1 Mix, Right: SX2 Mix .....	60
Figure 4-7: 21 Day Compression Results .....	61
Figure 5-1: Grain size distribution of CS (Max aggregate size No.4 sieve) and soil mixes (S100, S75, S67, S50, and S25) designed to optimize S replacement with CS according to dry [68] and wet sieve tests [71].....	73
Figure 5-2: Simple tests to determine the required water content for (a) a small batch in a controlled lab environment, too much water (b) a small batch in a controlled lab environment, optimum water content (c) a large soil batch under ambient field condition .....	76
Figure 5-3: Grain size distribution of S, CS, and S67 mix (Max aggregate size No. 16) chosen to add rice hull fiber (F) to.....	78
Figure 5-4: Forney compression machine.....	82
Figure 5-5: 3D Gantry printing system used in the Dana C. Wood Materials and Structures Lab at UNM [102].....	84
Figure 5-6: Diameter of nozzle: a) 5 mm; b) 15 mm; c) 20 mm; d) 25 mm; e) 40 mm [47]: Diameter of nozzle: a) 5 mm; b) 15 mm; c) 20 mm; d) 25 mm; e) 40 mm [47].....	85
Figure 5-7: Example of the extrudability test printing path for different printing speeds [102] .....	86
Figure 5-8: The extrudability test printing path for different printing speeds [102] .....	87
Figure 5-9: Flexure test set up .....	88
Figure 5-10: Cross-sectional views of a 3D printed vessel with a traditional 3D printing toolpath in which the width of each layer is constant (Left) and a toolpath generated by	

WeaveSlicer in which the width of the vessel wall is constant (Center-left). A view of a WeaveSlicer vessel print (Center-right). A sinusoidal curve with period and amplitude shown (Right) [104] .....	89
Figure 5-11: Left: Cross section of a wall with a constant width, generated by WeaveSlicer. Middle: Calculation of variable amplitude used in WeaveSlicer. Right: A top -down view of how the sinusoidal toolpath is constructed .....	90
Figure 5-12: Material consistency test for a large-scale batch of Mix ID S67 soil .....	92
Figure 5-13: (Mix 2.5) 3DSP: Test 1 .....	93
Figure 5-14: (Mix S67) 3DSP: Test 1.1 .....	94
Figure 5-15: a) Mixing the dry ingredients; b) Material consistency test for a large-scale batch of Mix ID S67F2 soil .....	96
Figure 5-16: (Mix S67F2) 3DSP: Test 2.....	97
Figure 5-17: Water content determination according to the consistency test (a) S75 with 35.5% water content; (b) S75 with 32% water content; (c) S50 with 23% water content; (d) S25 with 16% water content.....	99
Figure 5-18: Compressive strength results of S & CS mixes (Max aggregate size No. 4)...	101
Figure 5-19. Linear shrinkage results of the first set of soil mix to optimize the S replacement by CS.....	103
Figure 5-20. Crack pattern formation in various soil mixes after 3 days of drying.....	104
Figure 5-21: Compressive strength results of the second set of mixes with S, CS, F .....	105
Figure 5-22: Linear shrinkage results of the second set of soil mixes to optimize the S67 with the addition of rice hull fiber .....	106

Figure 5-23: Shrinkage samples of the second set of mixes with fiber added showing less cracks and shrinkage after 3 days of drying.....	107
Figure 5-24: (a) Extrudability zigzag test with variable printing speeds; (b) Extrudability zigzag test with constant printing speed of 15 m/s .....	108
Figure 5-25: (a) Buildability test prior to collapse; (b) Collapse of material at 25 <sup>th</sup> layer ...	109
Figure 5-26: 3DSP of mix ID S67F2 flexure samples.....	109
Figure 5-27: Modulus of rupture results for mix ID S67F2.....	110
Figure 5-28: Day 1 results (Mix S67, WC 20%) .....	111
Figure 5-29: Day 2 results (Mix S67, WC 20%) .....	112
Figure 5-30: Day 3 results (Mix S67, WC 20%) .....	112
Figure 5-31: Day 5 (Mix S67, WC 20%).....	112
Figure 5-32: Day 7 (Mix S67, WC 20%).....	112
Figure 5-33: Day 10 (Mix S67, WC 20%).....	113
Figure 5-34: (a) Photo of mix S67F2 2-foot dia. dome after printing; (b) measuring arc over the top of the dome after printing .....	114
Figure 5-35: Mix ID S67F2 day 3 results (a) side of dome; (b) top of dome; (c) over the top arc string measurement; (d) base of dome circumference string measurement.....	115
Figure 5-36: Mix ID S67F2 day 7 results (a) side of dome; (b) crack in the side of dome noticed; (c) top of dome; (d) over the top string measurement .....	116
Figure 5-37: Mix ID: S67F2 day 10 results (a) side of the dome; (b) additional crack observed; (c) first crack observed.....	116
Figure 5-38: Mix ID S67F2 day 13 results (a) side of the dome; (b) second large crack observed; (c) top of the dome .....	116

Figure 5-39: Mix ID S67F2 day 14 (a) top view of the dome; (b) side view of the dome; (c)  
second large crack observed ..... 117

## List of Tables:

Table 2-1: Sizes and weights of adobe made in NM (1987) [4] .....	21
Table 2-2: Composition of Soils that Make Good Adobe [20].....	22
Table 3-1: Test 1. Grain-size distribution of plain Belén soil.....	43
Table 3-2: Test 2. Grain-size distribution of plain Belén soil.....	45
Table 3-3: Test 3. Grain-size distribution .....	46
Table 3-4: USCS range of particle sizes [68] .....	50
Table 3-5: Comparing the size distribution of plain soil and soil classification of different tests .....	50
Table 4-1: Mixed proportions of soil mixes .....	56
Table 5-1: Comparing the size distribution of plain soil and soil classification of different tests [68], [69], [70], [94] .....	69
Table 5-2: Grain Size Distribution of CS (Max aggregate size: Sieve No. 4) according to ASTM C136 [66] .....	71
Table 5-3: Soil mix design to optimize S replacement with CS by their weight percentage .	72
Table 5-4: Percent of gravel, sand, silt/clay of the five mixes with S and CS.....	73
Table 5-5: Soil mix design to optimize S replacement with CS by their weight percentage .	77
Table 5-6: Preliminary Material Parameters (Mix ID S50) .....	90
Table 5-7: Material Parameters (Mix S67) ---- Test 1 .....	92
Table 5-8: G-code Printing Parameters (Mix S67) - Test 1 .....	92
Table 5-9: Material Parameters (Mix S67) - Test 1.1 .....	93
Table 5-10: G-code Printing Parameters (Mix S67): Test 1.1 .....	94
Table 5-11: Material parameters for Mix ID S67F2 – Test 2.....	95
Table 5-12: Printing parameters for Mix ID S67F2 – Test 2.....	96

Table 5-13: Traditional consistency test comments on the first set of soil mixes with S and CS  
(max aggregate size No. 4) ..... 98

Table 5-14: Traditional consistency test comments on the second set of mixes with S, CS (max  
aggregate size No.16), and F..... 99

**List of Equations:**

Equation 1: Compressive Strength.....	60
Equation 2: Compressive Strength.....	81
Equation 3: Change in length.....	83

### **List of Abbreviations and Acronyms**

3D	Three-Dimensional
3DP	Three-Dimensional Printing
3DSP	Three-Dimensional Soil Printing
NACA	Native American Community Academy
NM	New México
UNM	University of New México
BRCC	Building Resilient Communities Civil Engineering Course
TN	Intermountain West Transformation Network
IDS + A	Indigenous Design Studio + Architecture
CINVA	Centro Interamericano de Vivienda y Planeamiento
USCS	Unified Soil Classification System
ASTM	American Society for Testing and Materials International
USDA	United States Department of Agriculture
XG	Xanthan Gum
S	Plain Belén Soil
CS	Concrete Sand

## **ABSTRACT**

3D printing (3DP), or additive manufacturing, represents a dynamic and swiftly advancing manufacturing method in which diverse materials are deposited layer by layer through computer-controlled processes, creating intricate geometries. This technology has demonstrated success in various construction applications, including the construction of bridges, bus stop stations, and even residential homes. Nonetheless, the predominant application of 3DP in construction relies heavily on cement due to its robustness, convenience, and ease of use. Regrettably, the cement sector is a substantial source of greenhouse gas emissions, responsible for approximately 8% of worldwide CO<sub>2</sub> emissions. Investigating all facets of carbon emissions reduction is imperative to create sustainable buildings and infrastructure. Using 3D soil printing (3DSP) with locally sourced soil materials represents a promising stride toward achieving carbon-neutral construction. Sustainable construction should encompass a product's energy efficiency and the comprehensive evaluation of its local and global environmental, community, and economic impacts throughout the production process, from inception to completion. Vernacular structures made from locally available resources such as soil, clay, and fiber have been found worldwide. New México (NM) stands out in North America for its extensive history and techniques of building with local soil that has been passed down through traditions for thousands of years. This research explores the complexities of integrating contemporary engineering and traditional testing practices for 3DSP with local materials to create sustainable construction solutions. This research works towards creating a 3DSP traditional horno (outside oven) for the local Native American Community Academy (NACA). This exploration examines durability characteristics of local NM soil including soil mix composition, grain size distribution, mechanical properties, shrinkage rates, pumpability,

extrudability, and buildability of the studied earthen mixtures needed for 3DSP towards sustainable construction.

# **Chapter 1**

## **1. Introduction**

### **1.1 Preface**

The background for this research stretches across many different origins, cultures, traditions, beliefs, disciplines, departments, organizations, communities, partnerships, relationships, and generations. I have discovered there are many ways of knowing and being considered a Master of anything. Ancestral knowledge is wisdom passed down to us over generations through storytelling, written accounts, spiritual beliefs, values, and/or traditions. We have academic science and research accredited by universities, academic articles and journals, and others within that academic-scientific community to uphold high standards of ethics, expertise, codes, and specifications. We have family members who are experts in their own craft and can tell you if the tortilla (flour or corn) or adobe mix is adequate just by looking at it or feeling it in their hands. We have community knowledge that we can rely on to convey what is needed to assist in teaching the generation at hand and future generations - if we listen. Many different resources and references (recent and dated, conventional and traditional) have been utilized to develop this thesis.

As I began writing my thesis, I was distraught and consumed with anxiety about how I was going to explain everything I have learned, researched, and developed along with including and incorporating everyone who has played a role in that journey. I was then reminded and reawakened, by my brothers and sisters at NACA, to the idea of explaining my thesis like the story that it is. To be my authentic true self. Storytelling is a fundamental aspect of their traditions and program. They feel it is essential to integrate it into all aspects of learning and teaching. By telling

my story I will naturally honor all the work I have done and, in turn, honor all the collaboration work that has been accomplished with everyone involved. Prior to this awakening, I did not realize (or allow myself the time to reflect) how integrated my personal story, background, and upbringing were woven into my research until I was prompted to recall why this area of focus was important to me. I was so concerned about the classes, deadlines, tests, meetings, technical aspects, and results, I felt like I lost myself in the process. I had to reground myself. It was beautiful to reflect: on where I came from, how far I have come, and everyone in my family (and ancestors) who have provided me with the opportunity to be here and have the freedom to choose how I want to make a positive impact on the generations that are to come after me. I felt like Simba from The Lion King when Rafiki (community sage) bonks him on the head with the stick, and Mufasa's spirit (his father) reminds him to "remember who you are." Here I thought I was creating something that would change and improve the community, but instead, the community changed and improved me.

This research is not merely investigating a mud mixture's scientific durability improvements and properties needed for 3DSP. It is working towards solutions to weave the past with the future, academic science with traditional knowledge, university community with the local community, and modern technology with sustainable design in hopes that we will all come together to create, develop, and enhance the needs of the local community and environment by creating nurturing solutions and paths for current and future generations.

\*\*\*

In a small circular hut (15 – 20 ft. in diameter) with a thatched roof, earthen mud floors, and earthen walls built of pak-lum (thrown-mud in Mayan language), my Abuelita (paternal grandmother) Paula Saavedra (Zozaya Moguel-Chì) gave birth to my father, David Zozaya, in the village of Tekal de Venegas located in Yucatán, México. My father is the second to the youngest

of 6 children. The environment is a humid tropical jungle, the beds were made of woven hammocks and were hung in alternating layers, to optimize the small space available. On one occasion, Chi-chi-Zoni (great-grandmother) María Asunción Chí, was asleep on the top hammock and she heard rustling above, a mouse perhaps? The next thing she knew an enormous, and heavy, yellow snake fell coiled on top of her – nearly knocked the air out of her. Word of wisdom, be aware of sleeping in the top hammock in a Mayan hut. By 27 years old, Abuelita was a widow with 6 children. She and Chi-chi-Zoni worked hard every single day from sun up to sun down to provide for the family. All work was done by hand including washing clothes, making tortillas, panuchos, empanadas, and embroidering hipil's (Yucatecan women's blouses or loose-fitting dresses) as seen in Figure 1-1. My Father remembers them cooking outside the hut over an open fire surrounded by rocks that would contain the fire and also support the pots or comals (cast iron pan/skillet). At least twice a week the women would gather wood from the jungle. They would carry the wood on their back with a rope that had a piece of cloth attached to it that would come across their forehead, like a headband, to help support the load. Eventually, Abuelita had to find a better source of income, so she went to work in the city of Mérida at Hotel San Pablo where she was required to live on site. There she was real-life Cinderella working day and night shifts and was only allowed 1 hour off on Sundays to go to church. My Gpa (Manuel Saavedra) ended up staying at her hotel where they met and fell in love. He unfortunately, had to return to NM for business matters, but he promised that he would return. When he did, she was nowhere to be found due to all the children, including Chi-chi-Zoni, developing scarlet fever. Now this part of the story can seriously be turned into a movie, but Gpa turned into a detective and miraculously found her at the hut (with mud in between her toes), eventually married her, and moved her and all the children to Belén, NM where they were raised on a farm. A piece of the property they grew up on remains in the family and is the

land where I have gathered the soil material for this research. My Abuelita and Gpa are still alive and live in T or C, New México (NM).

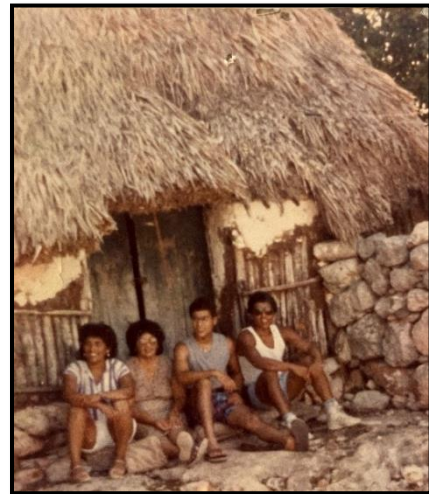


Figure 1-1: (left) Chi-chi-Zoni in her hipil, and Abuelita (Family Photo circa 1970's)

Figure 1-2: (right) From left: Martha Zozaya (Auntie Honey), Abuelita, my father David Zozaya, and Catalino Zozaya (Uncle Cat) in front of the pak-lum hut they grew up in Tekal de Venegas (Family Photo 1986)

One of the most distinct memories I have growing up is the smell of the wood-burning stove in the kitchen. My Nana (maternal grandmother), Filomena Romero Chávez, raised my two siblings and myself in an adobe home located in the South Valley of Albuquerque, NM. Nana was born in La Joya de Sevilleta, which is located south of Belén, NM. This small village was the southernmost Spanish settlement along the Camino Real de Tierra Adento during the eighteenth century before travelers embarked south. There, she also grew up in an adobe home, and she told me that she remembers her and her siblings making the adobes and letting them dry in the sun when they were young. She eventually married my Tata (maternal grandfather) Gregorio Chavez, and they moved to Albuquerque, where they purchased the adobe house that my siblings and I were raised in, sometime in the 1950s. The stove was a Majestic brand wood-burning stove; the surface of the stove had flat circular comals that you could lift with this cute little pry-bar-type handle that had a spiral at the end of it where you held it (can be seen in Figure 1-3 left of the stove

on the wall). It was very important always to put it back where it belongs; if it was misplaced, nobody could sleep till it was found. To the left of the stove is where the chopped wood would go. The top of the stove had these two little cupboards with a tiny latch, and the door would swing out towards you instead of sideways. It would warm the whole house and was a staple of the kitchen - and the entire house if you ask me. It is where we would all gather, where she would feed us, share stories with us, and drink her coffee. My Nana was born in 1925 and went to be with the Lord on August 5, 2016.



Figure 1-3: Nana posing by the Majestic wood stove on her 90th birthday (Nov. 2015) – Photo by Daiquiri Zozaya

Reflecting on how both sides of my family were raised in earthen homes and how cooking was essential to their nurturing makes this research come full circle and worthwhile. I want to continue learning and teaching these aspects of our history and traditions so that they may continue growing and radiating throughout our family, children, community, and future generations. My Nana and Abuelita run through my blood, and my connection to them has empowered me to follow my

dreams of building sustainable construction, beginning with a 3DSP horno for the NACA community. I know in my heart I am on the right path.

## **1.2 Motivation and Background**

The motivation for my passion for wanting to be a part of the construction world has been sparked and fueled by sustainability. I was introduced to sustainability while taking a Geology class as an undergraduate student at the University of New México (UNM). Sustainability opened my awareness to the resources we are depleting at an alarming rate - nationally and worldwide, global warming, the increasing population, drought, decreasing fresh water supply and the contamination of it, trash and plastic infecting our oceans and environment, increasing temperatures, increasing fires and natural disasters, and the awareness that some of these implications can be irreversible if better decisions, particularly in engineering practices, are not integrated at a faster rate. It will take many interdisciplinary networks and connections to mitigate these problems at hand. D. E. Williams sums it up appropriately stating, “three-dimensional problems require three-dimensional solutions [1].”

From the academic aspect, I have learned that sustainability is the multi-faceted challenge of creating, incorporating, maintaining, and/or meeting a present need without jeopardizing future needs. This awareness can be applied to almost any discipline as its three main pillars incorporate and take into consideration people, planet, and profit. These pillars can also be interpreted as community, environment, and economy.

The Indigenous aspect of sustainability is more wholesome and is considered a way of living, as well as having a place-based approach to the land and ecosystem where you live. Place-based means creating and developing a connection with the land and preserving and protecting it throughout time. The land is treated as an inheritance rather than a piece of property for

exploitation of its resources [2]. Remembering what the space was used for in the past, taking notice of the connection to that place and location on Earth, incorporating the larger phases of the cosmos, and creating a generational design for the future to look after are aspects to consider when developing any land [2]. Early Western development was focused on domination and exploitation of the land. The Indigenous are diligent in incorporating sustainability in every decision of approach, design, and planning, though their outlook has been ignored for many years. Building with earth is not a new concept but an expertise that must be remembered, renewed, restored, rejuvenated, and revitalized from every knowledgeable resource we can gather and learn from if we want to integrate it - sustainably, within our current construction industry.

### **1.3 Community Partnership With NACA**

In the Spring of 2022, I was encouraged to return to UNM for my master's in civil engineering by Mark and Asa Stone. The first class I took was an interdisciplinary course called Building Resilient Communities (BRC), where I was introduced to our beautiful NACA community. The partnership between NACA and the Intermountain West Transformation Network at UNM (TN, led by Mark Stone at that time) was initially formed between the NACA Land Based Healing and Learning team ("Land-Fam," led by Chuck Charleston, Whisper C.K., Alice Tsoodle, Victoria Martine, and Maya Kwon) and the UNM Civil Engineering course BRC (led by Mark Stone, Vidal Gonzales, and Asa Stone). The mission of NACA's Land-Fam team is to "strengthen our kinship with lands and waters to support the community in reclaiming our identity as beings who are integral to the ecology. We work to provide exposure and awareness to indigenous ways of knowing, allow space for application, and then support creation and design [3]." The class was created to introduce students to the principles and practices of the resilience theory as applied to community and environmental systems. Collaborating in developing NACA's East Mountain

property, located on the eastern slope of the Sandia Mountains just passed Cedar Crest, was one of the course outcomes. NACA shared that their long-term goals with the property are to: (i) build sustainable infrastructures, (ii) actively work towards a land management plan, and (iii) use the property as a site for land and place-based healing and learning for students, staff, and community members. The BRC course was comprised of six teams: wildfire/restoration, infrastructure, mapping, transportation, water, and education. Each of the six teams had a specific goal and worked directly with NACA throughout the semester to identify and design approaches to enhance community resilience [3].

I was part of the infrastructure team, and we worked towards creating a sustainable design for a shade structure and a bathroom facility. Initially, our group brainstormed on all the recycled materials we could utilize to build sustainably, and the options ranged from used tires, aluminum cans, plastic bottles, glass bottles, and adobe. When we discussed these options with NACA, they were very kind, yet adamant, that they would like the materials to be local and embrace the earth as much as possible. A structure made of used tires or fabricated material was not in the best interest of their cultural learning and teaching practices. The NACA team decided that an open shade structure made from reclaimed wood they had already acquired and a cord-wood bathroom structure, utilizing some of the wood from thinning the area for fire mitigation, would suit their outdoor learning needs best. The details of their preference for utilizing local earthen materials, which I cultured from this experience, redirected my graduate research to concentrate on creating something that falls within this category so it could benefit the community's needs as much as possible.

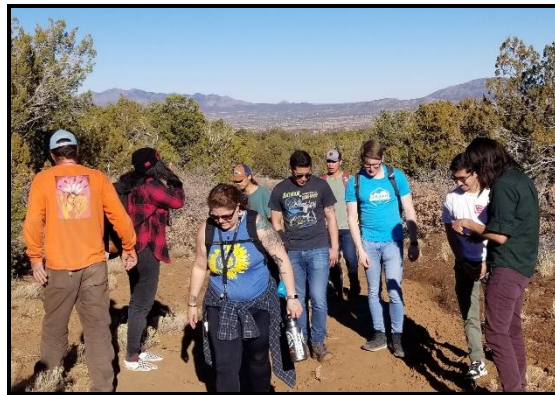


Figure 1-4: BRC class at NACA's East Mountain property (Spring 2022), photo by Daiquiri Zozaya

NACA is a tuition-free community-supported charter school located in Albuquerque, NM that provides a culturally integrated college preparatory education designed by and for Indigenous Students (grades K-12<sup>th</sup>). Students, represent more than 60 different tribal groups and five Indigenous languages are consistently taught (Dinè, Keres, Zuni, Tiwa, and Lakota) [4]. Land-Based Healing and Learning is one of the ways NACA teaches their students to strengthen their kinship with the land and water to support the community in reclaiming their identity as beings who are integral to the ecology. They work to provide exposure and awareness to indigenous ways of knowing, allowing space for application and support creation and design. Students and staff can choose to participate in one of the Keeper Pathways, which includes Medicine, Food, Water, Mountain, and/or Storykeepers [5]. Within each of these programs are regional and local experts (Knowledge Keepers) offering insight, traditional ecological knowledge and/or skill sets regarding local history, cultural practices, economy, ecology, science, etc. These experts work in collaboration with educators and NACA staff to more deeply localize, decolonize, and indigenize curriculum, pedagogy, and infrastructure [5]. NACA's unique way of approach and integrated way of teaching has helped me understand how to cultivate and express my own experience and story as a Knowledge Keeper.

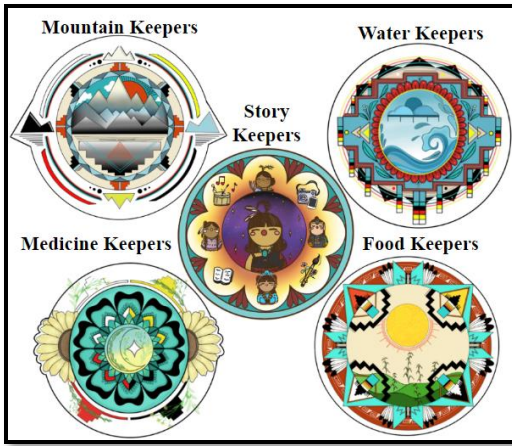


Figure 1-5: NACA's Land-Based Healing & Learning Keepers [5]

Another incredible implement used within their educational philosophy is NACA's Wellness Wheel. (It is with NACA's permission and blessing that I can share this information). Indigenous thinking and learning is a reflective process involving deliberate looking inward, self-awareness, and contemplation of deeper meanings [6]. The Wellness Wheel is a check-in tool utilized to reflect on how whole the individual is feeling within their intellectual, physical, social/emotional, and community & relationship wellness [6]. It can be a weekly, daily, or even hourly check-in. Some days, an individual may feel that their intellectual wellness is full because they have completed a lot of schoolwork (or thesis writing), but their physical and emotional wellness tanks are a little low and neglected. I cannot tell you how many times I came into a Land-Fam meeting full of stress, anxiety, and worry, and this simple check-in (combined with sageing) grounded and centered me. It reminded me to be gracious with myself and to be okay with providing space to reflect on what I need to be whole and balanced. Every time I left a meeting with NACA, I left feeling more whole, rejuvenated, and inspired. They also regularly fed us delicious dishes that were authentic and prepared with love. I could feel and taste that the food was nutritious and healing to my body, and it was usually harvested from their garden or prepared by their students. The cucumbers were so crisp and full of flavor; the tomatoes were sweet and juicy.

The fresh popped corn kernels were hard to put down, the chamomile tea was soothing, and the blue corn meal was nostalgic for my Nana's. NACA's Wellness Wheel has provided me with an awareness to remember to honor space for self-wellness and reflection.

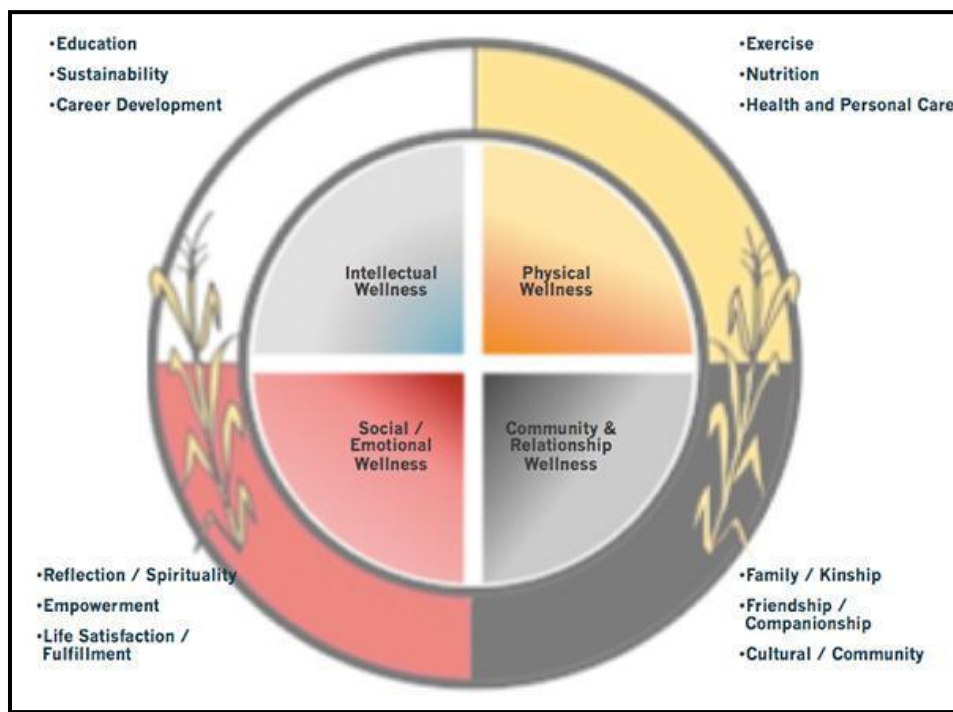


Figure 1-6: NACA's Wellness Wheel [6]

In the fall of 2023, our NACA-UNM partnership continued through the extension of a USDA-funded project in which the school received a Farm to School grant in 2018 to develop a school garden with a hoop house erected to provide year-round learning around food production [7]. The extension is part of a Turnkey-Edible Garden grant to support the continued growth and deepening of its Farm to School efforts focusing on Indigenous food cultivation and the development of skills that support Indigenous culture, values, and food sovereignty [7]. The extension includes designing an outdoor shaded cooking area and classroom – referred to as a “Cook-Shack” – where a portion of the food harvested from the gardens would be utilized to engage students in preparing, cooking, and enjoying healthy food onsite at the school property.

[7]. Through this project, students will be able to strengthen their Indigenous food sovereignty movement where classes can butcher, process, and cook animals, bake bread in a traditional Pueblo wood-fired adobe oven (horno) or an in-ground fire hole for cooking, have access to fresh herbs and produce grown in surrounding garden boxes, have adjacent storage for weekly harvests, and have an outdoor sink to ensure food freshness and safety [7].

During one of the collaboration meetings, the idea of creating a 3DSP horno – utilizing the local material mix I was developing for my graduate research – originated. An horno (pronounced or-no) is a traditionally built outdoor oven introduced from the Moors into the “New World” and introduced by the first Europeans to NM and can be found in most of the Pueblos in NM. Every horno is made differently, according to their generations-old family techniques and Pueblo traditions but is usually constructed utilizing adobes or puddled mud. The horno is dome-shaped with a door and a smoke hole, although not all are made with a smoke hole. Hornos are used just like a regular oven and can be used to cook bread, pudding, fish, pizzas, roast corn, chile, etc. Bread is an important part of many Pueblos’ culture and is baked at every celebration, feast day, funeral, and initiation. It is also an important economic tool, as baked bread can be a key source of income for many families. The art of preparing a horno for baking is pretty much standard across Pueblos: Once the firewood is burned down inside the horno, the flames recede, and the oven reaches the ideal temperature of around 450 degrees (which can vary); the hot coals are removed with custom-made tools; and the ashes are cleared off the floor of the horno with soaking-wet juniper branches (or burlap) [8]. The loaves of bread are placed in the oven, the opening is closed (usually a wooden door), and wet towels are stuffed into the cracks.



Figure 1-7: Jimmy Paywa (Zuni Pueblo) takes the cover off his traditional horno, considered the largest in NM [8]

We thought having a traditionally built horno and a small-scale 3DSP horno for the students would be beneficial for the students and the community. We could use it as a model to teach and explain the local soil mix used, how it was prepared, designed, 3D-printed, and compare the differences between the traditional and 3DSP versions. If successful, cook something in it. During this time, we collaborated with Professor Tamera Begay and the UNM School of Architecture and Planning Department. Tamera Begay is the Founder of Indigenous Design Studio + Architecture (IDS + A) and agreed to assist in the NACA partnership by designing the outdoor Cook-Shack utilizing her design studio class taught in the spring of 2024.

#### 1.4 Research Objective

The objectives of this thesis are as follows:

- Develop a sustainable building material mix using local materials that can be 3D printed, benefiting the community.
- Create a mix that meets the minimum strength and shrinkage requirements per New México earthen building codes and standards.

- Conduct an engineering analysis to minimize shrinkage and increase the strength of local soil materials while gathering traditional knowledge on past methods and techniques that can enhance current testing.
- Explore the journey of community engagement in the 3D printing of soil.

## **1.5 Research Approach**

My research approach in this thesis includes the following:

- Narrating my journey of being introduced to the NACA community and re-evaluating my research to establish a meaningful connection with them.
- Examining the characteristics of the local Belén soil and exploring ways to naturally and sustainably improve the material mix design, aiming to produce a 3D-printed horno for NACA's outdoor Cook Shack.

This research was conducted in four phases to investigate 3D printing of local soil material. In the preliminary phase, local soil, located in Belén, NM, was gathered and soil classification was investigated utilizing traditional and conventional testing methods ensuring the proper amount of clay, silt, and sand present. In addition, an X-ray diffraction test was conducted to determine the mineralogy of the clay. During the second phase, preliminary compression strength tests integrating xanthan gum, a biopolymer, with the soil was conducted resulting in a failed approach of increasing the compressive strength of the soil material. During the third phase, the local soil was enhanced with concrete sand in increasing amounts. The linear shrinkage and compressive strengths of each soil mix were tested and evaluated according to the NM earthen building code. The most suitable mix was chosen for a preliminary 3DSP of a 1-foot diameter dome. Results were examined, investigated and reevaluated. During the fourth phase, the soil mix was further enhanced by integrating rice hull fiber in increasing amounts to determine if the durability of the

material improved. Linear shrinkage and compression tests were conducted resulting in improved results. 3D printability was assessed by conducting an extrudability, buildability, and flexure test of the material and concludes with a 3D-printed 2-foot diameter dome.

## **1.6 Thesis Outline**

This thesis is presented in five remaining chapters. Chapter 2 covers the literature review on the history of different earthen building material and techniques with an emphasis on traditional adobe construction in NM, and current developments in 3D printing. Chapter 3 presents a conference paper scheduled for publication in Earth USA 2024, focusing on the preliminary study of characterizing soil. It primarily addresses determining the grain size distribution of local soil in both lab and field settings and modifying current ASTM tests to achieve more reliable results for high clay soils. Chapter 4 explores biopolymer additives and preliminary studies on their impact on soil applications in 3D printing. Finally, Chapter 5 includes a journal paper to be submitted as a result of this thesis, discussing methods to control the high shrinkage of high clay local soil by adding fine sand and rice hull, along with preliminary 3D printing tests. Chapter 6 concludes the thesis with research conclusions and future work recommendations. Chapter 7 is dedicated to references.

## **Chapter 2**

### **2. Literature Review**

#### **2.1 Human History of Earthen Material**

Human history has revealed that early civilizations survived in small mobile groups. To provide adequate food and shelter for themselves, hunting and gathering groups depended on a profound knowledge of their local environment [9]. Every aspect of their lives revolved around seasonal changes, local climate, and the landscape [9]. The nomadic way of life continued for thousands of years but eventually contributed to the decline of hunted animals and caused an impact on the environment. In time, the development of permanent settlements and agricultural cultivation brought an essential change in human history and was fundamental to all subsequent social developments [9]. The Neolithic Period (10,000 – 3000 B.C.) marks the gradual replacement of nomadic hunting and foraging with primitive agriculture and the domestication of animals [10].

Evidence of structures built with earthen materials have been found all over the world dating back thousands of years. Some of the earliest permanent shelters discovered are located in the Middle East, China, and the Indus Valley [11]. Jericho, located in the modern-day West Bank, is home to one of the oldest continuously inhabited cities in the world with an excavated site that dates to 8300 B.C. The houses found there were circular shaped, approximately 16 feet in diameter, and made of walls that contained loaf-shaped mud bricks, currently referred to as adobe [12].

In NM, the evolution of architectural styles utilizing earthen materials can be broken down into four periods: Indian (700-1598 A.D.), Spanish and Mexican Colonial (1598-1848 A.D.),

Territorial (1848-1880 A.D.), and American (1880 – present) [10]. The Indian period, during which most of the early earthen structures were constructed, is further described below in Figure 2-2.

Timeline	A.D. 1 to 350	350	700	900	1050	1350
	<i>Basket Maker II period</i>	<i>Initiation of the Basket Maker III period</i>	<i>Initiation of the Pueblo I period</i>	<i>Initiation of the Pueblo II period</i>	<i>Initiation of the Pueblo III period</i>	<i>Initiation of the Pueblo IV period</i>

Figure 2-1: Timeline of Indian period, Adobe Conservation, A Preservation Handbook, pg. 20 [13]

The word Pueblo translates to village or town and is associated with a sedentary settlement as opposed to nomadic (Apache and Navajo) [14]. During the Pueblo II Period, most Pueblos were constructed of stone masonry and hand-molded adobes. The kiva, a ceremonial chamber, became a standard feature [13]. Archeologists consider Pueblo III to be the Great or Classic period of the Anasazi architecture. Pueblo Bonito at Chaco Canyon, located in the Four Corners area of NM, Colorado, Arizona, and Utah, is renowned for its stone masonry construction. The stones were laid dry or set with mud mortar [13].



Figure 2-2: Interior view of Pueblo Bonito at Chaco Canyon, NM, constructed from the 9th to 12th century CE Photo Credit: Benjamin Oswald (2018) [15]

### **2.1.1 Adobe**

An adobe is a sun-dried mud brick that is more closely considered a masonry unit rather than a type of mud mixture; so, you need not say “adobe brick” when describing the term, or you would essentially be saying “brick-brick.” The word adobe is believed to originate from the Egyptian word “thobe,” meaning “mud brick.” In Arabic, this word translates to “at-tob,” which in Spanish means “adobe.” In French, it became known as “toub” [16]. The mixture includes mud (clay and sand), fibers (straw, rice hulls, reeds, etc.), and water. The mixture is compacted into a form (usually made from wood), released from the form, and left to dry in the sun. It is believed that the first attempts to make adobes were probably lumps of clay roughly shaped, dried in the open, and hardened by the sun [16]. Adobes have been found in many shapes and forms all over the world. The blunted cone or pear-shaped adobe can be found in West Africa and has been used for building shelter for over 5000 years. The conical-shaped adobe can be found in Perú at the Moche pyramid that dates to 1000 B.C. [16]. Fibers were utilized to accelerate drying, reduce cracking, and increase the tensile strength of the adobe. Egyptian hieroglyphics document the early use of adobes, and Biblical accounts (Exodus 5:18) refer to the use of mud bricks with straw for construction in the ancient world [13].



Figure 2-3 Bricks from Jericho, Pre-Pottery Neolithic A period, ca 9000 BC, Ashmolean Museum [17]

Through the writings of Roman Engineer Vitruvius (ca 30 B.C.), we know that the ancient Greeks had a refined system of adobe manufacturing and construction [11]. The rectangular Lydian adobe averaged  $45\text{ cm} \times 26\text{ cm} \times 10\text{ cm}$  (10 in.  $\times$  10 in.  $\times$  4 in.). The pentadoron adobe

(five palms square) was used for public buildings, measuring  $45\text{ cm} \times 45\text{ cm} \times 8\text{ cm}$  ( $18\text{ in.} \times 1\text{ in.} \times 3\text{ in.}$ ). For private buildings, the tetradoron adobe (four palms square) measured  $30\text{ cm} \times 30\text{ cm} \times 10\text{ cm}$  ( $12\text{ in.} \times 12\text{ in.} \times 4\text{ in.}$ ) [11], [16].

In the United States, one-third of the nation's adobe dwellings are located in New México (NM) [10], where the climate is arid or semiarid, and annual precipitation is low. The introduction of the wooden form by the Spanish in the late 1600s permitted the adobero (adobe maker) to control the size and weight of the bricks, which in turn allowed for greater construction flexibility [18]. According to the NM Bureau of Mines & Mineral Resources, during 1987-88, NM was one of the nation's largest producers of adobe and pressed-earth blocks, with 33 commercial adobe manufacturers in business, mostly located along the Rio Grande Valley [10]. Adobes can vary in size; below is a summary of the sizes produced in NM in 1987.

Table 2-1: Sizes and weights of adobe made in NM (1987) [4]

Type of adobe	Dimensions (inches)	Weight (lbs.)
Egyptian brick	$3 \times 5 \times 10$	8
Veneer brick	$4 \times 4 \times 16$	26
Half adobe	$4 \times 4 \times 8$	23
Quemado (burnt adobe)	$3\frac{1}{2} \times 8 \times 16$	30
New México standard adobe	$4 \times 10 \times 14$	30
Adobe (old style)	$4 \times 5\frac{1}{2} \times 16$	28
Adobe (old style)	$4 \times 12 \times 18$	50
Taos standard adobe	$4 \times 8 \times 12$	26
Terrón (Isleta Pueblo)	$7 \times 7 \times 14$	35
Dome brick (mosque)	$2 \times 10 \times 6$	8
México standard adobe	$3\frac{1}{2} \times 10 \times 16$	35
Salazar adobe	$4 \times 10 \times 15\frac{1}{2}$	37
Acoma Mission adobe	$3 \times 9 \times 18$	30

The early development of adobe most often occurred where trees were a limited building resource [11]. Due to deforestation or a lack of growth in the vicinity (desert area), communities had to rely on the most abundant local material available: earth. Adobes can be made from a variety of local soils. In NM, the most suitable soil found in the Rio Grande Valley is a sandy loam composed of approximately 55-85% sand and 15-45% finer material (generally more silt than clay) [10]. The Portalab Manual (NM) describes a similar type of mixture: 1-7% gravel, 65-80% sand, 18-20% clay [19]. The Mud Village Society (France, New Delhi, India) designates a comparable mixture of 55-75% sand, 10-28% silt, 15-18% clay, and less than 3% of organic matter that is best suited for making adobe [16]. NM State University suggests the following composition of soils that make a good adobe according to the soil textural name, as seen in Table 2-2 [20].

Table 2-2: Composition of Soils that Make Good Adobe [20]

Soil Textural Name	Percent Sand	Percent Clay	Percent Silt
Loamy sand	70 to 85	0 to 15	0 to 30
Sandy loam	50 to 70	15 to 20	0 to 30
Sandy clay loam	50 to 70	20 to 30	0 to 30

A balance of particle sizes is essential to ensure a quality adobe [10]. Clay gives strength to the adobe, but in excessive amounts will cause shrinkage; sand or straw is added to decrease the shrinkage and prevent cracking [10]. Too much sand will result in adobes that crumble easily because they lack sufficient binder to hold the grains together [18]. Additionally, a balance of particle sizes is essential to ensure a quality adobe, which will be discussed in detail in the next chapter. Adobe attracts moisture, which erodes its cohesiveness. An application of a firm mud or lime plaster coat will help prevent erosion, if applied well it can take several years for it to erode [21].

Adobe does not necessarily need to be restricted to arid and semiarid climates if the buildings are properly protected or certain soil stabilizers are used [22]. Adobes can be made stabilized or semi-stabilized to assist with durability, improve their strength, and increase their resistance to weather erosion (wind, sand storms, rainfall, snowfall, humidity). Probably the most widespread reason for adding stabilizers to soil bricks is the desire to increase the water resistance of the finished product [18]. The single biggest drawback of traditional un-stabilized adobes is their lack of water resistance and susceptibility to rapid erosion in heavy rains [18]. Moisture re-entering an adobe will cause the clay particles to swell and release their bonding so that the entire mass will slump [18]. The most common additives are cement and asphalt emulsion, but including these ingredients will increase their embodied carbon footprint. Asphalt, also known as bitumen, is primarily used for its waterproofing properties. It is used as an emulsion (in water), which provides good waterproofing qualities in the adobe [21]. Cement is used as a stabilizer mainly due to its bonding properties. Soils with high clay and silt content may require a cement stabilizer equal to 20% of the dry weight of the soil [21]. Lime can also be used as a stabilizer and is considered a more environmentally friendly additive due to its ability to absorb CO<sub>2</sub> as it dries, also known as carbonation. It doubles as a waterproofing and binder agent. It can be substituted for half the amount of cement required but is greatly enhanced when combined with cement [21]. It is important to note that adobe stabilized with lime or cement requires slow curing. Adding moisture or covering the material to retain it during drying will prevent the adobe from drying out too quickly [21].

Adobe is more widely recognized as environmentally friendly for its excellent thermal mass and insulating properties [11]. Thermal mass is now understood to moderate and stabilize the daily fluctuation of the interior air temperature of a structure by delaying the timing of the

maximum and minimum heat flow through the dense mass walls [13], [23]. Excess thermal mass beyond the needs of daytime heating is stored within the mass walls and floor. As the sun sets and the interior temperature drops, the stored solar energy is naturally released through the night to keep the home warm [11]. Adobe's high density (106 lbs/ft), thermal conductivity (0.3 BTU hr/ft<sup>2</sup>-°F/ft), and specific heat/ability to store thermal energy (0.24 BTU/lb-°F) make them an exceptional choice for improving a structure's thermal performance [23]. Adobe has other positive qualities, including fireproof, bulletproof, low sound transmission qualities, and biodegradable.



Figure 2-4: Hazel Zozaya assisting in making adobes at Valle de Oro workshop (Sept. 2023).  
Photographed by Daiquiri Zozaya

### 2.1.2 Limits in Adobe

Overall, the limits in structures built out of adobe are small compared to their positive, sustainable attributes. Adobe is considered more expensive because you have to consider the intensive labor required to make, lift, and move them several times before they are set in place. They are not naturally water resistant unless stabilized with chemicals, which alters their sustainability factor. If a natural mud mortar is used for plastering, it may have to be maintained more regularly. Adobes are lower in strength than concrete, wood, and steel unless reinforced or used in large masses. Adobe is weak in tension and shear and will crack when subjected to tensile

and shear forces. Adobe structures are sometimes hazardous in seismically active areas because of the low-strength materials used and can collapse if not reinforced properly [10]. Another limitation is that adobe, or earthen materials in general, is not taught in conventional education, so it is difficult to understand the engineering principles when the standards are only taught for cement, concrete, wood, and steel beams. Lastly, building with adobe is an art that takes time and effort, and usually extensive wisdom from someone to pass on that knowledge, which can be difficult to find, and a lifetime to master.

### **2.1.3 Puddled Adobe/Mud/Cob**

The mixture of mud, fiber, and water can be utilized in many ways and traditions to construct an earthen wall. In the American Southwest, puddled mud is a mud walling technique where the mud mixture is piled up and molded in layers by hand without the use of forms. In England, this mixture and technique is referred to as cob [11].

In England, structural monolithic mud walls were commonly made of cob, a mud and straw mix that is sometimes gravelly [11]. The walls constructed were usually 2 to 3 feet thick and could be as tall as 30 feet. Each course was approximately 18 to 24 inches thick and was allowed to dry for two weeks before the next course above it was placed. “In a typical English cob mix, the straw fibers are left fairly long to aid in binding and drying. Soil clay percentages typically range from 10% to 30%, with an average of 20% working well. Cob walls with clay percentages over 30% show shrinkage cracks after drying that are too large weakening the walls’ structure [11].” Cob walls were usually constructed upon a stone foundation 18 to 36 inches above the ground to protect it from water damage and direct rainfall.

NM is home to 19 Native American pueblos (Acoma, Cochiti, Isleta, Jemez, Laguna, Nambé, Picuris, Pojoaque, Sandia, San Felipe, San Ildefonso, San Juan (Ohkay Owingeh), Santa Ana,

Santa Clara, Santo Domingo, Taos, Tesuque, Zia, and Zuñi) [14]. Numerous pueblos have evidence of earthen-built structures, one of which is the ancient tradition of puddled adobe located in Taos Pueblo. Taos Pueblo is the only Native American community that is designated both a National Historic Landmark (1960) and a World Heritage site (1992) [14]. Two of the main buildings located there are considered the oldest continuously occupied structures in the USA [14]. Within the pueblo, subterranean and semi-subterranean pit houses have been found that are ten feet deep and contain walls lined with puddled mud 6 inches thick and 18 inches high that date back to 1200 A.D. [11], [13]. The housing structures resemble a terraced pyramid, as seen in Figure 2-5, built by erecting large rectangular buildings with five stories, each smaller by the width of a room than the one below it [14]. The ancient use of passive solar design can be observed in the positioning of the buildings (southern facing), utilizing the winter sun to its advantage and blocking the wind from the north in the winter.

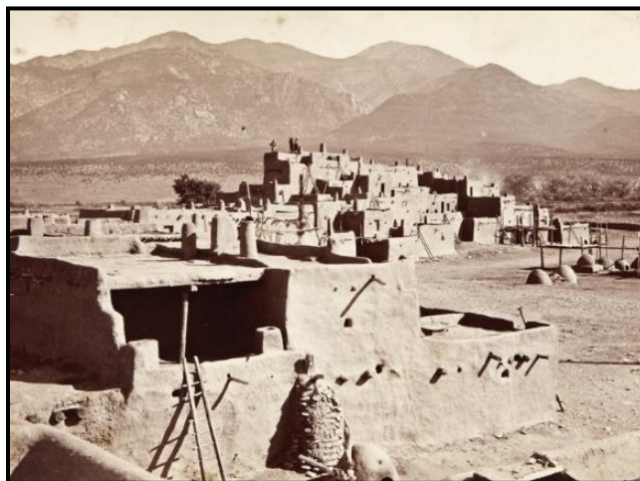


Figure 2-5: Taos Pueblo, New México, 1880. Photo by John Hillers

#### 2.1.4 Rammed Earth/Pisé De Terre

Rammed earth, also known as pisè de terre in France, is another type of earthen building technique used to construct monolithic walls. The walls are built by pounding lifts of 6 to 8-inch

layers of moistened soil material, usually 18 to 36 inches wide, into a moveable form with a bottomless frame [11]. The ramming may be done manually with a hand tool or a pneumatic tamper. The soil must be rammed till it is dense and extremely firm. After lift compaction is complete, the frame is then moved and repositioned for continued construction. Suitable soil for ramming usually has a 20% clay content, 80% sand with small gravel content, and soil moisture content of about 10% [11]. Sometimes, a small amount of cement is added to the mixture for stabilization and weatherproofing, but this increases the product's environmental unfriendliness. Rammed earth has the advantage of forming structural walls in place with much less handling than the adobe, because the forming and curing (drying) take place on the wall itself [11]. Earthen walls built 2 to 3 feet thick possess good thermal qualities, moderating the interior living space temperature against winter cold and summer heat and requiring only small amounts of supplemental energy (if any) for rooms not passively heated by the sun [11]. Massive rammed earth walls often require no exterior insulation to bolster their thermal performance as opposed to thinner adobe walls or wood frame construction.

Archeological work shows early evidence of rammed earth dating to 7000 B.C. in China [24]. This technique evolved so that by 200 B.C., the Great Wall of China, comprising the largest and longest defense walls ever constructed, was partially built with rammed earth [11]. Rammed earth was one of the most common materials used to build large structures in the ancient world [25].

Due to the monolithic strength of the massive walls, rammed earth is suitable for multi-storied buildings. In Carthage, near present-day Tunis on the north coast of Africa, remains of rammed earth walls built in 700 B.C. can be found [11]. By 200 B.C., the craft was so refined that some of their buildings attained heights of six stories [11]. In 1837, a seven-story rammed earth building was constructed in the town of Weilburg, Germany, and is still being occupied today[11], [26].

### **2.1.5 Compressed Earth Block (CEB)**

CEBs are usually made with a soil mixture similar to rammed earth and just enough water to hold its shape. It can be compressed into a block with a gasoline or diesel-powered hydraulically operated machine or a manual hand-operated press, often referred to as a “CINVA-Ram” [10]. The CINVA-Ram machine was designed by Chilean engineer Raúl Ramírez in 1956 and patented in 1958 [27]. Widely used in Colombia, the machine was also exported all over the Americas up to Africa, Asia, and Europe [27]. The blocks can be stabilized by adding cement or lime to increase their waterproofing and strength capabilities. The pressed blocks dry and shrink in the sun before they are laid, making walls crack-free [28]. The powered machines can produce several thousand blocks a day [10]. Due to the high mechanical pressure applied by the hydraulic press, the CEBs usually test high in compressive strength and modulus of rupture [10].

### **2.1.6 Pak Lum/Wattle and Daub/Jacál**

In the Yucatan peninsula, locals utilize a technique called pak lum, which roughly translates in English to “thrown mud,” where “pak” literally represents the sound the mud makes when it is slapped on, and “lum” means mud or earth [29]. This technique is also known as wattle and daub. Local materials such as bamboo or reed canes are tied together, usually with rope, as the frame for the structure, known as a hut by locals. Flexible branches are sometimes weaved in between the poles, and a mud mixture, similar to a cob, is then pressed (or thrown) into the frame on both sides to form a wall [30]. The hut roof was usually thatched utilizing palm leaves and overhung past the walls to protect the walls from moisture. The exterior walls were usually covered with a lime-wash to stabilize and protect them from the tropical environment. As far back as 1100 B.C., the Maya have used lime products to construct residential and public architecture [31]. Burnt lime was used for construction, sanitary, dietary, and other purposes. The ubiquity and the large quantities of

labor and raw materials involved would have made lime production an important socio-economic endeavor throughout the area [31].

In NM, Early Pueblo I people also used jacál (post-in-adobe) construction – a technique of infilling woven vertical wood posts with mud [13]. Jacál can also be translated as “modest home.”

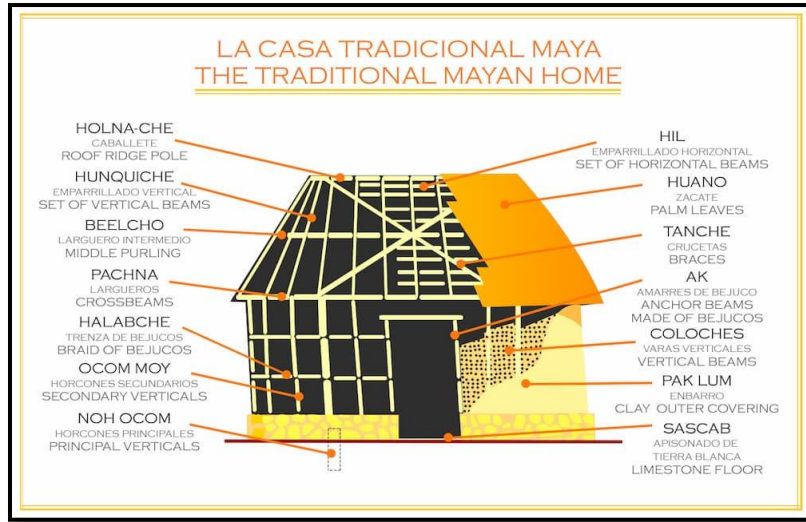


Figure 2-6: Traditional Mayan wattle and daub (pak lum) home with translations in Mayan/Spanish/English [32]

### 2.1.7 Terrón

The Spanish word “Terrón,” meaning “ a flat clod of earth,” refers to the type of adobe made of cut sod or turf material found in boggy river-bottom locations, particularly in the Rio Grande floodplain areas [33]. When the river would flood, grass would start to grow, and they would cut blocks out of the soil, silt, and topsoil that had the grass roots to hold it together. Many of the older buildings at Isleta Pueblo are constructed with terrones..

## 2.2 Earthen Building Codes and Standards

NM is unique and special when it comes to earthen construction. It is one of the few states in the USA to have a state-wide building code dedicated to earthen material and also one of the only states to allow the construction of an adobe, rammed earth, or CEB building to be two stories in

height (shall not exceed) [34]. The code also specifies that a qualified soil means any soil, or mixture of soils, that attains an average minimum compressive strength of 300 psi and an average modulus of rupture of 50 psi. Shrinkage cracks for adobe and CEB are allowed, providing that these cracks do not jeopardize the structural integrity of the blocks. The International Building Code Empirical Design of Adobe Masonry [35] suggests the same compressive strength and modulus of rupture requirements as the NM code but the shrinkage requirements state that adobe units shall not contain more than three shrinkage cracks and any single shrinkage crack shall not exceed 3 inches (76 mm) in length or 1/8 inch (3.2 mm) in width. These minimum requirements were followed while designing and developing the local soil material to be 3DSP in this research.

### **2.3 Sustainability in Construction**

The demand for environment-friendly and sustainable construction alternatives is currently rising. Concrete forms the backbone of modern society providing roads, bridges, homes, schools, hospitals, dams, storm sewers, and a myriad of other structures, but its massive production poses fundamental and compounding sustainability challenges: climate change and destructive resource extraction [36], [37]. Concrete production significantly contributes to CO<sub>2</sub> emissions due to the high energy required to produce cement, the primary binding agent in concrete [38]. Cement is one of the most extensively utilized construction materials, and the demand for it is increasing worldwide [38]. Global cement production has increased more than 30-fold since 1950 and almost 4-fold since 1990; total emissions from the cement industry have been estimated to contribute as much as 8% of global CO<sub>2</sub> emissions [39].

The construction sector, as a whole, is a highly active industry responsible for 40% of global energy consumption, 38% of global greenhouse gas emissions, 12% of global potable water use, 40% of solid waste generation in developed countries, and 50% of the world's processed raw

materials [40], [41]. This has led to researching and investigating more sustainable construction materials such as soil, fibers, and water. There are very few peer-reviewed articles on this topic, which has also made the development of this research difficult. Earthen construction remains one of the least studied methods of construction, though it may be the oldest. One of the major setbacks of utilizing an earthen-based material vs. a cement-based material is the convenience of higher strength, workability, and reliability that concrete offers. It is also difficult to compete with concrete when the mix design already has an established code and specifications for its use. Utilizing concrete for 3DP is a step forward in the digital construction world but a step back in sustainability.

## **2.4 The 4<sup>th</sup> Industrial Revolution: Digital Manufacturing**

The first industrial revolution began in 1760 with the invention of the steam engine and the transition to coal as the main energy source for power trains, which were the primary means of transportation [42]. The biggest changes came in the industries in the form of mechanization. Mechanization was why agriculture started to be replaced by industry as the backbone of the societal economy [43]. The second industrial revolution began in 1900 with the invention of the internal combustion engine; this led to an era of rapid industrialization using oil, gas (fossil fuels), and electricity to power mass production [42], [43]. Other inventions during this era include the development of steel demand, chemical synthesis, and methods of communication such as the telegraph and the telephone [43]. The third industrial revolution started in 1960 and was characterized by the implementing of electronics and information technology to automate production and assembly lines [42]. This era brought forth the rise of computers, the internet, programmable logic controllers, nuclear energy, space expeditions, and robots [36]. The fourth industrial revolution now involves cyber-physical systems, cloud computing, artificial

intelligence, and computer-generated product design, including digital manufacturing and 3DP/3DSP.

The recent push to lower the earth's global carbon dioxide emissions has led to the construction industry looking for faster and more sustainable building practices as well as production. Architects and engineers have been attempting to migrate into the digital manufacturing process as it offers solutions in productivity, time, labor, freedom of geometric design, and large-scale assembly opportunities. In construction, there are four main digital manufacturing methods: additive, subtractive, formative, and assembly, as seen in Figure 2-7. 3DP, with earthen materials, is considered a branch of additive digital manufacturing because it is built layer upon layer with the aid of a computer-based program guiding the 3D printer.

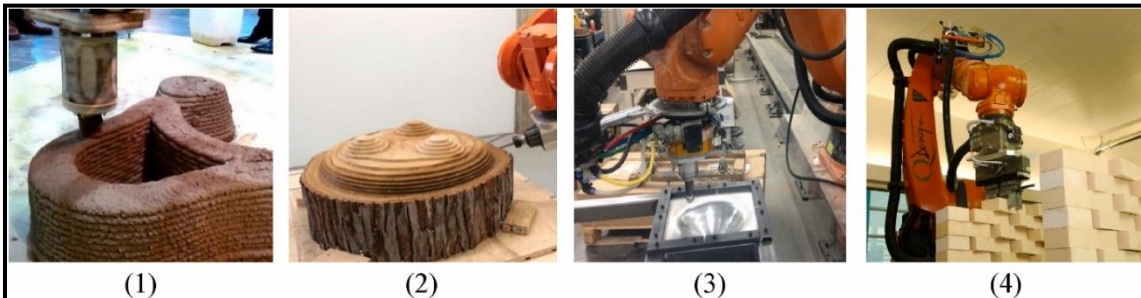


Figure 2-7: Examples of digital manufacturing methods – 1) Additive, 2) Subtractive, 3) Formative, 4) Assembly [44]

Two types of printers are commonly used in 3DP; the first is a gantry-style printer with three degrees of freedom (movement) in the x, y, and z coordinates. This printer's downside is that it can only print vertically in the z-direction, and it can be difficult to transport to the building site. The second type of printer available consists of an industrial robotic arm that has 6 degrees of freedom. The downsides include that it is very heavy, some need to be anchored to the ground, and the arm extension has limits and must be moved, or a second robotic arm printer is needed for large prints. Many companies are trying to develop ways to automate this process in the construction industry,

but there are several bottlenecks and complications in making this procedure full-scale, including material design, material delivery system, manufacturing technologies, and performance properties of the printed material.

## 2.5 Digital Manufacturing with Earth

The first recorded attempt to digitize earthen materials was in Egypt and Morocco in 2011. German designer Markus Kayser experimented with on-site additive manufacturing and created the Solar Sinter machine that utilizes solar energy to melt sand and power the printing system to create glass shapes layer by layer, as seen in Figure 2-8 [44].



Figure 2-8: Solar sintering of sand by Markus Kayser (2011) [44]

In 2014, the Italian company WASP<sup>®</sup> created the first recorded project of 3D clay printing for construction purposes. The project used red clay collected on-site in the village of Ait Ben Haddou in Morocco to produce prototypes of building components [44]. In 2016, WASP<sup>®</sup> conducted the first attempt at 3DP with an adobe mixture, presenting an early concept of a 3DP earth house. By 2018, they joined forces with Rice House and presented the world's first complete 3DP earth house using their newly upgraded 3DP system, Crane WASP<sup>®</sup>, as seen in Figure 2-9. The 3D printed house was named Gaia, and was produced entirely on-site utilizing a mixture composed of 25% soil taken from the site (30% clay, 40% silt, and 30% sand), 40% straw-chopped rice, 25% rice hull, and 10% hydraulic lime [45]. The printing process of the walls took 10 days

and covered 30 square meters with a wall thickness of 40 cm; the total cost of the materials used in the wall structure was € 900 (\$973 USD) [45]. The walls were not load-bearing, timber frames were used to support the roof loads but it was a remarkable accomplishment at the time [44].



Figure 2-9: (left) Earth house prototype by WASP<sup>®</sup> in Italy, (right) Crane WASP<sup>®</sup> 3DP system, 2018

In 2021, WASP<sup>®</sup>, in collaboration with Mario Cucinella Architects, presented their largest 3DP earth construction, TECLA (which takes its name from Technology and Clay), constructed in Ravenna, Italy [45]. The preliminary design combined two interlinked cells; both were 3D printed simultaneously using two synchronized Crane WASP printers [44]. The construction process consumed 60 cubic meters of raw material, 200 hours of printing, 7000 machine codes (G-code), 350 layers of 12 mm, and 150 km of extrusion, while the average energy consumption was below 6 kW [44], [45], see Figure 2-10.



Figure 2-10: TECLA project WASP<sup>®</sup> and MCA, 2021

The research on automating earth construction has increased and shown significant development over the last 10 years. Utilizing earth as a building material has sustainable advantages but lacks workability and structural performance qualities when compared to well-established cement-based materials. Challenges that hinder the process include manufacturing technologies such as the type of printer (gantry vs. robotic arm), delivery system (extruders, pumps, rheology), manual preparation and mixing; performance aspects such as shrinkage, structural, and thermal performance; and research reliability, validity, and visibility [44].

## 2.6 3DP Requirements

When designing a mix for 3DP or 3DSP the material has to follow certain parameters in order to be printed successfully. These requirements include pumpability, extrudability, and buildability. Pumpability refers to the mix's rheology (deformation or flow behavior of a material), setting time, and the physical ability to be pumped to or flow to the hopper of the 3D printer. Extrudability refers to the mix's ability to easily be pushed through the printer nozzle (think of a tube of toothpaste), filament size, deformation of the material, printing path length and speed, and rheology of material. Buildability refers to the mix's ability to hold its shape while successive

layers are printed on top of it. This includes the filament height, layer height, buckling, and rheology of the material [46].

## 2.7 Previous Work

Previous work on 3DSP with earthen materials has been conducted at UNM's Advanced Sustainable Construction lab by one previous student, Shiva Bhusal, who conducted his Master's research on 3D Printing of Earthen Materials: Toward the Carbon-Zero Construction [47]. In his research, he collected soil from 6 local areas and tested the soil characteristics; where he found the most suitable material collected was from Belén, NM, due to its high plasticity content. Mr. Bhusal created cob mix designs by adding type S hydraulic lime, wheat straw fiber, and pozzolana in different proportions. The results showed that the plain soil's compressive strength was 6.1 Mpa (884.73 psi), and the modulus of rupture was 4.15 MPa (601.90 psi), which met the minimum compressive and flexure strength requirements but failed in the shrinkage requirements with excessive cracking. Adding lime stabilized the mix but still had high shrinkage cracks and a decrease in compression and flexure strengths by more than  $\frac{3}{4}$  of the plain soil. The addition of type S lime and fiber helped control the shrinkage and cracking but further reduced the compression and flexure strength. The addition of lime, fiber, and pozzolana further improved the shrinkage characteristics, but the increased water-to-dry-mix ratio needed for hydration resulted in an increase in the mix's flowability, thixotropy, over-extrusion, and deformation in the lower layers of the printed specimen.

In conclusion, further research must be conducted on improving the soil mix's shrinkage characteristics while maintaining the minimum compressive and flexural strength, and 3D printability requirements including pumpability, extrudability, and buildability.

## **Chapter 3**

### **3. Evaluating Grain Size Distribution of Local Soils for 3D Printing in Sustainable Construction**

This chapter's objective is to:

- i. Highlight soil collection and conventional geotechnical soil characterization (Test 1 and Test 2)
- ii. Examine alternative soil characterization (Test 3 and Test 4)
- iii. Investigation of conventional and alternative characterization results
- iv. XRD Analysis

#### **3.1 Abstract**

This research focuses on the carbon-neutral development of utilizing local soil in 3D printing (3DP) construction. Integrating locally sourced soil into construction materials aims to minimize carbon footprints associated with material production, transportation, and biodegradability to foster environmental conservation. Our previous studies [48], [49] employed ASTM C136 tests to characterize local soil for 3DP and determine the clay content. However, the property results of the local soil did not match the measured clay content characterized by ASTM C136, indicating lower clay content than expected. This study aims to achieve a more appropriate grain size distribution method for the lab and field by modifying the conventional ASTM approach and incorporating an alternative traditional field test for characterizing the size distribution of local soil for 3D printing. First, a dry sieve analysis using ASTM C136 (Test 1), and a modified version

(Test 2) showed clay contents of 5.22% and 7.43%. However, the soil's high bonding, strength, and shrinkage properties suggested higher clay content. A wet sieve test (Test 3) and a shake jar test (Test 4) both indicated about 61.4% clay/silt content, displaying similar outcomes. Tests 3 and 4 provided more accurate and reliable results, aligning with the material properties of 3D-printed soil samples. The shake jar test is also proposed as a simple and practical traditional field test that could be adapted to quickly determine the sand, silt, and clay content at various construction sites.

### **3.2 Introduction**

3DP is the additive deposition of material through a computer-controlled process that played a crucial role in the fourth industrial revolution in many fields of the manufacturing industry [50], [51]. Recently, 3DP has been successfully used in construction, building components like pedestrian bridges, bus stops, and houses [52], [53], [54]. This technology offers more sustainable, affordable, and safer construction by minimizing human involvement and reducing material production, transportation, and waste [55], [56], [57]. Concrete is commonly used in 3DP for its flowability and mechanical performance, but its sustainability is questioned, prompting the need for alternative materials like local soil [9], [33], [36], [37], [44].

Earthen construction, such as adobe, is popular due to its low environmental impact and biodegradability [9], [44], [58], [59]. Adobe, a sun-dried mud brick widely used in New México, consists of local materials such as sand, silt, clay, and various fibers. Recent research explores the use of traditional materials found in Adobe that can be used in 3DP to enhance the product's sustainability [11], [44], [58], [59]. Preliminary studies on 3D soil printing (3DSP) have evaluated the properties of 3D-printed soil components, focusing on creating flowable and buildable mixtures with adequate mechanical performance.

Several studies have explored different soil mixtures for 3DSP, incorporating materials like alginate, sodium silicate, lime binder, and fiber such as straw and rice hulls to improve compressive strength [44], [60], [61], [62], [63], [64], [65], [66]. While some mixtures achieved promising results, higher cement content was often needed for significant strength, compromising the material's sustainability. Additionally, minimizing shrinkage in printed soil filaments is crucial to prevent cracking.

The Advanced Sustainable Construction (ASC) lab at the University of New México (UNM) has been developing a local soil material for 3D printing that meets NM earthen building code requirements [34]. Soil characterization was conducted on six locations surrounding the UNM campus, and it was found that soil collected from Belén, NM, contains the adequate amount of clay and plastic properties beneficial for 3DSP, requiring the material to be buildable, extrudable, and pumpable [47]. However, the high strength and high shrinkage responses of the local soil did not correspond with the amount of clay content determined by soil characterization. Understanding the correct amount of gravel, sand, and clay present in the soil is important for adobe-making and can correlate with 3D printing applications. Therefore, this study attempts to revise the conventional geotechnical test methods used for grain-size distribution of local soil and compare the results of four different tests to find a more reliable technique to perform for 3D printing of local soil material.

### **3.3 Significance of Soil Particle Size Distribution in 3DSP**

In 3DSP, the distribution of particle sizes plays a crucial role. An acceptable soil mix is essential for the printing process and the final product's properties. For smooth and even extrusion, the right balance between large gravel (which can cause blockages), medium-sized sand (providing structure), and fine clay (acting as a binder) is necessary. This balance also influences the final

product's strength and shrinkage. By understanding the particle size distribution, researchers can optimize the mix design to achieve both printability and a strong, dimensionally stable final product.

In local soil, sand helps prevent shrinkage in adobe and 3D printing mixes, but too much can weaken the material. Clay provides strength and bonding but also increases shrinkage, especially swelling clays in the smectite group, such as montmorillonite and nontronite. Unlike sun-dried adobes that shrink individually before construction, 3D-printed structures are monolithic and experience forces throughout, so shrinkage is more critical. Swelling clay particles are tiny and hold onto water, leading to higher shrinkage in high-clay content mixes. Therefore, the high shrinkage measured in the preliminary work [47] indicated that the clay content was higher than what was observed by traditional geotechnical tests, and the soil characteristics needed to be further investigated for the sake of using local soil in 3DP. This research explored four methods for measuring soil particle size in labs and fields. It also compared these methods to find the most accurate one for 3DSP applications. In addition, XRD analysis was conducted to determine the clay mineralogy of the soil.

### **3.4 Collecting Soil from Belén, NM and Initial Soil Preparation**

From the preliminary study on 3D printing with locally available earthen materials in New México, soil from Belén, NM, showed the most promise in terms of plasticity [47]. The soil was sourced from a family property in Belén, NM, for this study (different location from preliminary study). Belén is located approximately 30 minutes South from UNM as depicted in Figure 3-1.

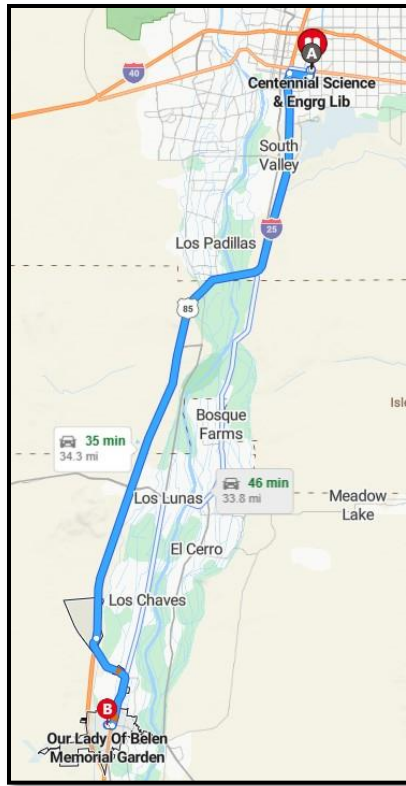


Figure 3-1: Google map of Belén, NM located South of UNM campus

When collecting material from the site, native vegetation was scraped off, and the upper 6-12 inches of topsoil was removed. The material was then collected from the area below this. An onsite field test (as displayed in Figure 3-2; b-c) was conducted to determine if the material had adequate clay content. This was done by slowly adding water to a walnut-sized sample of the soil material and determining if it would roll into a ball. If the material crumbles and falls apart easily, it contains a high sand content; if it coheres and forms a ball, it contains some clay. If the material can be rolled into a skinny snake shape or form a ribbon when squeezed through your fingers, the higher the clay content it possesses [19]. The material collected was transported to the UNM Lab, where it was cleaned of organic debris such as leaves, roots, and twigs. Due to the material being hard and containing large clumps of clay, it was manually crushed with a steel 8 in. x 8 in. hand tamper. Clumps of clay collected on sieve sizes 3/4", #4, and #8 were re-crushed with the hand

tamper until all material was crushed into a fine powder before further characterization, as demonstrated in Figure 3-2; d-e.

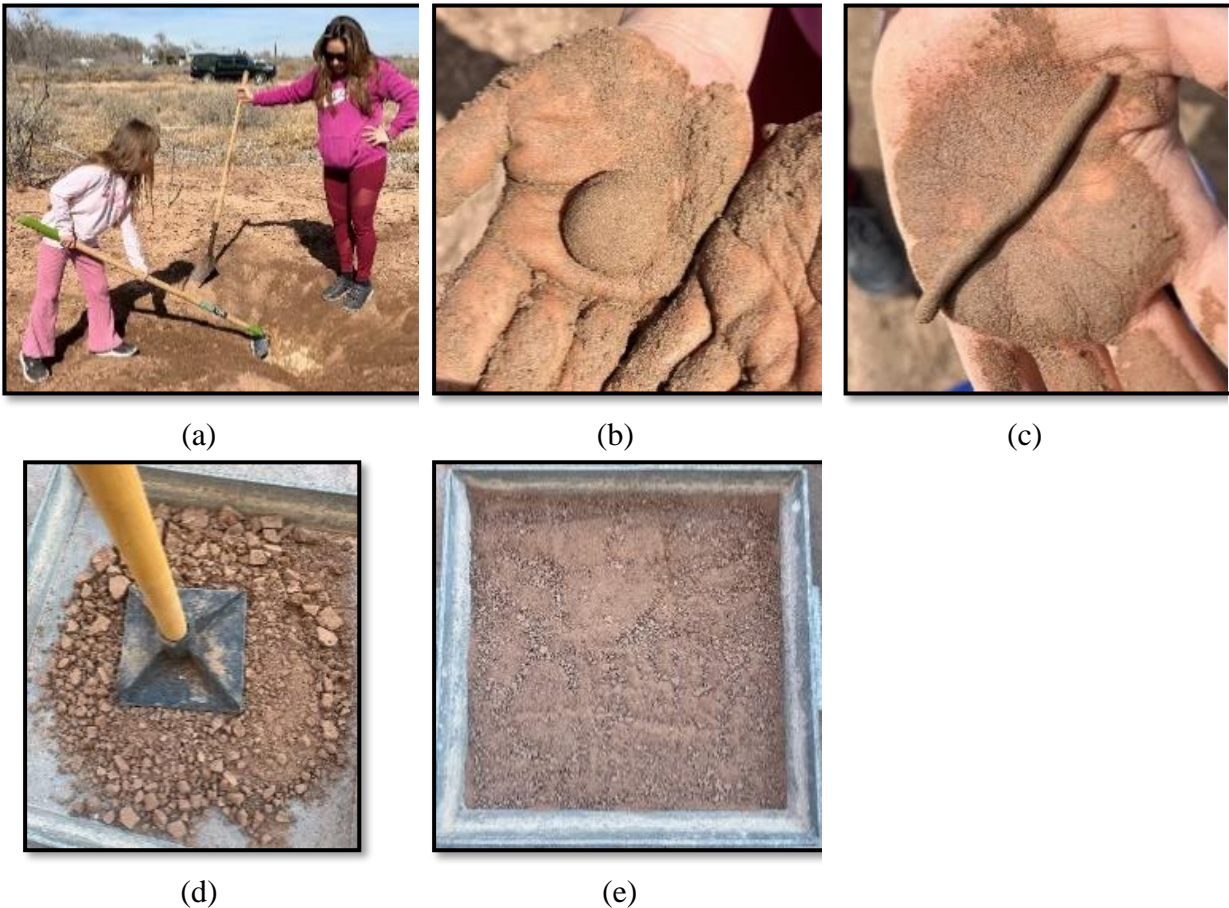


Figure 3-2: (a) collecting local soil from family property located in Belén, NM; (b), (c) field examining soil material; (d), (e) crushing soil with a hand tamper into a fine powder

### 3.5 Lab Tests for Particle Size Distribution of Soil

The standard engineering research guide is the American Society for Testing and Materials International (ASTM). This standard adopts the USCS system for classifying soils, which Professor Casagrande developed for airfield construction during World War II [67]. The classification system is based on determining a material's particle-size characteristics, liquid limit, and plasticity index. Notably, many of these standards are utilized for the testing of cementitious materials and mortars. There are very few specified standards for earthen buildings, and none have

been developed thus far for 3DSP. This section explores three lab methods and one traditional field test for analyzing soil particle size distribution. We'll delve into variations of the standard ASTM C136 and ASTM C117 sieve tests, examining how different preparation and sieving techniques can impact the results.

### **3.6 Test 1. Conventional ASTM C136 Dry Sieve Test**

After initial material preparation (crushing the material into a fine powder), it was dried for 24 hrs. at 230°F (110°C) and sieved according to ASTM C136 [68]. The Atterberg limits utilizing ASTM D4318 [69] resulted in a liquid limit of 36.12%, a plastic limit of 17.69%, and a plasticity index of 18.43%. The soil had a D<sub>60</sub> of 0.50 mm, a Cu (coefficient of uniformity) of 5, and a C<sub>c</sub> (coefficient of curvature) of 0.8. Therefore, per ASTM D2487 [70], the material falls under the coarse-grained soils category and is classified as poorly graded sand (SP). This conventional sieve test reported a low clay/silt content of 5.22%. However, this value doesn't match the high strength and shrinkage observed in the pure soil samples. This suggests the possibility of limitations in the standard sieve test for our specific application. The grain-size distribution results from Test 1 of the plain Belén soil are displayed in Table 3-1.

Table 3-1: Test 1. Grain-size distribution of plain Belén soil

Sieve # (US/SI)	Mass (g)	% Retained	Cum. Retained	% Passing
No. 4 (4.75 mm)	0.3	.06	.06	99.94
No. 8 (2.36 mm)	5.1	1.02	1.08	98.92
No. 16 (1.18 mm)	81.3	16.26	17.34	82.66
No. 30 (0.60 mm)	80.8	16.16	33.5	66.5
No. 50 (0.30 mm)	125.4	25.07	58.57	41.43
No. 100 (0.15 mm)	118.7	23.74	82.31	17.69
No. 200 (0.075 mm)	62.4	12.48	94.79	5.21

Pan	26.1	5.22	100.0	0.0
-----	------	------	-------	-----

### 3.7 Test 2. Modified ASTM C136 Dry Sieve Test

Noticing that some of the larger particles retained were not coarse aggregates but rather hard clumps of clay that had not been broken up, the characterization of the material was further investigated. Test 2 was conducted similarly to the conventional Test 1, but after the material was manually tamped, it was soaked in water to help break up larger clay particles. The material was then dried for 24 hours at 230°F, re-tamped into a fine powder, and sieved according to ASTM C136 [68]. After drying, the material was re-hardened, and large shrinkage cracks were noticed, as seen in the center picture of Figure 3-3. The soaking of the material initially assisted in breaking up the clay clumps, but since the material had to be completely re-dried, according to the standard ASTM procedures, it did not make the soil easier to break up compared to Test 1. However, the material appeared to have a slightly finer consistency. The soil remained under the coarse-grained soils category but, due to the slight increase in fines, was reclassified as poorly graded sand with clay (SP-SC) [70]. The grain-size distribution results from Test 2 of the plain Belén soil are displayed in Table 3-2.

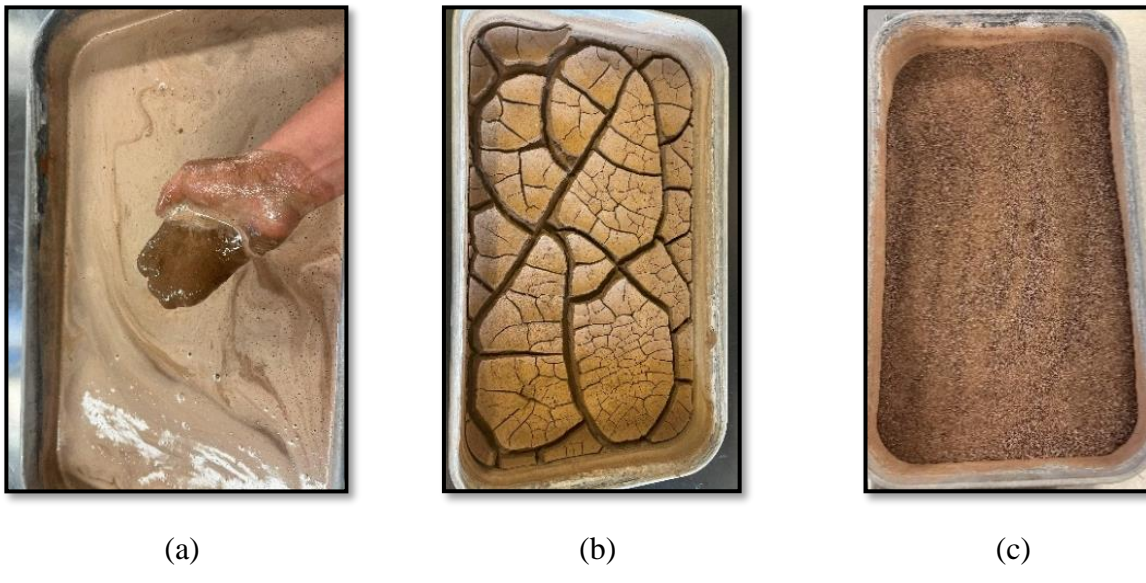


Figure 3-3: Test 2 – Belén soil soaked (left), dried (center), and re-tamped (right)

Table 3-2: Test 2. Grain-size distribution of plain Belén soil

Sieve # (US/SI)	Mass (g)	% Retained	Cum. Retained	% Passing
No. 4 (4.75 mm)	0	0	0	100
No. 8 (2.36 mm)	0.3	.06	.06	99.94
No. 16 (1.18 mm)	27.7	5.54	5.60	94.40
No. 30 (0.60 mm)	44.9	8.98	14.58	85.42
No. 50 (0.30 mm)	108.5	21.70	36.27	63.73
No. 100 (0.15 mm)	171.8	34.35	70.63	29.37
No. 200 (0.075 mm)	109.2	21.84	92.46	7.54
Pan	37.1	7.42	100.0	0

### 3.8 Test 3. Modified ASTM C117 Wet Sieve Test

To investigate the proper grain size distribution further, a sieve analysis by washing was conducted in Test 3. The soil was re-sieved according to the author's experience, and ASTM C117 [71] was utilized as a guide. Each sieve was manually "washed" with distilled water until the smaller soil particles were dissolved and pushed through the wire mesh with only the accurate

particle size retained on the sieve, as shown in Figure 3-4. Material that remained on each sieve was carefully collected and placed in a separate pan, dried, and individually weighed. The grain-size distribution results from Test 3 of the plain Belén soil are displayed in Table 3-3.



Figure 3-4: Test 3. Wet sieve test

Table 3-3: Test 3. Grain-size distribution

Sieve # (US/SI)	Mas s (g)	% Retained	Cum. Retaine d	% Passing
No. 4 (4.75mm)	0	0	0	100
No. 8 (2.36mm)	0	0	0	100
No. 16 (1.18mm)	0.4	.08	.08	99.92
No. 30 (0.60mm)	1.7	.34	.42	99.58
No. 50 (0.30mm)	27.6	5.52	5.94	94.06
No. 100 (0.15mm)	96.9	19.38	25.31	74.69
No. 200 (0.075mm)	66.5	13.30	38.61	61.39
Pan	307	61.39	100.0	0

The results of the washed sieve analysis show that there was more silt and clay (fine-grained material) than originally anticipated from the dry sieve analysis. According to the USCS standards, the soil is now considered fine-grained soil (where more than 50% of the material passes

No. 200) and is classified as sandy lean clay, whose group symbol is a clay loam (CL). These results now correlate closely to the shake jar test results, explained in the next section, where the material's USDA classification is considered a clay loam (CL). The Portalab Manual [19] also mentions that soils suitable for adobe and rammed Earth are sandy loam and light clay loam. The results from both tests now correspond with one another, and we can confidently move forward knowing that the classification of clay loam is verified in more ways than one, and the clay/silt content is around 61.4%. This classification is matched with the properties of the high strength and shrinkage properties of soil.

### **3.9 Field Test for Particle Size Distribution of Soil: Test 4. Shake Jar Test**

In addition to the sieve analysis lab tests mentioned earlier, various traditional field tests assess soil suitability for adobe construction, which can also be considered and possibly adapted for 3DSP. This research employed a similar approach to compare the field test results with the lab tests. The shake jar test, depicted in Figure 3-5, is a field method used to evaluate soil suitability for adobe making (i.e., printability for 3DSP) by determining the soil's approximate percentages of sand, silt, and clay. For the test shown in Figure 3-5 a glass graduated cylinder with a rubber plug lid was used instead of a jar for a clearer depiction of the different layers sediments . Once these percentages are calculated, the USDA soil texture classification chart, shown in Figure 3-6, can be used to classify the soil. This serves as an alternative method to the USCS dry sieve analysis. The instructions for the shake jar test were followed from The Portalab Manual: Low-Cost Soil-Engineering Tests for Constructing Earthen Buildings [19]. To conduct the test, place approximately 6 inches of soil material in a glass jar with a lid (a one-quart mason jar can be used), and slowly add water until the soil is submerged and the water level in the jar is almost full. Screw the lid on tight and gently shake the jar in a circular motion reversing ends at least 50 times. Place

the jar on an even surface and let the contents settle for 10-45 minutes. Once settled, you can visually inspect and measure the different layers. Rock and gravel, if present, will be at the bottom, followed by coarse and medium sand; silt will be in the middle (dense and darker in color), and fine clay will be at the top layer.

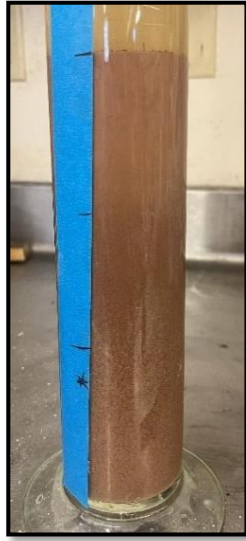


Figure 3-5: Test 4. Shake jar test

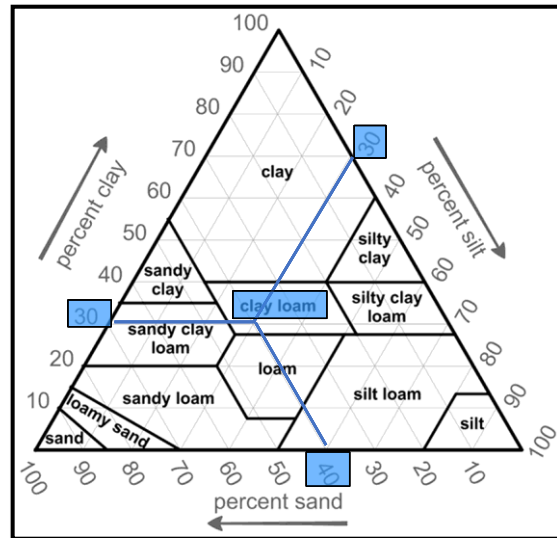


Figure 3-6: USDA Soil Textural Classification Chart [72]

The shake jar test results determined that the Belén soil's sand content was 38.55%, the silt content was 30.12%, and the clay content was 31.33%. From this information, the soil is classified as a clay loam (CL) on the USDA chart. These results or percentages do not coincide with the initial USCS classification determined from the dry sieve analysis utilizing ASTM C136 [68] in Test 1 and Test 2, where the material was considered a poorly graded sand (SP).

### 3.10 Comparing the Particle Size Distribution Results

The grain-size distribution results from sieve tests conducted in the lab (Test 1, Test 2, and Test 3) are shown in Figure 3-7. As it is demonstrated, from Test 1 to Test 3, there was a noticeable decrease in the percentage retained on the larger diameter sieve sizes #4, #8, #16, and #30 and an increase in finer particles retained on the #200 sieve (i.e., 5.22% in Test 1, 7.43% in Test 2 and

61.39% 9 in Test 3). This is because particles within high clay content, such as Belén soil, tend to clump together and adhere to the sand particles, which prevents them from being completely broken down and properly sieved during the soil classification process using ASTM C136 [68] in Test 1 and Test 2. The soil classification varied depending on the method used because of the differences in the size distribution plot. However, when comparing the lab tests to the field test, it is notable that Test 3 resulted in a soil classification similar to that of Test 4 as seen in Table 3-5 where the size distributions are compared between the four different tests.

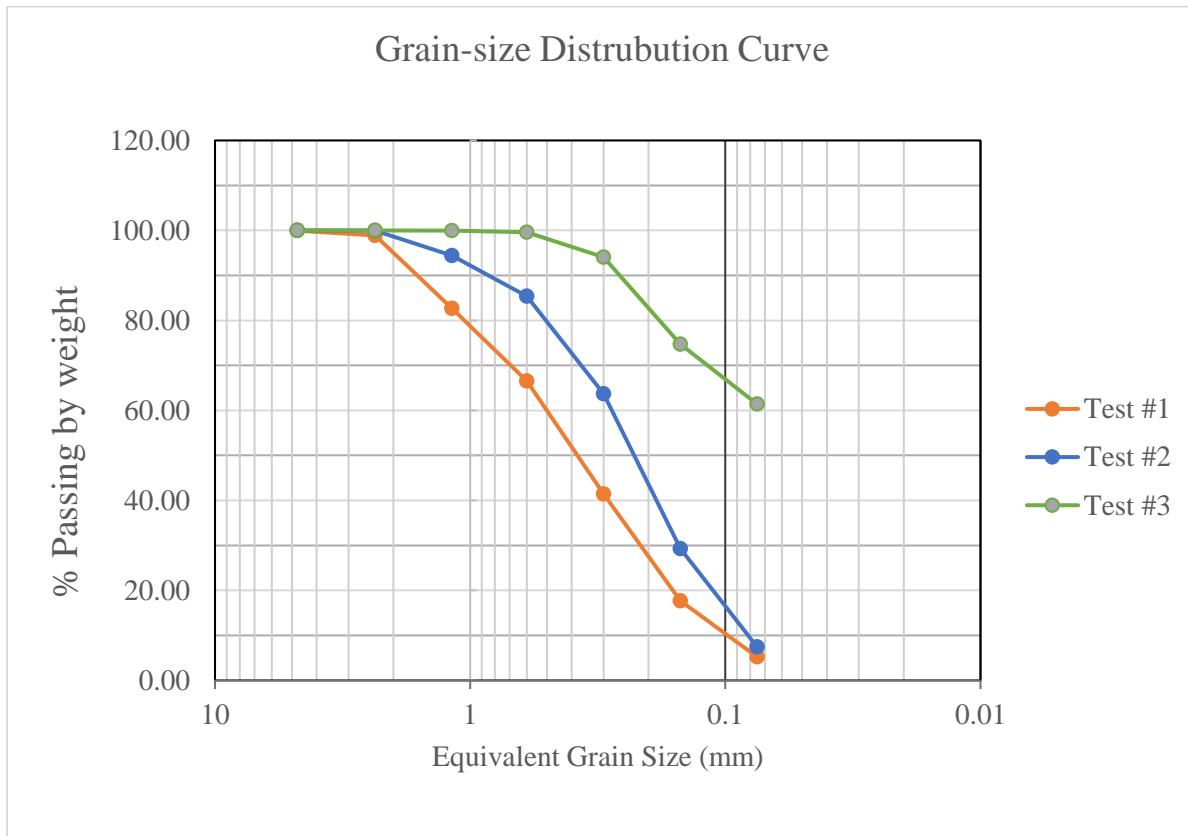


Figure 3-7: The grain-size distribution curve of plain Belén soil

ASTM D2487 [70] defines terminology for identifying soils, as seen in Table 3-4. The percentages for each category were calculated for both lab and field tests and are displayed in Table 3-5. The size distribution results indicate that Test 3 and Test 4 are well aligned and show

high agreement, while Test 1 and Test 2 displayed completely different and coarser size distributions. Despite the high bonding properties and shrinkage measures observed in a previous study [47] suggesting high clay content in the local soil, Test 1 and Test 2 results were inconsistent and inaccurate. The clay particles in high clay soil, like the Belén soil, tend to clump together and stick to the sand particles, preventing proper breakdown and sieving during the soil classification process. Therefore, Test 3 and Test 4 yielded more accurate results in determining the clay content of the local soil and could be used as alternative tests for the size distribution of any local soil.

Table 3-4: USCS range of particle sizes [70]

Soil		Size (mm)
Boulders		Larger than 300 mm
Cobbles		Between 75 and 300 mm
Gravel	Coarse	Between 19 and 75 mm
	Fine	Between 4.75 and 19 mm
Sand	Coarse	Between 2 and 4.75 mm
	Medium	Between 0.425 and 2 mm
	Fine	Between 0.075 and 0.425 mm
Silt and Clay		Smaller than 0.075

Table 3-5: Comparing the size distribution of plain soil and soil classification of different tests

Test No.	Gravel	Medium to Coarse Sand	Fine grain Sand	Silt	Clay	Soil Classification
Test 1	1.08%	57.49%	36.21%	5.22%		SP
Test 2	0.06%	36.26%	56.26%	7.43%		SP-SC
Test 3	0.00%	0.42%	38.19%	61.39%		CL
Test 4	0.00%	38.55%		30.12%	31.33%	CL

Note: SP = poorly graded sand; SP-SC = poorly graded sand with clay; CL = clay loam

### 3.11 Conclusion

This study compares conventional ASTM and alternative traditional field tests for characterizing the grain-size distribution of local soil for 3D printing. First, a dry sieve analysis using ASTM C136 (Test 1), and a modified version (Test 2) were performed, revealing clay contents of 5.22% and 7.43%, respectively. Despite these results, the soil's high bonding quality,

strength, and shrinkage suggested a higher clay content. A wet sieve test (Test 3) and a shake jar test (Test 4) indicated about 61.4% clay/silt content, showing good agreement. Overall, Test 3 in the lab and Test 4 in the field for high-clay local soil provided more reliable results, matching well with the material properties of 3D-printed soil samples. The shake jar test (Test 4) and roll ball/snake test are simple field tests that could be easily adapted for various construction sites.

### **3.12 X-Ray Diffraction Analysis**

An XRD analysis test was conducted on the soil material to determine the mineralogical composition of the clay and if it was comparable with the previous study [47]. XRD analysis is a nondestructive technique that provides detailed information about a material's crystallographic structure, chemical composition, and physical properties [73]. XRD analysis tests were conducted by UNM's Earth and Planetary Sciences Department utilizing the SmartLab X-ray diffractometer Rigaku machine. A flow diagram recognized by the US Geological Survey [74] was determined to classify the clay minerals in the soil, as seen in Figure 3-8.

### **3.13 XRD Results**

The material was air dried, and based on the oriented mount of  $14.9\text{\AA}$ , it was treated with ethylene glycol, and the material expanded to  $17\text{\AA}$ . The material was then heated to  $400^\circ\text{C}$ , where it collapsed to approximately  $10\text{\AA}$  with a very weak  $5\text{\AA}$  peak. No chlorite peak indicated that there was a kaolinite peak present. The randomly oriented aggregate mount of clay fraction dropped to  $1.54\text{\AA}$ , indicating that the soil could be nontronite clay as seen in Figure 3-9. The scans also indicated montmorillonite, kaolinite, illite, and quartz peaks were present, although determining the percentages is semi-quantitative and would require further quantitative analysis.

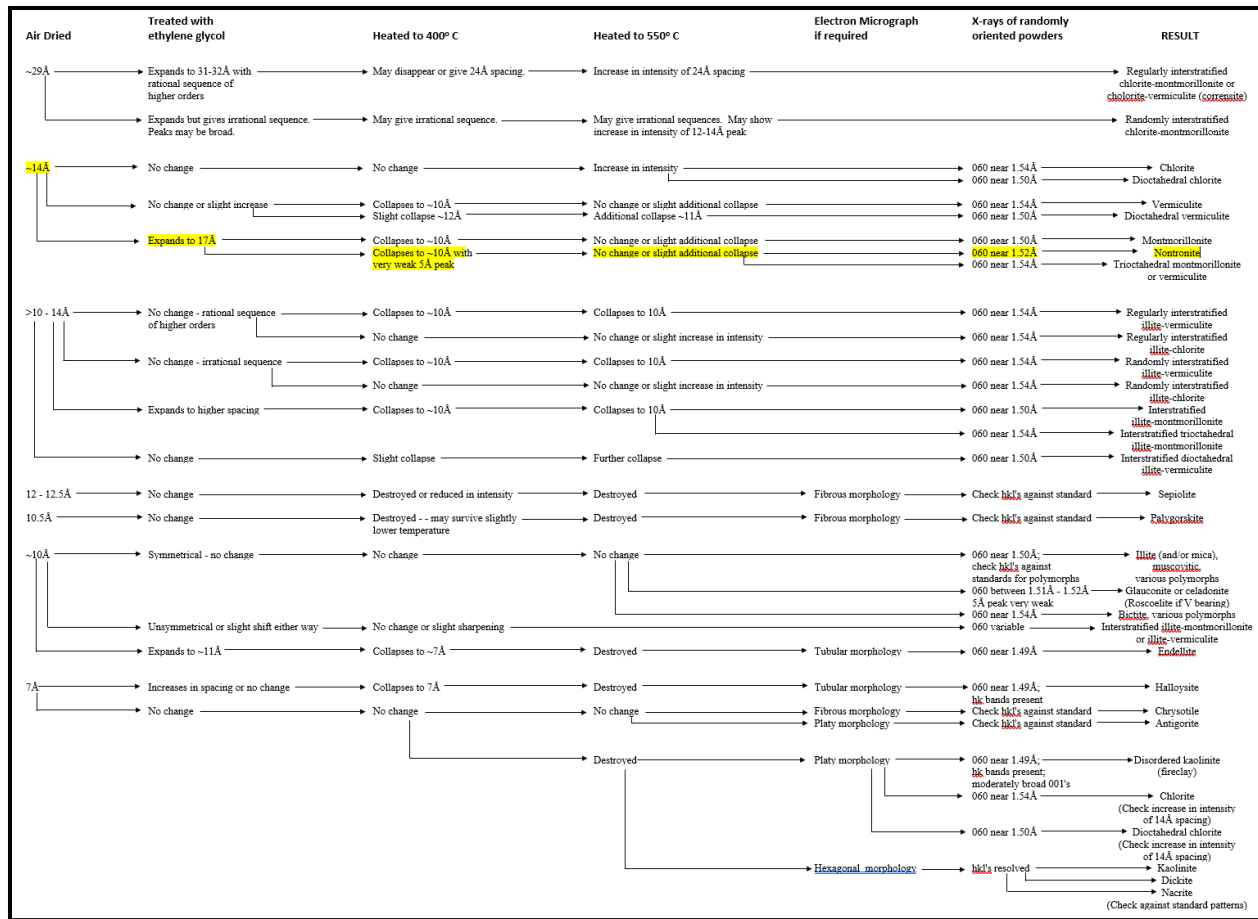


Figure 3-8: USGS Clay Mineral Identification Flow Diagram (XRD)

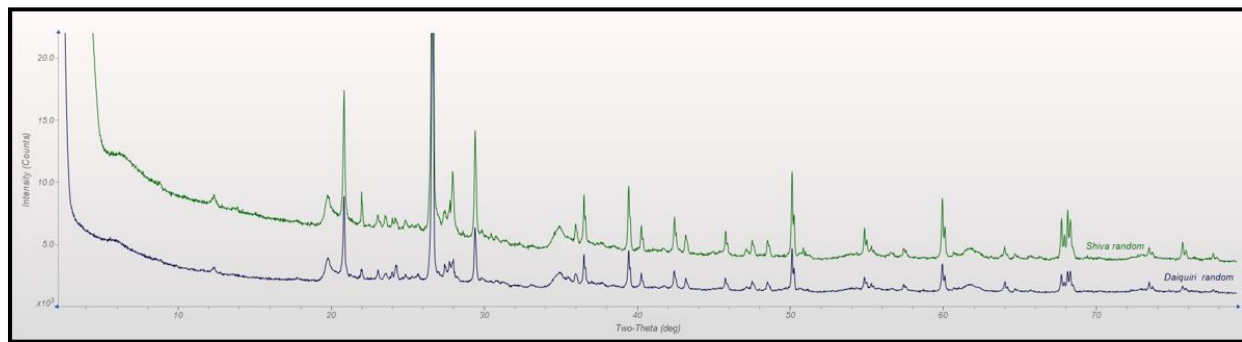


Figure 3-9: Random-oriented scan results for Belén soil samples

### 3.14 XRD Discussion

Conducting an XRD analysis on the soil used in 3DSP can assist in understanding the mineralogical composition of the material used, in turn, can assist in what type of clay (swelling

vs. non-swelling) the material possesses and can aid in determining what additives can contribute (or not contribute) to the materials strength and shrinkage properties.

According to a 1989 study conducted by the NM Bureau of Mines & Mineral Resources [10], 33 commercial adobe producers, 28 owners of pressed-earth-block machines, and 2 rammed-earth contractors in NM were located, and 41 samples of the soil material used for their products were investigated, as seen in Figure 3-10. Mineralogy analyses of the clay-size fraction of the soils used in adobe, pressed-earth blocks, and rammed-earth walls indicated that although the mineralogy varies greatly, there are four clay-mineral groups commonly represented in the clay-size fraction of adobe soils in NM: kaolinite, illite, smectite, and the mixed layer illite/smectite [10]. Expandable clay minerals include the smectite and mixed-layer illite/smectite groups, and the nonexpedable clay minerals include kaolinite, illite, and chlorite. The high-aluminum kaolinite and high-potassium illite constitute approximately 50% of the clay minerals. The calcium or sodium-rich smectite and mixed-layer illite/smectite make up the other 50%. In addition, quartz and calcite are the next common minerals. Clay-size fractions high in expandable clay minerals relative to nonexpedable clay minerals have been shown to increase the compressive strength of adobe material. This is to say that a soil material with a small amount of expandable clay in the smectite group will be comparable to an adobe material with a larger amount of nonexpedable clay minerals [10]. Particle-size analyses showed that the sand fraction is far more abundant than previously thought. Acceptable blocks can be made from material containing up to 89% sand +/- size and as little as 1% clay-size particles [10].

Understanding the type of clay present and realizing that more sand and less clay could be utilized to make adobe can assist in understanding the ratios needed for 3DSP. With this information, a re-evaluation of the soil characteristics was needed.

Particle sizes (sand +, silt, and clay) and minerals of the clay-size fraction (particles less than 2 micrometers or <2 of adobe bricks, pressed-earth blocks, and rammed-earth production materials in New Mexico. Clay-mineral analyses are semiquantitative (parts in 10). FS, mixed-layer illite/smectite; tr, trace amount; –, not present.

Producer	Map no. Table (Fig. 1A no. or 1B)	Particle-size percentages					Clay minerals					Other minerals in clay-size fraction in order of abundance	
		Sand +	Silt	Clay	Smectite	I/S	Illite	Kaolinite	Chlorite				
A. D. Adobe Co.	4	1	85%	13%	2%	4	1	3	2	–	quartz and calcite		
Adobe International	5	1	69%	22%	9%	3	tr	2	5	–	calcite and quartz		
Adobe Bricks of New Mexico	4	2	81%	16%	3%	6	1	2	1	–	calcite		
Adobes Unlimited	5	2	67%	31%	2%	1	2	3	4	–	calcite		
Aguires Services	4	3	52%	45%	3%	1	3	2	3	1	quartz and calcite		
Big "M" Sand & Cinder	4	5	34%	60%	6%	3	2	2	3	–	quartz and calcite		
Corrections Industries (resample)	4	6	54%	40%	6%	–	3	3	4	–	quartz		
Coyote Adobe, Inc.	5	5	72%	24%	4%	3	3	2	2	–	calcite, quartz, and feldspar		
DeLaO Adobe Brick Mfg.	4	7	71%	21%	8%	1	4	3	2	–	calcite and quartz		
Eloy Montano Sand & Gravel	4	8	61%	35%	4%	2	2	3	3	–	calcite and quartz		
Gallegos Sand & Gravel	4	9	84%	10%	6%	2	4	1	3	–	calcite		
Huston Construction Company	7	A	68%	25%	7%	1	4	3	2	–	calcite		
(resample)	7	A	69%	25%	6%	2	4	2	2	–	calcite and quartz		
Jaquez Construction	5	9	69%	26%	5%	2	2	1	5	–	calcite and quartz		
Paul Martinez	4	10	55%	36%	9%	1	4	2	3	–	quartz and calcite		
Medina's Adobe Factory	4	11	76%	9%	15%	1	5	2	2	–	quartz and calcite		
Ralph Mondragon	4	12	54%	42%	4%	1	5	1	3	–	calcite and quartz		
New Mexico Earth	4	14	78%	18%	4%	2	4	1	1	2	quartz and calcite		
Northern Pueblo Housing Authority													
Nambe Pueblo	5	15	40%	55%	5%	2	2	4	2	–	quartz and calcite		
Pojoaque Pueblo	5	15	57%	37%	6%	3	4	2	1	–	calcite		
Picuris Pueblo	4	16	41%	55%	4%	3	3	2	2	–	calcite and quartz		
Pueblo of Isleta Adobe and Cinder Enterprise	4	17	89%	10%	1%	2	3	2	3	–	calcite and quartz		
(resample)	4	17	89%	10%	1%	2	3	2	3	–	calcite and quartz		
Ridge Adobe	5	18	71%	24%	5%	tr	3	3	4	–	quartz, feldspar, and calcite		
Rio-Abajo Adobe Works	4	18	77%	21%	2%	1	1	2	6	–	quartz and calcite		
Archie Rivera	4	19	83%	15%	2%	1	3	3	3	–	quartz, calcite, and feldspar		
Jim Rivera	4	20	60%	31%	9%	1	2	1	6	–	quartz		
Rodriguez Brothers	4	21	63%	30%	7%	1	4	3	2	–	quartz and calcite		
Steve Romero	4	22	77%	19%	4%	4	2	2	2	–	calcite and quartz		
Manuel Ruiz	4	23	73%	20%	7%	2	4	2	2	–	calcite, quartz, and feldspar		
Roman Sandoval	4	26	27%	68%	5%	1	3	3	3	–	quartz		
Candelario Saucedo	4	27	66%	26%	8%	2	2	2	4	–	calcite and quartz		
Carl & Lorraine Steiner	5	21	55%	37%	8%	1	4	2	3	–	quartz and calcite		
The Adobe Farm	5	24	50%	41%	9%	2	3	2	3	–	quartz		
The Adobe Patch	4	28	80%	18%	2%	tr	2	5	3	–	calcite, dolomite, and quartz		
Tim's Adobes	4	29	81%	8%	11%	1	4	3	2	–	calcite and quartz		
Elias Vargas	4	31	83%	16%	1%	1	4	4	1	–	quartz and calcite		
Trini Velarde	4	32	48%	47%	5%	2	3	2	3	–	calcite and quartz		
Western Adobe	4	33	83%	13%	4%	2	4	1	3	–	calcite and quartz		

Figure 3-10: Particle-size and clay-size-mineralogy analyses of NM adobe producers [10, p. 50]

## **Chapter 4**

### **4. Addition of Xanthan Gum to Plain Belén Soil**

#### **4.1 Soil and Xanthan Gum - Mix Design**

The initial conventional characterization tests determined that the soil obtained from the family Belén property was comparable with previous studies' [48], [49] soil obtained from Belén and would be considered decent soil to continue researching for 3DSP. Additionally, according to the dry sieve test (Test 1) using ASTM C136, the clay/silt content of the soil was as low as 5.22% before modifying the gradation method. Thus, the next step in the process was to improve the soil's strength and reduce the shrinkage – as sustainably as possible. Cement and lime are the most common chemical agents used for soil stabilization [75]. With the production of cement contributing to environmental concerns, one alternative sustainable solution for soil stabilization is the utilization of biopolymers [65], [66], [75], [76]. Extensive experimental results have shown that soil strength increases with increased biopolymer concentration and curing time [65], [75]. Biopolymers are produced by different biological organisms in natural sources [75]. Plants, animals, microorganisms, and agricultural wastes are examples of natural biological sources of biopolymers [75]. Plant sources, such as rice, maize, wheat, sorghum, yams, cassava, potatoes, banana, tapioca, corn, cotton, and barley biopolymers can be produced chemically from monomeric components, such as oils, sugars, and amino acids [76]. Biopolymers are renewable, biodegradable, and potentially reduce CO<sub>2</sub> emissions by increasing soil stabilization as an alternative to cement [75]. Various researchers investigated the effect of Xanthan Gum (XG) on soil properties, and it was found that XG can considerably increase the compressive and shear

strength of soils, especially of soils that contain a significant amount of fine-grained aggregates [65], [66], [75].

Soil collected from the Belén property was prepared for initial experiments with 1% and 2% XG added to see if the compressive strength of the soil would increase. The XG used for this research was obtained from Cargill (Satiaxane CX 91), a food additive product used as a texturant. The base mix (with no XG added) was 100% plain (Belén) soil mixed with a 38% water-to-dry mix ratio. The water content was adjusted according to the plasticity range determined in the characterization step. Due to the consistency of the mixture, the water required for each was unknown and experimental at this time, as seen in Table 4-1.

Table 4-1: Mixed proportions of soil mixes

Mix ID	Plain Soil (%)	Xanthan Gum (%)	Water to Dry Mix Ratio
S	100	0	.38
SX1	99	1	.55
SX2	98	2	.75

Each soil mix material was mixed in a Kitchen Aid mixer according to the Standard Mechanical Mixing of Hydraulic Cement Pastes and Mortars of Plastic Consistency ASTM 305-20 [77]. Note that this standard was used as a guide, as there is no specified mixing standard for a soil mixture. First, the dry materials were weighed and added to the mixing bowl. The dry ingredients were mixed at the lowest mixing speed (60+/-5 rpm), and the specified amount of water was gradually added as it was mixed for 2 minutes. After mixing at low speed, the mixer was paused, and the soil mix material was scraped off the sides of the mixing bowl with a spatula. The mixture was continued at medium speed 4 (140 +/-5 rpm) for an additional 2 minutes. After mixing at medium speed, the mixer was paused, and the material was scraped off the walls. The mixer

was allowed to continue mixing at high speed 8 (225 +/- 5 rpm) for the final 2 minutes. The total combined mixing time was 6 minutes.

#### **4.2 Soil and Xanthan Gum - Compressive Strength Preparation**

To measure the compressive strength of the material, the Standard Test Method for Compressive Strength of Hydraulic Cement Mortars ASTM C109 [78] was followed. Note that this was used as a guide as there is no specified standard for compression of soil material to be 3DP. After each soil mix material was mixed, it was placed into a plastic 2 in.  $\times$  2 in.  $\times$  2 in. (50 mm  $\times$  50 mm  $\times$  50 mm) cube form in 3 equal lifts and gently compacted with a rectangular plastic probe. The form was tapped on the ground, each lift, to release any air bubbles. Mixes were made for 7-day and 21-day compression tests.

The consistency of the plain soil (S) was smooth and a little grainy. It was not too wet or dry, as seen in Figure 4-1.



Figure 4-1: Plain (Belén) Soil Mix

As the water was added to the SX1 mix, the consistency of the biopolymer-soil mixture became very gummy and similar to a thick, sticky dough. More water was slowly added due to the consistency of the material sticking together in the mixer. The final step of mixing at high speed for 2 minutes was impossible, and adding more water did not seem to improve the consistency.

The material was placed into the compression cube form in 3 equal lifts and compacted with a plastic probe, but it wasn't easy due to the mix being gummy and dry, as seen in Figure 4-2.



Figure 4-2: SX1 Soil Mix

For the SX2 soil mix, the water-to-dry mix ratio was increased to .75 due to the results observed from the SX1 mix. After adding the water, the consistency of the mix was smoother than the SX1 mix, but it appeared to have too much water now. After mixing was complete, the consistency of the material had a slightly fluffy texture and was similar to a frothy chocolate pudding; it was more soupy than the SX1 mix, as seen in Figure 4-3.



Figure 4-3: SX2 Soil Mix

The curing procedure was a work in process as the cube forms used for the compression tests usually require a lid on the forms as they are curing material that usually contains cement or lime. Initially, the lids were placed on the forms, but by the 3<sup>rd</sup> day, the material in the forms for

the SX1 and SX2 had risen, and the material was not drying properly, as seen in Figure 4-4 and Figure 4-5. Since this is a soil material and does not contain any cement, it does not need to be “cured” but air dried (similar to adobes individually drying in the sun). The excess risen material was scraped off and left to dry without the lid at an average ambient room temperature of 70°F (21°C).



Figure 4-4: 3 Day Results - Left: S Mix, Center: SX1 Mix, Right: SX2 Mix

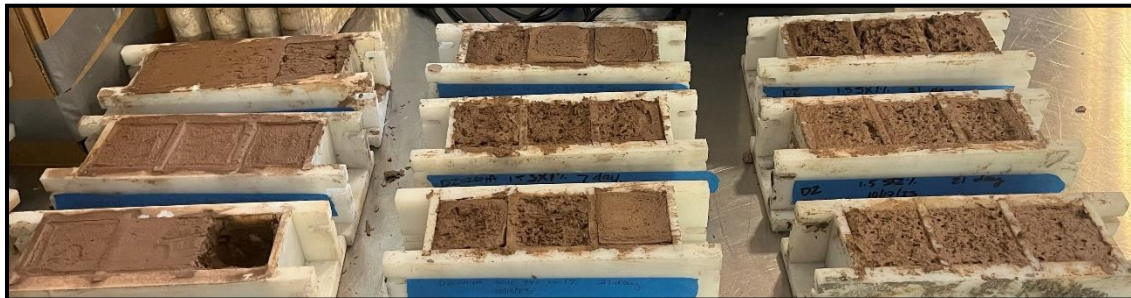


Figure 4-5: 3 Day results after removing lids and scraping excess material off – Left: S Mix, Center: SX1 Mix, Right: SX2 Mix

By the 7<sup>th</sup> day of drying, the SX1 and SX2 mixes had cracked severely and were sticking to the sides of the cube forms, as seen in Figure 4-6. Only 3 specimens of the SX1 were salvageable for testing. SX2 specimens could not be used for compression analysis as they broke into pieces when the forms were removed. The 7-day compression tests could not be conducted due to the inconsistent drying and the material being stuck to the sides of the forms.

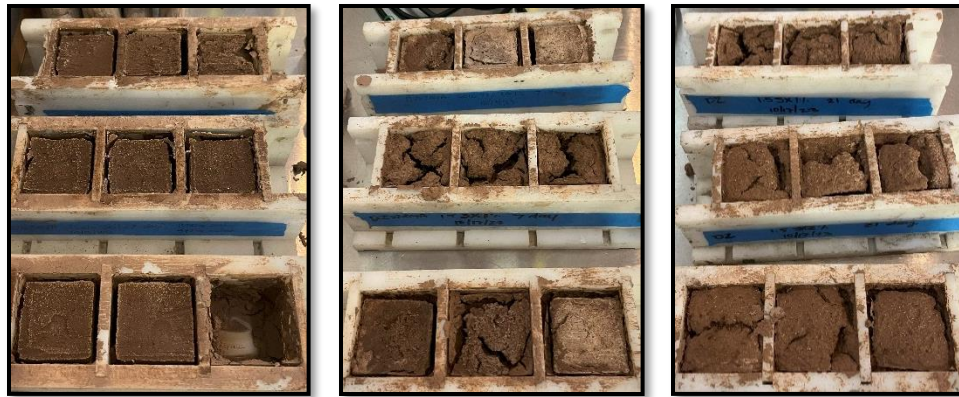


Figure 4-6: 7 Day Results - Left: Plain Soil Mix, Center: SX1 Mix, Right: SX2 Mix

#### 4.3 Xanthan Gum and Soil - Compressive Strength Results and Discussion

Compression tests were conducted on the 21<sup>st</sup> day on a high-strength concrete testing Forney machine. Each cube was weighed and measured before testing. The compressive strength ( $\sigma$ ) was calculated as the axial force per unit area of the contact surface of the cube specimen.

Equation 1: Compressive Strength

$$\sigma \text{ (psi)} = \frac{P}{A}$$

Where,

$\sigma$  = Compressive strength

P = Axial load applied

A = Area of the surface of contact of the cube specimens

The load compressed the samples at .00066 in/s (1 mm/min), and the ramp rate was 50 psi/s. The results concluded that the plain soil had an average 21-day strength of 731.5 psi, and the SX1 sample had an average 21-day strength of 397 psi, as illustrated in Figure 4-7. Although the SX1 mix was lower in strength, it still meets the minimum compressive strength of the NM Earthen Building Code of 300 psi. This could be due to the inconsistency of the material when mixing, the

amount of water added, the amount and type of clay present, and the drying process that occurred during the investigation.

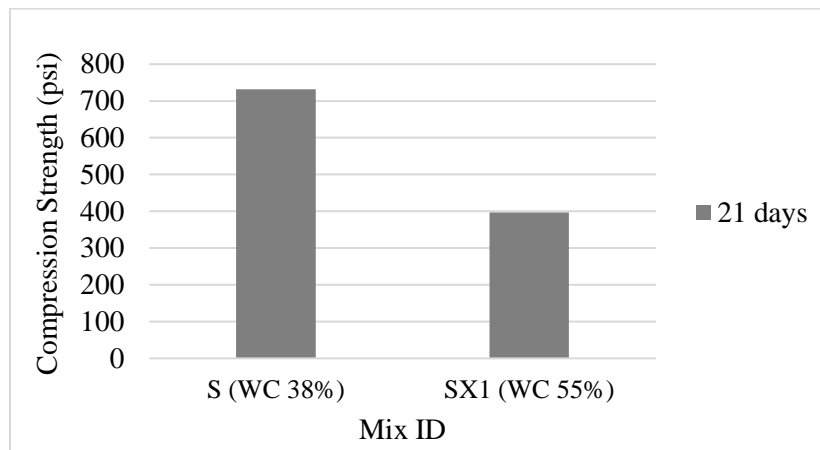


Figure 4-7: 21 Day Compression Results

This section investigated the addition of xanthan gum to the plain Belén soil which resulted in a mix that had less strength than originally anticipated. This could be due to the inconsistency of the material when mixing, the amount of water added, the amount and type of clay present creating a binder-to-binder issue between the biopolymer and clay, and the inconsistent drying process that occurred during the investigation. From the results, the high fines present, and the grain size distribution should be investigated on a deeper level to improve the mix.

## **Chapter 5**

### **5. Improving the Durability Performance of Local Soil Mix for 3D Printing**

This chapter's objective is to:

- i. Reduce shrinkage of soil mix by adjusting the proportion of local soil and concrete sand
- ii. Investigate shrinkage and compression results of the mixes of concrete sand and soil
- iii. Test mix with a primary 3DSP of 1-foot diameter dome
- iv. Further improve soil's durability characteristics by lowering maximum grain size and addition of rice hull fiber
- v. Investigate shrinkage and compression results of improved mix
- vi. Test mix with a secondary 3DSP of 2-foot diameter dome

#### **5.1 Abstract**

The use of earth-based materials in construction has a rich worldwide historical context, yet their application in 3D printing sustainable structures is relatively emerging and largely uncharacterized. This study investigates the adaptation of local New Mexican soil towards 3D soil printing applications, aiming to develop a sustainable soil mix that is both printable and structurally durable. Initial test results highlighted significant shrinkage issues, with recorded material contraction up to 12.33%, limiting its practical use. We employed a series of experimental modifications to the soil composition and printing process to mitigate these shrinkage effects. The results indicate a reduction in shrinkage to 3.48%, an overall reduction of 8.85 % and improved

(required) mechanical strength from previous studies, demonstrating the potential for using local soil in sustainable 3D-printed construction. These findings address critical material limitations and pave the way for innovative applications in community-based construction projects, such as the 3D printing of traditional hornos (ovens). This research contributes to the broader effort of integrating sustainable materials into modern building technologies.

## 5.2 Introduction

3D printing (3DP) is the additive deposition of material, layer by layer, through a computer-controlled process, playing a crucial role in the fourth industrial revolution across various fields of the manufacturing industry [50], [51]. Recently, 3DP has been successfully utilized in construction, producing building components such as houses, bridges, and bus stops [44], [52], [53], [54]. This technology offers further flexibility for architectural design, increased construction speed, and a more affordable, sustainable, and safer approach to construction by minimizing human involvement, formwork, material transportation, and waste [54], [55], [56], [79]. Concrete is commonly used in 3DP due to its flowability and robust mechanical performance. However, cement-based products are causing rising concerns over the environmental implications, prompting the search for alternative sustainable construction materials like local soil [9], [36], [44], [53], [58], [80], [81], [82]. Concrete production significantly contributes to carbon emissions due to the high energy required to produce cement, the main binding agent in concrete [38]. The cement industry is responsible for approximately 8% of global carbon emissions, additionally, 3D-printed concrete structures can require a higher concentration of cement for the material to be printable and extrudable making the product a less sustainable option [38], [39], [58], [83]. As the world's population continues to increase, ethical and social responsibility from engineers and architects are pressed to design in harmony with the environment in ways that guarantee sufficient

resources for future generations [11], [84], [85]. This study aims to explore the use of local soil in New México (NM) for 3D soil printing (3DSP), working to make it a mechanically viable option that meets the requirements of 3DP and structural performances established by the NM earthen building code [86]. By utilizing local resources, this research seeks to enhance the sustainability of construction practices while maintaining the necessary structural and durability standards.

The use of earth as a building material boasts a rich history worldwide. NM stands out in North America for its extensive history of Indigenous Pueblos, churches, and traditional homes constructed with local soil in various ways. In particular, structures made of adobe, a sun-dried mud brick comprised of soil, water, and fiber such as straw, have been a cornerstone of New Mexican architecture for centuries, preferred for their utilization of the high-quality soil located along the Rio Grande Valley which is ideally suited for adobe construction [10], [11], [13], [47], [48], [49]. In the United States (USA), one-third of the nation's adobe dwellings are located in NM [10]. Taos Pueblo, located in northern NM, is home to one of the oldest continuously occupied structures in the USA, constructed puddled earth and adobe [14]. It is the only Native American community that is designated both a National Historic Landmark and a World Heritage site [14]. Understanding the soil mixes and tests used for traditional adobe construction can aid in determining a suitable soil mix for 3DSP.

Adobe has been favored in NM due to its excellent thermal mass and insulation properties, freedom of design, affordability, repairability, durability, sustainability, and biodegradability. Adobe is also known to have other positive qualities that include being fireproof, termite-proof, bulletproof, and having low sound transmission [10]. Unlike concrete where cold joints can be a structural issue, adobe can be repaired by being re-wetted (re-awakened) with a lime-water solution and repaired with mud plaster or new adobe [13]. The introduction of the wooden form,

by the Spanish in the late 1600s permitted the adobe makers to control the size and weight of the bricks, which in turn allowed for greater construction flexibility [18]. Adobes can be made from a variety of local soils, but the most suitable soil found in the Rio Grande Valley is a sandy loam, from alluvial or pediment deposits, composed of approximately 55-85% sand, and 15-45% finer material (generally more silt than clay) [10]. A balance of particle sizes is essential to ensure a quality adobe. When grain size in mud is too similar, its adhesion properties are diminished [13]. Clay gives strength to the adobe, but in excessive amounts will cause shrinkage: sand or straw can be added to decrease the shrinkage and prevent cracking [10]. Indigenous peoples and early settlers recognized the local soil's suitability for building robust, long-lasting homes capable of withstanding the arid climate. This tradition of adobe construction has been handed down through generations, creating a rich architectural heritage that continues to influence modern building practices.

Beyond its practical benefits, adobe construction is deeply ingrained in NM's cultural and historical identity. Using local soil not only reduces the environmental impact of construction but also fosters a sense of continuity with past and future generations, creating a place-based approach. Place-based implies creating and developing a connection with the land and ecosystem, as well as preserving and protecting it throughout time [2]. This approach creates an opportunity for enhanced community engagement as adobe construction is quite a labor intensive, and assisting in mixing, or any stage of production, is culturally enriching - at any age. As contemporary builders and researchers pursue sustainable design options, NM's adobe heritage lessons provide valuable insights into the potential of earth-based materials for modern applications, such as 3D printing. By merging traditional knowledge with advanced technology, there is an opportunity to develop innovative and environmentally friendly building solutions that honor the region's architectural

legacy. This can be accomplished by creating structures made of local material that the community can benefit from and utilize for teaching, such as learning facilities, or a 3DSP horno, known as a traditional oven, which is used in many of the Native Pueblos for cooking bread, roasting corn or chile, making pizza, or pudding.

Although there is a long history of using earth for construction, the application of this material in 3D printing houses is relatively new. Recent research explores using traditional materials similar to adobe or cob mixtures in 3DSP to enhance the product's sustainability [44], [58], [59], [61], [80], [82]. Some previous studies have explored how to use this sustainable material for construction, and there have been a few successful large-scale 3D printed structures utilizing local soil by organizations like IAAC (Pylos, TerraPerforma, 152 Travessera de Garcia), WASP (Gaia, TECLA), and Emerging Objects (MUD Frontier projects: The Hearth, Beacon, Lookout Kiln, and Casa Covida) [87], [88], [89], [90]. The MUD Frontier project started along the Rio Grande watershed, beginning near the El Paso and Juarez border and ending near the headwaters of the Rio Grande in Colorado's San Luis Valley [90]. However, a reliable, printable, durable, and structurally stable soil mix for wide-use and large-scale production remains elusive. As a consequence, the pursuit of fully implementing 3D earthen material in modern construction remains hindered by a limited amount of published research describing the material reproducibility and mechanical properties, as well as a lack of engineering guidance for the structural design of such mixes [80], [82], [91].

In previous research conducted by our team at The University of New México (UNM) [48], [49], we studied the properties of local soil and adapted it for 3D printing. Despite these efforts, we observed significant shrinkage of the material—up to 7.7%—and compressive strength that fell below the required 300 psi established by the NM Earthen Building Code [86], which limits

its application for construction. Through the Transformation Network (TN) [92], UNM partnered with The Native American Community Academy (NACA), a tuition-free community-supported charter school located in Albuquerque, NM, that provides a culturally integrated college preparatory education designed by and for Indigenous Students (grades K-12) [4]. Land-Based Healing and Learning is one of the ways the school teaches their students to strengthen their kinship with the land and water to support the community in reclaiming their identity as beings who are integral to the ecology [93]. This current study is also part of a community engagement project with the school aiming to create a 3D-printed traditional horno (oven) using local soil that will be used as a learning tool in their outdoor cooking area. The paper focuses on addressing the mechanical material limitations, particularly shrinkage and compressive strength, to develop a sound and reliable product for this application. By improving the soil mix as naturally as possible, we aim to balance printability, mechanical strength, and shrinkage stability, thereby expanding the potential for using local soil in sustainable 3D-printed construction for any community needs.

### **5.3 Materials and Methods**

In our preliminary study on 3DP with local earthen materials in New México, soil from Belén, NM, showed the most promise in plasticity [48], [49]. The soil for this study was sourced from a family property in Belén (a different location from the preliminary study), where native vegetation was scraped off, and the top 6-12 inches of soil were removed. The material was collected from below this layer. An onsite field test determined approximate clay content by adding water to a walnut-sized soil sample and feeling the texture, cohesion, and clay content by hand by assessing its ability to form a ball, snake, or ribbon shape [13], [19], [28]. The soil was transported to the Dana C. Wood Materials and Structures Lab at UNM, cleaned of organic debris, and manually crushed with a steel hand tamper to a fine powder for further characterization. The next section

presents soil characterization, soil mix design, and test methods for casting and 3D printing of designed soil mixes.

### **5.3.1 Soil Characterization**

The particle size distribution of soil significantly impacts its compressive strength and shrinkage properties. Soils with a high proportion of fine particles, especially swelling types of clay, tend to expand when moist and shrink significantly upon drying. Clay is also recognized for enhancing soil strength; research indicates that expanding clay minerals in the smectite group, i.e., montmorillonite and nontronite, exhibit greater strength compared to non-expanding clays, i.e., kaolinite, illite, and chlorite of equivalent composition [10]. Achieving a balanced particle size distribution is crucial for producing high-quality adobe, and this principle likely applies similarly to 3D printing with earthen materials.

In another study by our team [94], we compared three different grain size distribution tests in the lab and one in the field to identify the best method for characterizing local soil for 3D printing. The test methods are thoroughly explained in Zozaya et al. [94]. The results indicated that a wet sieve test (Test 3) for the lab and a shake jar test (Test 4) for the field provided practical and reliable assessments, aligning with the properties of 3D-printed soil samples. These methods are suitable for quickly determining the sand, silt, and clay content of high-clay local soils for 3D printing applications and adjusting the clay content with a well-graded grain size distribution to achieve a more printable, mechanically strong soil mix. The wet sieve test (Test 3) and the shake jar test (Test 4) indicated about 61.4% clay/silt content, showing good agreement between the two tests. Table 5-1 compares the size distribution of the plain soil with the results from Test 3 and Test 4, which demonstrate this consistency. According to the USDA chart, the soil is classified as clay loam (CL) [72].

Table 5-1: Comparing the size distribution of plain soil and soil classification of different tests [70], [71], [72], [94]

Test No.	Gravel	Medium to Coarse Sand	Fine grain Sand	Silt	Clay	Soil Classification
Test 3	0.00%	0.42%	38.19%	61.39%		CL*
Test 4	0.00%		38.55%	30.12%	31.33%	CL*
CS**	14.86%	38.59%	46.20%	0.36%		SP***

Note: \*CL= Clay Loam; \*\*CS= Concrete Sand; \*\*\*SP=Poorly-Graded Sand

Additionally, an X-ray Diffraction (XRD) analysis was performed on the fine clay fraction of the soil samples (those passing through a No. 200 sieve). This provided essential information about the soil's mineralogy and identified specific types of clay present in the samples.

XRD tests indicated montmorillonite, kaolinite, illite, and quartz peaks were present, although determining the exact percentages is semi-quantitative and would require further quantitative analysis. According to a 1989 study conducted by the NM Bureau of Mines & Mineral Resources [10], 33 commercial adobe producers in NM were located, and 41 samples of the soil material used for their products were investigated. Mineralogy analyses of the clay-size fraction of the soils used in the adobe indicated that although the mineralogy varies greatly, there are four clay-mineral groups commonly represented in the clay-size fraction of adobe soils in NM: kaolinite, illite, smectite, and the mixed layer illite/smectite [10]. Expandable clay minerals include the smectite and mixed-layer illite/smectite groups, and the nonexpendable clay minerals include kaolinite, illite, and chlorite. The high-aluminum kaolinite and high-potassium illite constituted approximately 50% of the total clay minerals. The calcium or sodium-rich smectite and mixed-layer illite/smectite made up the other 50%. Quartz and calcite were the next common minerals found in the adobes. Clay-size fractions high in expandable clay minerals relative to nonexpendable clay minerals have been shown to increase the compressive strength of adobe material [10]. The information from this study on the commonly represented clay-mineral groups correlates with the XRD results conducted on the local Belén soil in this study and in the previous

study [48], [49] indicating that the current material contains similar mineralogy to acceptable adobe mixes and could be a good indicator of suitable material for 3DSP.

### 5.3.2 Soil Mix Design

Our previous study [48], [49] explored the use of local soil in construction, focusing on its printability and properties in fresh and hardened states. It investigated the impact of various regional and natural admixtures, such as type-S hydraulic lime, natural wheat fiber, and pozzolana, on the performance of the soil mixes. Contrary to expectations, type-S hydraulic lime and pozzolana did not improve strength or reduce shrinkage. However, adding fibers reduced shrinkage to some extent, but the minimum linear shrinkage observed was with a soil/lime/pozzolana/fiber mix that resulted in 2.6% (0.46 mm). The International Building CodeCodeCodeCode states that adobe can be used for construction if it does not have shrinkage cracks 76mm in length and 3.2 mm in width [35], which in length did not meet the requirements. We discovered that an ineffective soil gradation technique, specifically the ASTM C136 [68] dry sieve test, classified the soil as Well-Graded Sand and failed to reflect the accurate clay content in the local soil. By employing a modified soil gradation technique explained in Zozaya et al. [94], we re-classified the soil as CL (clay loam), indicating a very high clay content, likely the main reason behind the significant shrinkage observed.

To address this issue, the mix design in this study aims to mitigate shrinkage by reducing the clay content with proper grain-size distribution and adding new natural fibers to achieve a more structurally stable soil mix. We replaced part of the local Belén soil with concrete sand to lower the clay content while closely monitoring the compressive strength to ensure it does not fall below the minimum strength requirement of 300 psi suggested by the New México Earthen Building Code [86].

This section presents two different sets of mixes designed to address naturally improving the compressive strength and shrinkage of soil mixes used for 3DSP: one with plain soil and concrete sand and the second with plain soil, concrete sand, and rice hull fibers.

### **5.3.3 Optimizing Soil Mix Design: Substituting Local Soil with Concrete Sand**

To improve the grain size distribution of local plain Belén soil (S), concrete sand (CS) was obtained (donated) from Vulcan Materials Company, a local producer and distributor of construction aggregates located in Placitas, NM. CS is used in concrete mixes, so it should be free of fine particles according to ASTM standards [95]. Accordingly, performing a dry sieve test (ASTM C136 [68]) is sufficient to determine the size distribution of the CS. The CS was washed at the plant, and afterward, a standard dry sieve analysis (ASTM C136 [68]) was conducted at the Dana C Wood Materials and Structures lab at UNM. Due to the size of the printer nozzle chosen, 20 mm in diameter, the CS was further sieved in the lab to have a max aggregate size of sieve No.4 (0.187 in./4.75 mm), the smallest sieve through which 100% of the sample must pass. Having too large of an aggregate can clog the system and affect the pumpability and extrudability of the material being printed. Grain size distribution results of the sieved CS are shown in Table 5-2 and Figure 5-1.

Table 5-2: Grain Size Distribution of CS (Max aggregate size: Sieve No. 4) according to ASTM C136 [68]

<b>Sieve # (US/SI)</b>	<b>Mass (g)</b>	<b>% Retained</b>	<b>Cum. Retained</b>	<b>% Passing</b>
No. 4 (4.75mm)	0.00	0.00	0.00	0.00
No. 8 (2.36mm)	70.80	14.28	14.86	85.14
No. 16 (1.18mm)	57.90	12.15	27.00	73.00
No. 30 (0.60mm)	126.0	26.44	53.44	46.56
No. 50 (0.30mm)	169.70	35.61	89.05	10.95
No. 100 (0.15mm)	43.90	9.21	98.26	1.74
No. 200 (0.075mm)	6.60	1.38	99.64	0.36
Pan	1.70	0.36	100	0.00

Five soil mixes were formulated to optimize the replacement of S with CS. Each mix replaced varying amounts of soil with CS, as detailed in Table 5-3. The mix ID denotes the percentage, by weight, of plain Belén soil (S) in each formulation. For instance, S75 indicates that the soil mix weight comprises 75% S and 25% CS. The literature guides this substitution [10], [16], [19], [20], [82], suggesting that adobe mixes typically require between 15-45% clay. Referring to Table 5-1, which indicates the plain soil contains clay/silt content of approximately 61.4%, efforts were made to achieve a clay quantity comparable to that used in traditional adobe soil mixes. The clay/silt content by weight ranges between 16.2-61.4%.

Table 5-3: Soil mix design to optimize S replacement with CS by their weight percentage

Mix ID	Plain (Belén) Soil (S)	Concrete Sand (CS)	Clay/Silt content (%)	Liquid Limit (%)	Water /(S+CS)
S100	100	0	61.39	36.12	36.00
S75	75	25	46.67	35.5	32.00
S67	67	33	41.89	-	20.00
S50	50	50	31.61	35.37	23.00
S25	25	75	16.17	25.03	16.00

To better understand the particle size distribution for each designed soil mix combining the ASTM C136 dry sieve test [68] result for CS and wet sieve test [71] result of S, Figure 5-1 illustrates the particle size distribution of the five formulations and Table 5-4 summarizes each soil mix's weight percentage and clay/silt content according to this particle size distribution. As shown in Figure 5-1 and Table 5-4, the coarser soil mixes were achieved by incorporating more CS into S, and the silt/clay content was reduced from S100 (61.39%) to S25 (16.17%). Additionally, Figure 5-1 shows that adding more CS to the S improves the soil's gradation from a uniformly graded to a more well-graded soil.

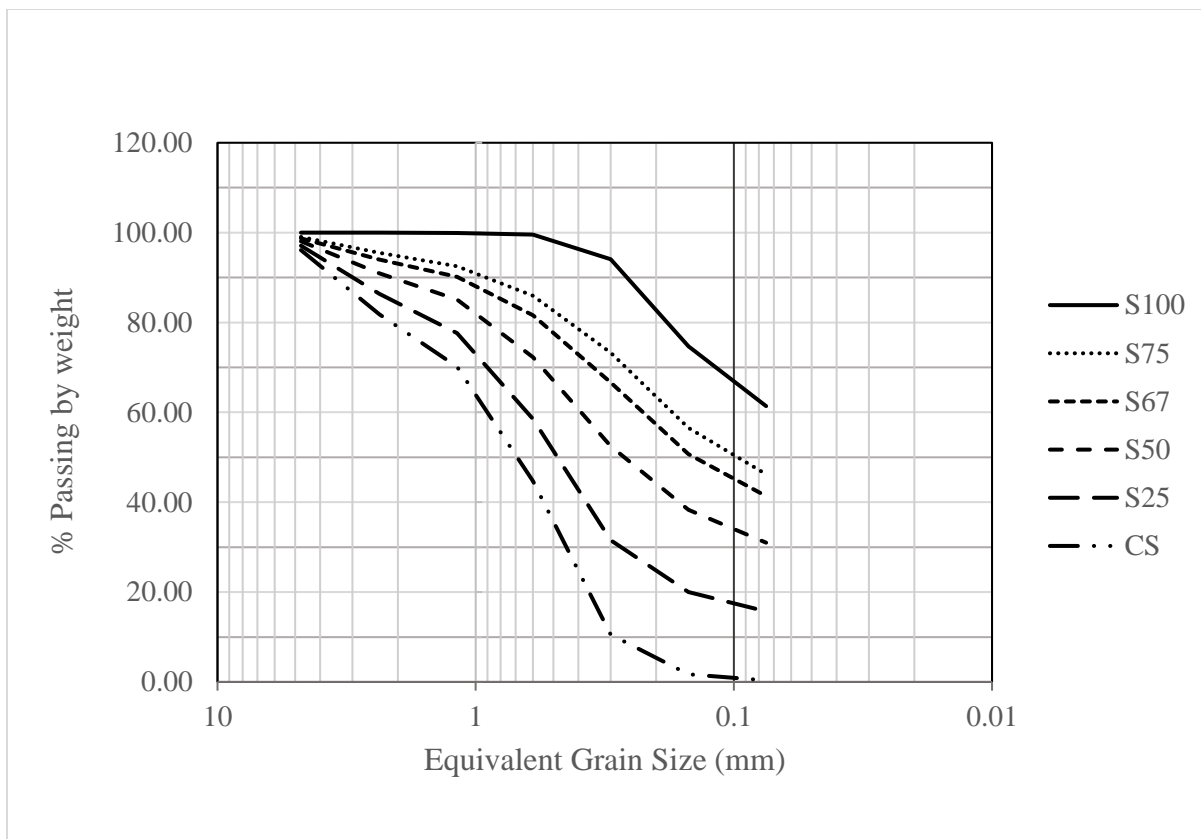


Figure 5-1: Grain size distribution of CS (Max aggregate size No.4 sieve) and soil mixes (S100, S75, S67, S50, and S25) designed to optimize S replacement with CS according to dry [68] and wet sieve tests [71]

Table 5-4: Percent of gravel, sand, silt/clay of the five mixes with S and CS

Mix ID	Gravel	Medium to Coarse Sand	Fine grain Sand	Silt/Clay
S100	0.00	0.42	38.19	61.39
S75	3.58	9.62	40.12	46.67
S67	4.75	12.61	40.75	41.89
S50	7.25	19.04	42.10	31.61
S25	11.01	28.70	44.13	16.17

Beyond particle size distribution, accurately determining the optimal water content for each mix is critical. While previous studies [49] explored flow table tests and rheology measurements for this purpose, flow tables have limitations in the context of soil mixes for 3D printing. This

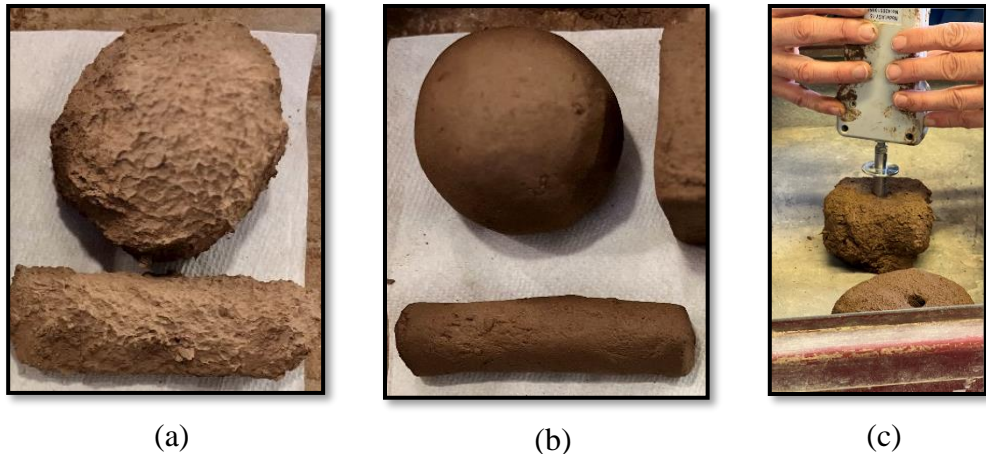
paper tested the Liquid Limit (LL) of each new soil mix according to ASTM D4318 [69]. This method determined the approximate baseline water content needed for each mix, as displayed in Table 5-3. Note that the missing LL for S67 will be discussed further in sections 5.3.10 and 5.4.1.

Determining the optimal water content for each soil mix was crucial for successful 3D printing. Two methods were employed depending on the batch size and the ambient condition. For small batches in a controlled lab environment (i.e.,  $73^{\circ}\text{F}$  ( $23^{\circ}\text{C}$ )  $\pm 2^{\circ}$  and an average indoor humidity of  $16\% \pm 2\%$ ), the LL value served as a starting point. This value reflects the maximum water content where the soil behaves like a liquid. However, adjustments were made based on the results of the traditional consistency test, reported in the last column (Water/ (S+CS)) of Table 5-3. This test allowed for a more delicate evaluation of the desired consistency for 3D printing - a balance between smooth extrusion and adequate structural integrity. The chosen method for determining the water content of each soil mix is based on a traditional texture-by-feel consistency test established from the author's experience and literature for testing soil and adobe material in the field as a guide [19], [28], [82], [94], [96]. This test offers a straightforward approach to finding the required water content. In this test, an amount of water below the LL was added to the soil, and a sample of the soil mix was kneaded and rolled into a ball approximately 1.5-2 in. (50 mm) in diameter and a sausage shape approximately 3.9 in. in length (100 mm) and .78 in. (20 mm) in diameter, as displayed in Figure 5-2a. The water content was determined by examining the consistency of the mix in the ball and sausage form; if the material crumbled and could not be rolled into a ball it did not have enough water, and 5ml at a time was added to the soil, re-kneaded, and re-tested. The added water was recorded as optimal if the material was covered and rolled into a ball. Too much water was added if the material was too sticky or slumped. For instance, the LL measured for mix S25 was 35.5% when the material was tested in a small batch; at this water

content, the material was watery and slumpy, as displayed in Figure 5-2a. A small batch of 500g of the soil mix was measured by weight, and 20% (100 ml) of water was initially added. 5ml of water at a time was added to the mix until the material could roll into a ball and sausage easily which occurred at 32% (160 ml), as displayed in Figure 5-2b. It was found that the more CS was added to S, the lower the optimum water content was determined from the LL.

For larger batches of soil mix intended for 3D printing, a different approach for optimal water content was necessary. The larger batches were mixed in a standard-size wheelbarrow with a shovel and by hand. Access and funding to a large pumpable mixer was not possible for this study. The water content was initially estimated based on the values obtained from the traditional consistency test explained earlier. This initial estimate was then refined during the mixing process using a penetration technique Figure 5-2c with a portable digital penetrometer hardness tester [97] to achieve the optimal water content for printability. This technique allowed for a more precise adjustment of the water content to achieve the optimal printability characteristics required for successful 3D printing with larger batches. Note that the LL for mix ID S67 was not determined prior to the traditional consistency test and when the preliminary 3DSP was conducted.

To do this test, a small portion of soil material was formed into a cube shape approximately 1.5-2 in. (50 mm) on each side and placed on a flat surface. The penetrometer was slowly inserted into the soil, perpendicularly, and the measured hardness was recorded. The recommended hardness scale can differ with each printer; for this study, the optimum hardness scale ranged from .36 to .42 kg/cm<sup>2</sup>, which translated to a slightly higher water content than the traditional test results and will be discussed further in the next section.



(a)

(b)

(c)

Figure 5-2: Simple tests to determine the required water content for (a) a small batch in a controlled lab environment, too much water (b) a small batch in a controlled lab environment, optimum water content (c) a large soil batch under ambient field condition

### 5.3.4 Optimizing Soil Mix Design: Including Natural Fibers

A new set of mixes was formulated to further reduce the shrinkage observed in the previous set of soil mixes after 3D printing trials, considering the limitations of the nozzle size. The soil mix S67 (with CS max aggregate size No.4) was chosen for the preliminary 3D printing trials, and in the second set of mixes, the CS was further sieved in the lab to have a max aggregate size of No.16 (0.046 in./1.18 mm). Having too large of an aggregate can clog the printing system and affect the pumpability and extrudability of the material being printed. Grain size distribution results of the sieved CS are shown in Table 5-5 and Figure 5-3. This second set of mixes also incorporated natural rice hull fibers supplied by Victor's Home Brew Supply in Albuquerque, NM. As a result of rice grain processing, a large amount of waste (approximately 20%) is produced from rice as the hull [98]. Due to their poor nutritional value, low bulk density, and high ash content, rice hulls have become a growing space and environmental pollution problem [99]. An average length of 8-10 mm rice hull fibers were chosen for this study due to their consistent length and the possibility that rice hull waste can be recycled and reused for 3DSP to reduce shrinkage as a more sustainable option. If straw or hemp fibers were chosen for this study, the fibers would

have to be cut to be smaller than the nozzle size of 20 mm and lengths could vary and affect the extrudability of the material. This can be a labor-intensive process for large prints, where more material would be needed. Rice hull fibers are the perfect size, naturally. The rice hull fibers were measured by weight and added to the soil mix at four different weight fractions (.5, 1, 1.5, and 2%), guided by previous studies [47], [58], [100], [101].

The second set of mixes consists of five soil mixes utilizing mix S67 (max aggregate size No. 16) with increasing amounts of rice hull fibers, as detailed in Table 5-5. The mix ID denotes the percentage, by weight, of plain Belén soil (S), concrete sand (CS), and rice hull fiber percentage (F) in each formulation. For instance, S67-F0.5 indicates that the soil mix weight comprises 99.5% of S67 (67% S, 33% CS) mix and 0.5% F.

The optimum water content was estimated according to the traditional texture-by-feel consistency test described in the previous section (5.3.3) and is noted in the last column (Water/(S+CS)) of Table 5-5. Figure 5-3 describes the grain size distribution of the improved S, CS, and S67 mixes used to add rice hull fibers.

Table 5-5: Soil mix design to optimize S replacement with CS by their weight percentage

Mix ID	Plain (Belén) Soil (S)	Concrete Sand (CS)	Total % of (S+CS)	Clay/Silt content	Fiber Content	Water /(S+CS)
S67-F0	.67	.33	100	45.87	0	22
S67-F0.5	.67	.33	99.5	45.64	.5	22
S67-F1.0	.67	.33	99	45.41	1.0	22
S67-F1.5	.67	.33	98.5	45.19	1.5	22
S67-F2.0	.67	.33	98	44.95	2.0	22.5

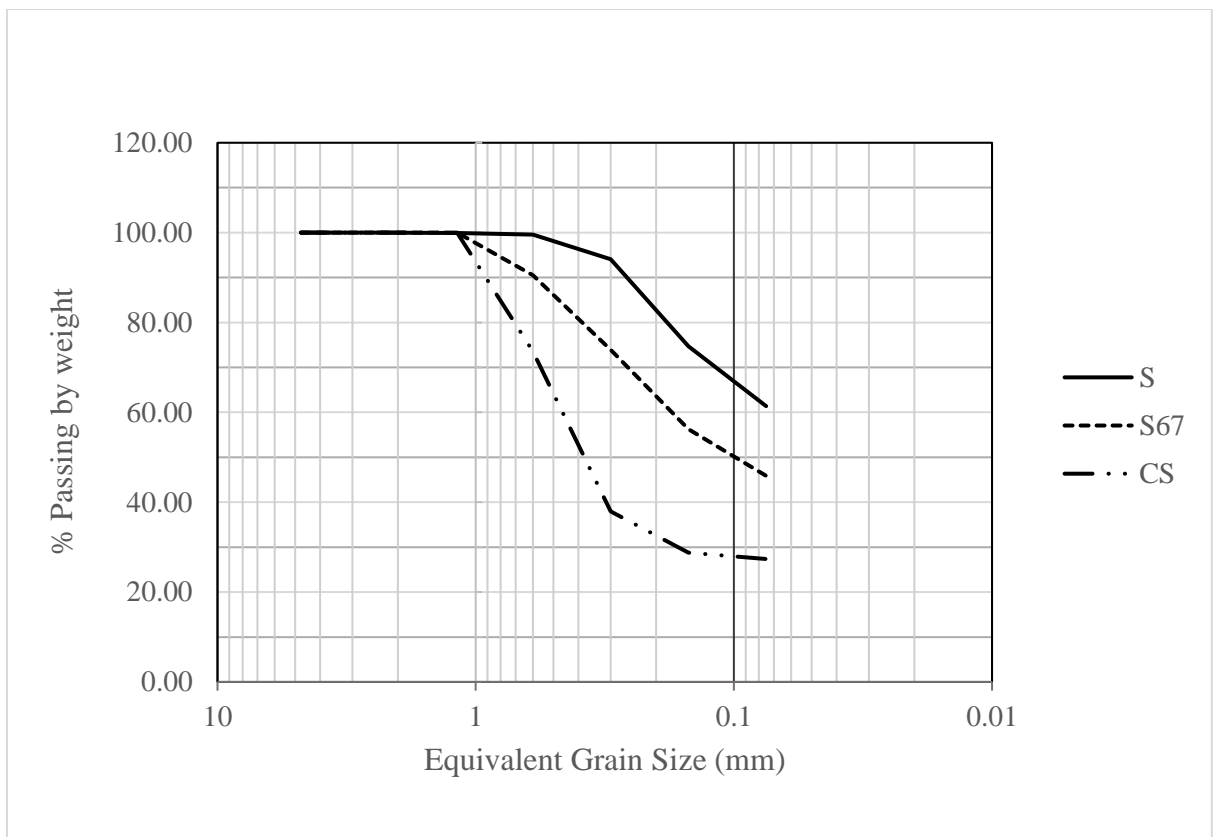


Figure 5-3: Grain size distribution of S, CS, and S67 mix (Max aggregate size No. 16) chosen to add rice hull fiber (F) to

### 5.3.5 Mixing procedure for soil mixes

For small-scale soil batches, each soil mix was blended in a Kitchen Aid mixer according to ASTM 305-20 [57]. Note that this standard was used as a guide, as there is no specified mixing standard for an adobe/cob type of soil mixture. First, the dry materials were measured by weight and added to the mixing bowl. The dry ingredients were mixed at the lowest mixing speed (60+/- 5 rpm), and the specified amount of water was gradually added as it was mixed for 2 minutes. After mixing at low speed, the mixer was paused, and the soil mix material was scraped off the sides of the mixing bowl with a spatula. The mixture was continued at medium speed 4 (140 +/- 5 rpm) for an additional 2 minutes. After mixing at medium speed, the mixer was paused, and the

material was scraped off the walls. The mixer was allowed to continue mixing at high speed 8 (225 +/-5 rpm) for the final 2 minutes. The total combined mixing time was 6 minutes.

For large-scale soil batches, the preparation was quite labor-intensive and required a team of 7-10 people to prepare the batches to be printed. Each large batch made was 20,000g or 45,000g in weight. First, the S was crushed with a steel 8 in. x 8 in. steel hand tamper until the consistency was a fine powder. The CS was sieved according to mix set, and fiber was measured by weight according to the fraction determined for each mix ID. After all the dry materials were measured, they were mixed in a standard-size wheelbarrow with a hoe. Water was slowly added according to the traditional consistency test results and mixed by hand in a kneading manner, which can be extremely labor-intensive. As the mix reached the traditional consistency test water content, it was clear that the material was still too dry, and more water was measured out 10% at a time, mixed, and tested with the penetrometer as described in section 5.3.3.

In our initial experiments on 3D-printed domes, we relied on a manual hand-mixing technique to achieve the desired consistency in the soil mix. While effective for smaller batches, hand mixing becomes incredibly labor-intensive and impractical as the scale of the 3D printing project increases. This limitation highlights the need for mixing solutions for large-scale 3D printing applications. In the adobe industry, large stockpiles of the appropriate soil material are mixed with a front-end loader, water is added, which is usually allowed to soak overnight in a mud pit, and then the material can be transferred by front-end loader or conveyor pugmills to the modeling forms [10]. This may be an alternative method to mix the soil for 3DSP, but it will need to be further examined and tested. Fortunately, various industrial mixers are available that can efficiently handle larger volumes of soil, significantly reducing manual effort and ensuring consistent mix properties throughout the printing process. These mixers could range from simple

drum mixers to more sophisticated pug mills, depending on the specific needs of the project. Implementing such solutions would be crucial for scaling up 3D printing with local soil materials and supporting the growth of the adobe industry.

### **5.3.6 Test Methods**

Having formulated the soil mixes and established a consistent mixing process, we conducted a series of tests to identify the optimal material for 3D printing soil structures such as a dome, which is the closest shape related to a traditional horno. These tests focused on printability, mechanical strength, and dimensional stability.

First, we reviewed established methods for evaluating cast soil specimens, such as compressive strength tests on soil blocks and shrinkage tests on soil bars. Based on these evaluations, the most promising soil mix for 3D printing was selected.

Finally, this chosen mix underwent printability assessments, including tests for extrudability (smooth flow through the printer nozzle), flexure strength (stress at failure in bending or modulus of rupture) and buildability (ability to form and retain desired shapes during printing). These evaluations ensured the successful 3D printing of domes in the final stage of the study. All test methodologies are explained in detail in the following sections.

### **5.3.7 Measurement of Compressive Strength in Cast Soil Cubes**

The compressive strength of the soil mixes was measured following the ASTM C109 [58] standard as a guide. Each soil mix was blended according to section 5.3.3 for small-scale soil batches and placed into a 50 mm × 50 mm × 50 mm (2 in. × 2 in. × 2 in.) plastic mold in three equal lifts and gently compacted with a rectangular plastic probe each lift. After each lift, the mold was tapped on the ground to release air bubbles. Three specimen cubes were prepared for each mix

for 7-day and 28-day compression tests, with 7 days chosen based on the required drying time for soil mixes. Molds were left uncovered, and the walls were removed on the third day to facilitate proper drying. The specimens dried in ambient laboratory conditions, with an average temperature of 73°F (23°C) and 16% ± 2% indoor humidity.

To measure the compressive strength at the given ages, the cube samples were tested using a high-strength concrete testing Forney machine, as shown in Figure 5-4.. The load compressed the samples at .00066 in/s (1 mm/min), and the ramp rate was set to 50 psi/s. Each cube was weighed and measured before testing. The compressive strength ( $\sigma$ ) was calculated according to Equation 2 as the axial force per unit area of the contact surface of the cube specimen.

Equation 2: Compressive Strength

$$\sigma \text{ (psi)} = \frac{P}{A}$$

Where,

$\sigma$  = Compressive strength

P = Axial load applied

A = Area of the surface of contact of the cube specimens



Figure 5-4: Forney compression machine

### 5.3.8 Measurement of Shrinkage in Cast Soil Samples

Following ASTM C490 [64] to assess length change, the shrinkage characteristics of each mix were evaluated. Prepared according to section 2.2.3 for small-scale soil batches, the mixed material was cast into steel prism molds measuring 12 in.  $\times$  2 in.  $\times$  2 in. (300 mm  $\times$  50 mm  $\times$  50 mm). To eliminate air bubbles, the material was compacted in two equal lifts using a rectangular plastic probe and a tamping motion. After three days, the mold walls were removed to facilitate proper drying. The specimens were then cured under laboratory ambient conditions, with an average temperature of 73°F (23°C)  $\pm$  2° and an average relative humidity of 16%  $\pm$  2%. In triplicate (three samples per mix), the shrinkage was assessed, and the average values represented the shrinkage of each mix.

Specimen length was monitored daily for seven days to assess shrinkage, with the change in length recorded. This timeframe was chosen as the specimens typically dry completely within a week, minimizing further volume changes. Measurements were taken on opposite sides of each

specimen and averaged to account for potential variations. Even in the presence of cracking, the total length was determined by measuring each cracked piece and summing the individual lengths (cracks themselves were excluded). The final shrinkage value for each mix was calculated as the average change in length across the three replicate specimens and calculated according to Equation 3.

Equation 3: Change in length

$$\varepsilon_{sh-l}(t) = \frac{l_t - l_0}{l_0} \times 100$$

Where,

$\varepsilon_{sh-l}(t)$ = linear shrinkage of the soil prism in % at the age of t;

$l_t$ = length of the prism at the age of t;

$l_0$ = length of the prism after casting.

### 5.3.9 3D Printability Tests and Mechanical Properties of 3D-Printed Soil Samples

In this section, we will detail the 3D printer used for our soil sample tests, including its specifications and capabilities. The 3D printer utilized at the Dana C. Wood Materials and Structures Lab at UNM is a gantry 3D printer with a steel frame measuring 2m x 2m x 2m, with 3 degrees of freedom in the x, y, and z planes. The system is controlled by a computer control unit that interprets and converts STL files into G-code. The system uses cartesian coordinates with no rotational movement. The nozzle system contains a small hopper where you can feed the material. It is equipped with a rotating auger that extrudes the material downward from the nozzle head onto the printing bed. The circular nozzle head can be removed and replaced with different-sized nozzles, as seen in Figure 5-6. A 15 mm and 20 mm nozzle were used in this study, allowing for precise soil mix extrusion. The nozzle system is guided by drive motors that move in horizontal and vertical directions along moving guide rails. The printer's extrusion speed can be adjusted

between 1 to 5cm/s and 1 to 5 rad/s, respectively, providing flexibility for different material properties and printing requirements. Figure 5-5 is an image of the 3D printer setup, showcasing all its components, including the nozzle, guide rail, control unit, drive motor, and printing bed [102].

The following subsections will explain the procedures for extrudability, buildability, and mechanical properties tests. These tests are crucial for determining the feasibility of using soil mixes in 3D printing applications.

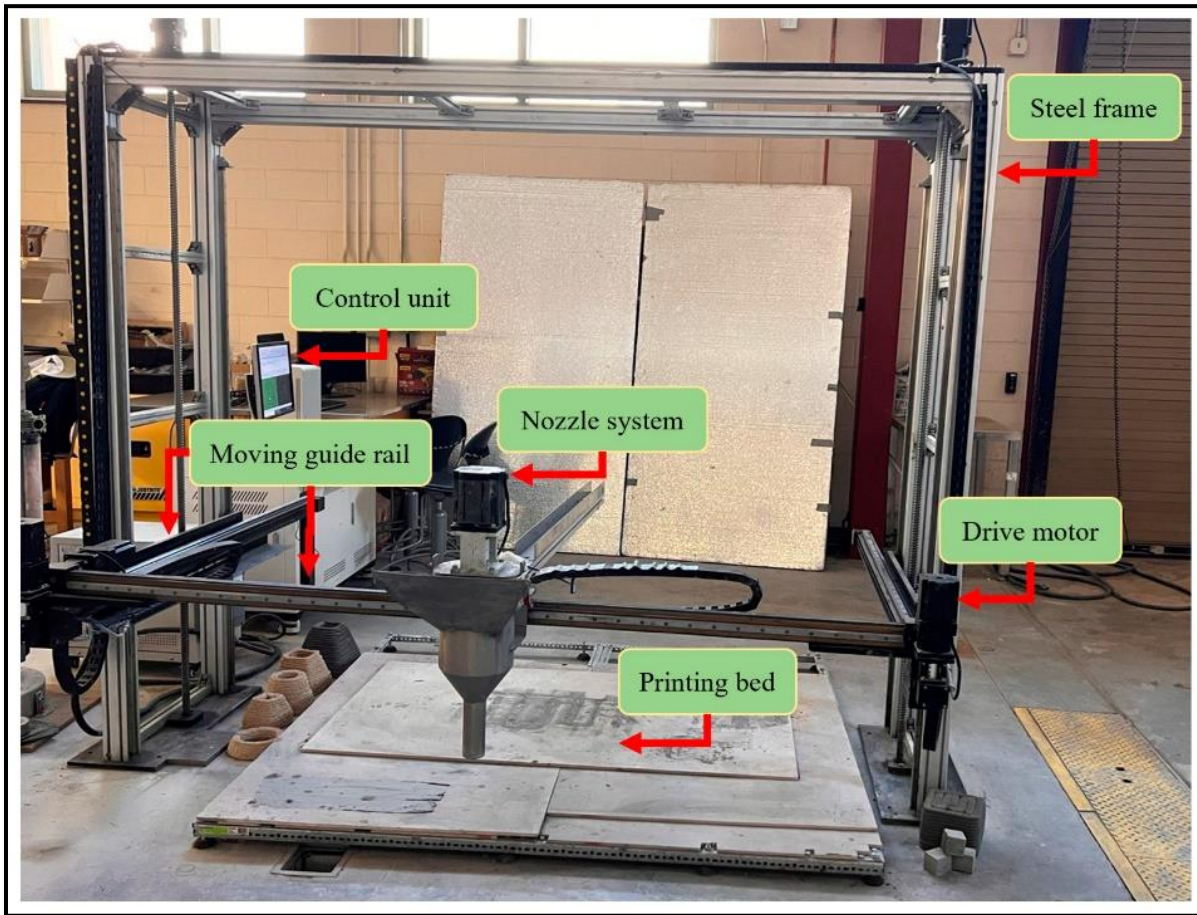


Figure 5-5: 3D Gantry printing system used in the Dana C. Wood Materials and Structures Lab at UNM [102]

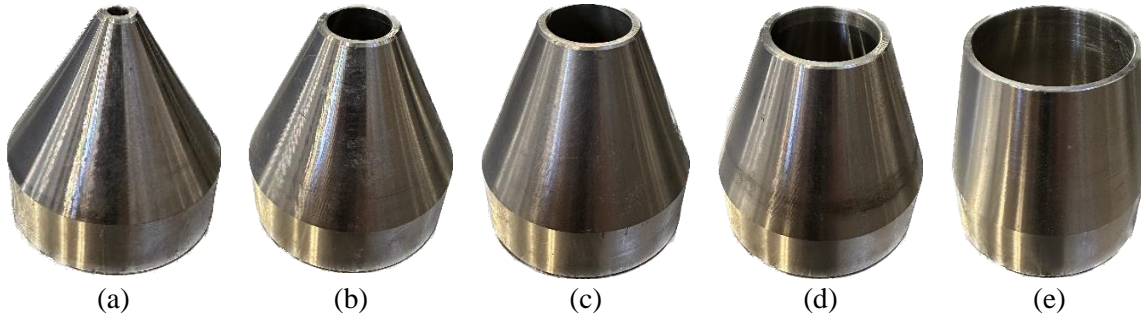


Figure 5-6: Diameter of nozzle: a) 5 mm; b) 15 mm; c) 20 mm; d) 25 mm; e) 40 mm [47]; Diameter of nozzle: a) 5 mm; b) 15 mm; c) 20 mm; d) 25 mm; e) 40 mm [47]

### 5.3.9.1 Extrudability Tests

Extrudability refers to the ease with which the soil mix can be extruded consistently through the nozzle without clogging, breaking the flow, or causing cracks and maintaining dimensional accuracy (similar to the ease of toothpaste being squeezed out of its tube). The test involves running the soil mix through the 3D printer at different printing speeds to find the optimal settings. The consistency of the extruded material is observed and recorded. To measure the extrudability, a zigzag pattern with six different legs was printed. A 20 mm nozzle was chosen for this test. A constant layer height of 10 mm and extrusion rate was set for 0.15 rounds/s. Each leg of the zigzag pattern (in total, six legs) was 3D printed with varying printing speeds set at 10 mm/s, 15 mm/s, 20 mm/s, 25 mm/s, 30 mm/s, and 35 mm to obtain an optimized printing speed which resulted in consistent filament width that was as close to the design width, of 20mm, as possible.

Figure 5-7 is a schematic representation of the extrudability test setup.

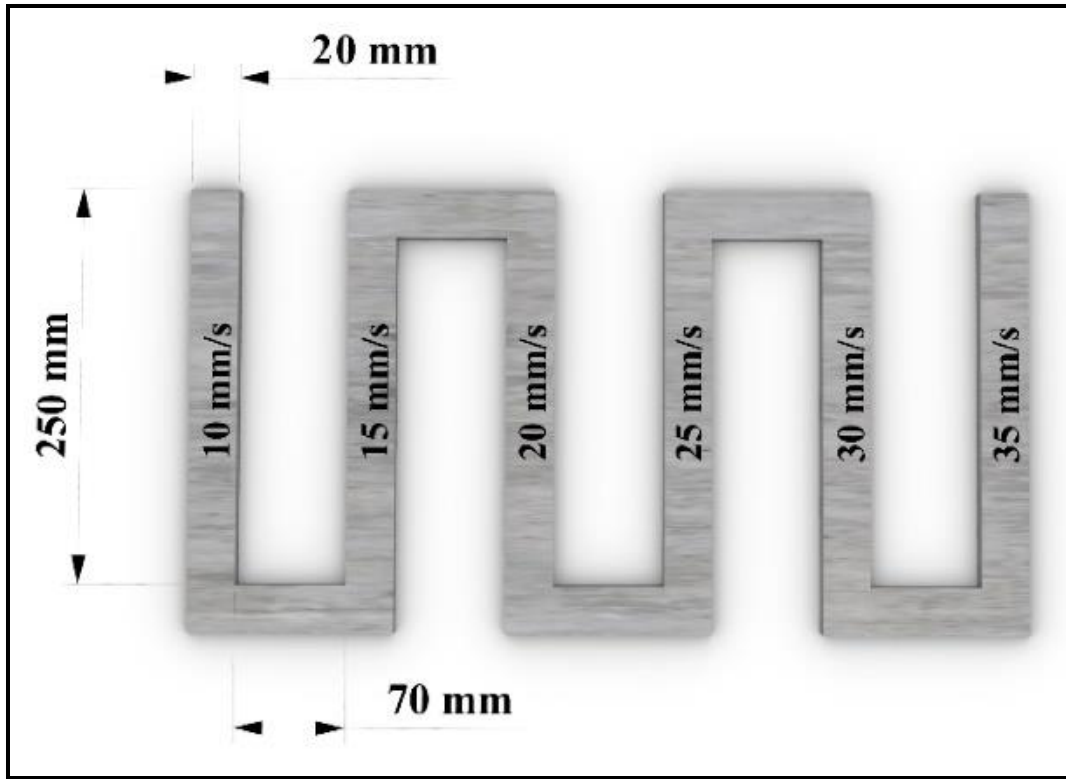


Figure 5-7: Example of the extrudability test printing path for different printing speeds [102]

### 5.3.9.2 Buildability Tests

Buildability assesses the soil mix's ability to form stable layers without collapsing or deforming. This test involves printing multiple layers of the soil mix and evaluating the structural integrity of the printed object. The buildability evaluation was performed by printing a 20 mm x 300 mm wall where the maximum layer height that was printed before failure was recorded. A schematic representation of the buildability test setup is shown in Figure 5-8.

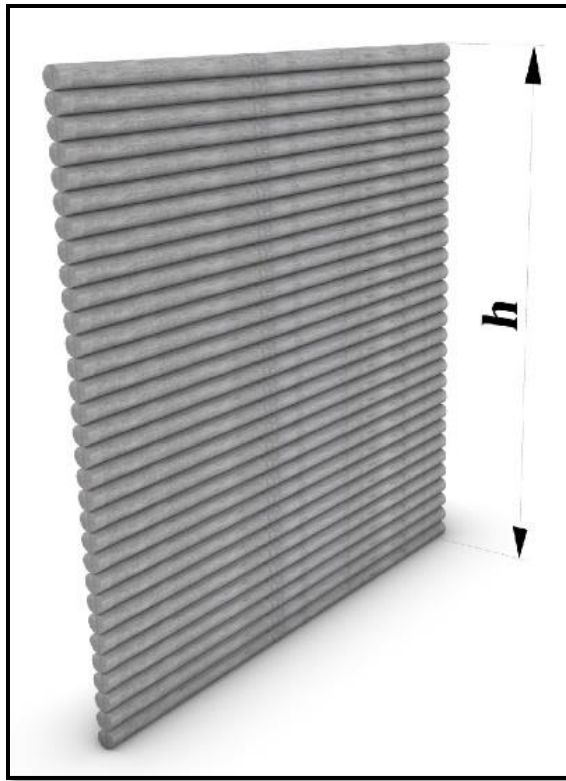


Figure 5-8: The extrudability test printing path for different printing speeds [102]

### 5.3.9.3 Mechanical Properties of 3D Printed Specimens

Flexure tests on the 3D-printed samples were conducted to measure the modulus of rupture (MOR). ASTM C293 [103] was used as a guide for the soil-printed specimens. Five specimen samples were initially printed at 200 mm x 40 mm x 40 mm and, after printing, while still wet, were cut down to 160 mm x 40 mm x 40 mm to eliminate any discrepancies in shape that could have occurred during the printing process and attain the best rectangular shape as described in the specifications. The specimens were then cured under laboratory ambient conditions, with an average temperature of 73°F (23°C)  $\pm$  2° and an average relative humidity of 16%  $\pm$  2%. The samples were supported on the two endpoints during testing as shown in Figure 5-9: Flexure test. The loading was applied in the middle of the span at a rate of 0.1 mm/min. The MoR was calculated according to Equation 3.

Equation 3: Modulus of Rupture

$$\sigma = \frac{3Pl}{2bd^2}$$

Where,

P = Axial load applied on the prism specimen

l = Length

b = breadth of specimen

d = depth (height) of the specimen

$\sigma$  = modulus of rupture



Figure 5-9: Flexure test set up

### 5.3.10 3D Printability of Soil Samples on a Larger Scale

As material mix design research was being conducted in the Dana C. Wood Materials and Structures lab at UNM, a group from the UNM Computer Science Department was concurrently working on small-scale ceramic clay 3DP utilizing a software they developed called WeaveSlicer [104]. WeaveSlicer optimizes 3DP with clay by implementing an oscillating toolpath that keeps the wall thickness of the prints constant, as seen in Figure 5-10 [104]. The constant wall thickness is generated by the amplitude of the oscillation, which is determined by the form's overhang angle, as seen in [104]. The team was interested in collaborating in an interdisciplinary approach so the WeaveSlicer code could be tested at a larger scale, and we in turn, could test our selected soil mix's ability to be printed with this new approach. The software is an open-source software library that can be used in the Grasshopper Rhino [105] program environment. For the preliminary 3DSP, a g-code for a 1-foot diameter dome – the best shape that resembles a horno – was created.

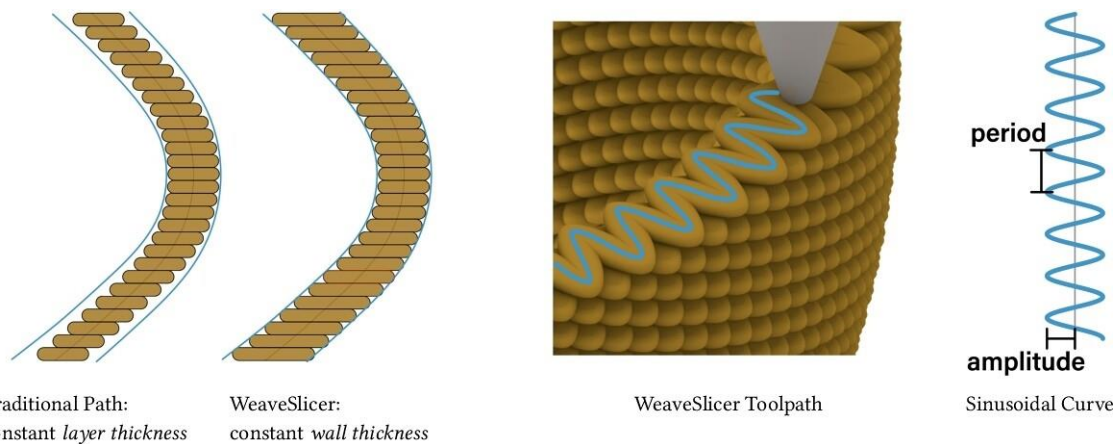


Figure 5-10: Cross-sectional views of a 3D printed vessel with a traditional 3D printing toolpath in which the width of each layer is constant (Left) and a toolpath generated by WeaveSlicer in which the width of the vessel wall is constant (Center-left). A view of a WeaveSlicer vessel print (Center-right). A sinusoidal curve with period and amplitude shown (Right) [104]

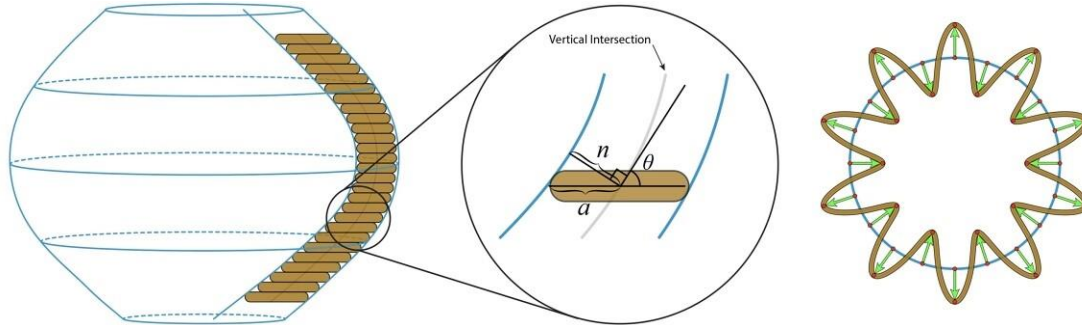


Figure 5-11: Left: Cross section of a wall with a constant width, generated by WeaveSlicer. Middle: Calculation of variable amplitude used in WeaveSlicer. Right: A top -down view of how the sinusoidal toolpath is constructed

The first large-scale 3DSP was conducted in one day. Mix ID S50 (50% S, 50% CS), with CS max aggregate size No. 4, was initially chosen due to the minimal shrinkage and compressive strength results observed (which will be described further in the results section). The material parameters for the preliminary mix are described in Table 5-6. This mix did not advance to the printing stage due to the consistency of the mix being too sandy during the mixing phase of the large-scale batch. When only 10% of the water was added, from the desired 23%, established from the traditional consistency test, it was evident that the material was not exhibiting enough cohesiveness, as shown in Figure 5-8b.

Table 5-6: Preliminary Material Parameters (Mix ID S50)

Plain Belén Soil, S, (g)	15,000
Concrete Sand, CS, (g)	15,000
Water Content (%)	10
Water (ml)	3,000



(a)



(b)

Figure 5-8: a) Mixing dry ingredients; b) Preliminary material consistency test on Mix ID S50

During the mixing phase, it was determined that a 2:1 ratio of S to CS would be a good consistency. This decision was based on the shrinkage and compression results in addition to the traditional consistency test. This new mix was between mix ID S75 and mix ID S50 so it was named mix ID S67, which correlates with the 2:1 composition of the S to CS percentage (CS max aggregate was No. 4). An additional 15,000 g of S material was added to the mix and water was measured and slowly added as the material was mixed with a hoe and by hand in the wheelbarrow. When the water added reached 20%, the mix was inspected for texture and cohesiveness as seen in Figure 5-12. The material was then tested with the penetrometer and noted in the material parameters as described in Table 5-7. Initial G-code printing parameters were set as described in Table 5-8.



Figure 5-12: Material consistency test for a large-scale batch of Mix ID S67 soil

Table 5-7: Material Parameters (Mix S67) ---- Test 1

Plain Belén Soil, S	30,000 g
Concrete Sand, CS	15,000 g
Water Content	20 %
Water	9000 ml
Hardness	0.36 kg/cm <sup>2</sup>

Table 5-8: G-code Printing Parameters (Mix S67) - Test 1

Nozzle size	15 mm
Layer height	7.5 mm
Period	20 mm
Amplitude (half of wall width)	30 mm
Extrude rate	0.5 mm/mm

Speed	500 mm/min.
-------	-------------

While conducting the initial test print with Mix S67 it was determined that the print was too dense, the period was too small, and the layer height was too small, see Figure 5-13. The material was also becoming stuck and clogged in the auger and 15 mm size nozzle. The CS max aggregate size of No. 4 sieve may have been too large for the nozzle.



Figure 5-13: (Mix 2.5) 3DSP: Test 1

Keeping the material parameters the same, see Table 5-9. The printing parameters were adjusted, as shown in Table 5-10. This test will be called Test 1.1. The nozzle size was increased to 20 mm, layer height increased to 13 mm, period increased to 40 mm, and speed increased to 750 mm/min. With the g-code adjustments made, the pumpability and extrudability of the material were enhanced without having to adjust the material mix parameters. Once the correct parameters were in place, the dome with a 1 ft. diameter was printed in 1 hour, as seen in Figure 5-14.

Table 5-9: Material Parameters (Mix S67) - Test 1.1

Plain Belén Soil, S	30,000 g
Concrete Sand, CS	15, 000 g

Water Content	20%
Water	9000 ml
Hardness	0.36 kg/cm <sup>2</sup>

Table 5-10: G-code Printing Parameters (Mix S67): Test 1.1

Nozzle size (mm)	20 mm
Layer height (mm)	13 mm
Period (mm)	40 mm
Amplitude (half of wall width) (mm)	30 mm
Extrude rate (mm/mm)	0.5 mm/mm
Speed (mm/min.)	750 mm/min.
Dome radius (mm)	75 mm

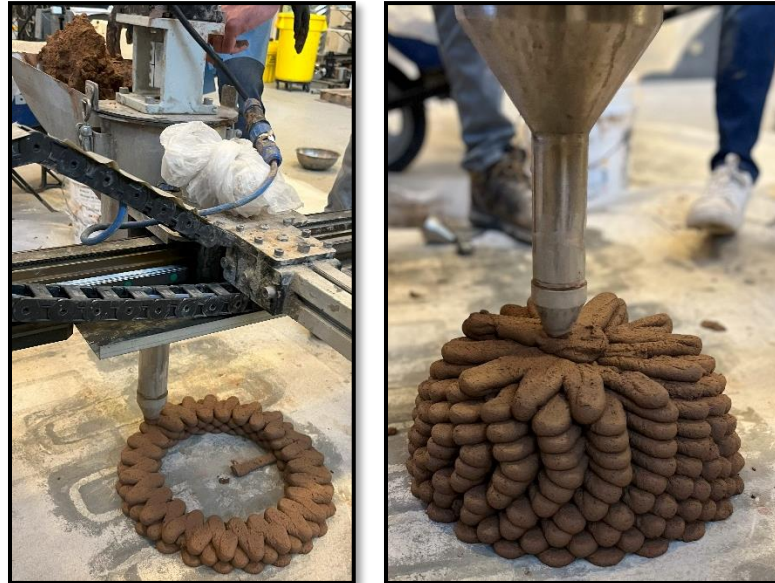


Figure 5-14: (Mix S67) 3DSP: Test 1.1

The second large-scale 3DSP was conducted in one day, Mix ID S67F2 (98% of 67% S, 33% CS, and 2% F) with CS max aggregate size No. 16 was chosen due to the minimal shrinkage and compressive strength results observed (which will be described further in the results section). The material was weighed in three batches (20,000g each) and was required to print a 2-foot

diameter dome. The dry material was measured according to weight, and the ingredients were mixed in a standard-size wheelbarrow. With a hoe as seen in Figure 5-15a. Water, determined from the traditional consistency test, was slowly added as the material was mixed with a hoe and by hand. Once the material reached the optimum moisture content, determined from the consistency test, the feel and hardness were evaluated with the penetrometer. The material was still too hard, measuring  $60\text{kg}/\text{cm}^2$ , so more water was measured and added to the mix (27%) until the consistency of the material could be easily squeezed through the fingers, as seen in Figure 5-15b and hardness measured  $.48\text{ kg}/\text{cm}^2$ , for the first large-scale batch. For the second and third batches, the water required was 25.5%, and hardness was measured at  $.39\text{ kg}/\text{cm}^2$ . The material parameters are described in **Error! Reference source not found.**, and the G-code. The printing parameters utilized were enhanced to accommodate the larger diameter size dome and to overcome some of the issues encountered with the first print, such as cracking due to large periods and amplitudes which are described in Table 5-12. Once the correct parameters were in place, the 2-foot diameter dome was printed in approximately 2 hours as seen in Figure 5-16.

Table 5-11: Material parameters for Mix ID S67F2 – Test 2

Total weight of soil, sand, fiber	20,000 g
Plain Belén Soil, S	13,131 g
Concrete Sand, CS	6,468 g
Fiber	2.0%
Water Content	25.5 —%— 27% %
Water	5100 – 5400 ml
Hardness	.48 and $0.39\text{ kg}/\text{cm}^2$

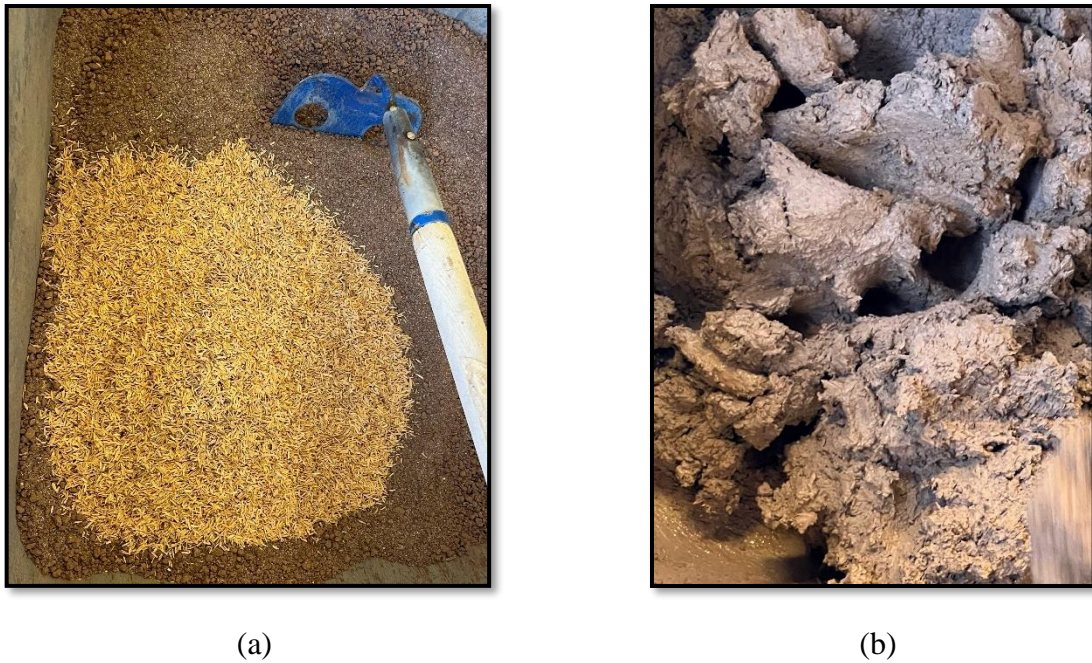


Figure 5-15: a) Mixing the dry ingredients; b) Material consistency test for a large-scale batch of Mix ID S67F2 soil

Table 5-12: Printing parameters for Mix ID S67F2 – Test 2

Nozzle size (mm)	20 mm
Layer height (mm)	12 mm
Period (mm)	30 mm
Amplitude (half of wall width) (mm)	30 mm
G-code Extrude rate	0.2 mm/mm
G-code speed	1000 mm/min.
Printer Extrude rate (mm/mm)	0.2 -.45 rounds/second
Printer Speed (mm/min.)	40 mm/s
Dome radius (mm)	150 mm



Figure 5-16: (Mix S67F2) 3DSP: Test 2

## 5.4 Results and Discussion

### 5.4.1 Traditional Consistency Examination of Mixes

In this section, the results of the traditional consistency test performed on the first set of mixes with S and CS (max aggregate size No. 4)4 used in the preliminary 3DSP of the 1-foot diameter dome and the second set of mixes with S, CS (max aggregate size No. 16), and F used in the second print of the 2-foot diameter dome will be discussed.

It was determined that the optimum consistency of a soil material could be variable depending on the batch size. This could be due to the amount of clay present, the amount of water added at a time, the amount of time the water was allowed to soak, the amount of time elapsed during mixing, the ambient temperature conditions, and the mixing procedure (kitchen aid vs hand mixing or with a hoe). It was found that determining the LL on 250g of material, as described in ASTM D4318 standards [69], was a good starting point for the baseline of assessing the optimum water content. Once the LL was established, the traditional consistency test could be conducted on

500g of material, beginning with a water content well below the LL and slowly adding measured-out water until the material was able to roll into a ball, as described in 5.3.3.

Comments on the consistency of the first set of mixes are described in the last column of Table 5-13, and pictures of the ball and sausage tests performed on the first set of mixes are shown in Figure 5-17. Note that the LL for Mix ID S67 was not conducted prior to the traditional consistency test, this mix was created during the first print and since the traditional consistency test showed to be a more accurate way of determining the optimum water content, it was decided that the LL was not necessary.

Table 5-13: Traditional consistency test comments on the first set of soil mixes with S and CS (max aggregate size No. 4)

Mix ID	Plain (Belén) Soil (S)	Concrete Sand (CS)	Clay/Silt content (%)	Liquid Limit (%)	Water /(S+CS)	Traditional Consistency Test Comments
S100	100	0	61.39	36.12	36.00	Thick but smooth and creamy, sticky, slippery, similar to peanut butter
S75	75	25	46.67	35.5	35.5	Very sticky, slurry, and slumpy. Not able to roll into a ball or sausage
S67	67	33	41.89	-	20.00	Thick but smooth, semi-sticky, semi-grainy, semi-slippy feel
S50	50	50	31.61	35.37	23.00	More manageable, medium sandy, less sticky, medium-grainy, less slippery
S25	25	75	16.17	25.03	16.00	Very crumbly, very sandy, slumpy but able to cohere into a ball

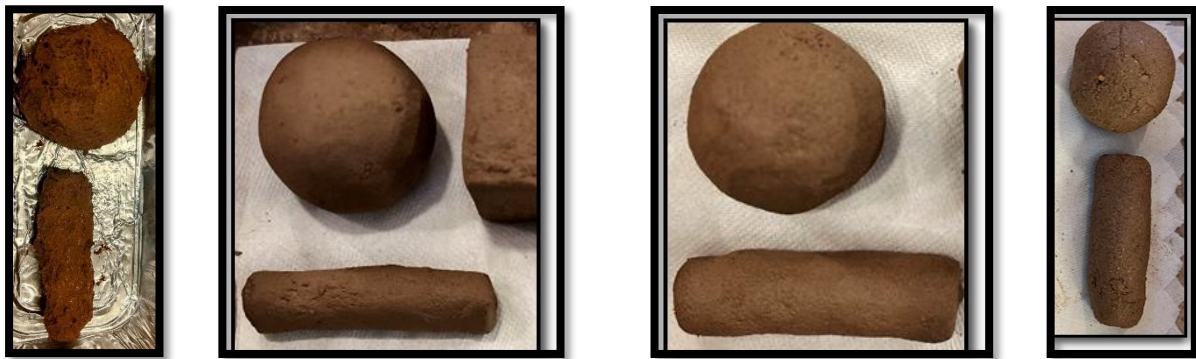


Figure 5-17: Water content determination according to the consistency test (a) S75 with 35.5% water content; (b) S75 with 32% water content; (c) S50 with 23% water content; (d) S25 with 16% water content

Comments on the consistency of the second set of mixes were very similar due to the mix (S67) being consistent in terms of S and CS and only the fiber amount being adjusted from .5- 2%. The amount of fiber added did not seem to affect the consistency of the mix. Four out of the five mixes of fiber required 20% water utilizing the traditional consistency test. Only one mix required .5% more water than the rest for the mix, which contained 2% fiber as described in Table 5-14.

Table 5-14: Traditional consistency test comments on the second set of mixes with S, CS (max aggregate size No.16), and F

Mix ID	Plain (Belén) Soil (S)	Concrete Sand (CS)	Total % of (S+CS)	Clay/Silt content	Fiber Content	Water /(S+CS)	Traditional Consistency Test Comments
S67-F0	.67	.33	100	45.87	0	22	Thick but smooth, semi-sticky, semi-grainy, semi-slippery feel
S67-F0.5	.67	.33	99.5	45.64	.5	22	Thick but smooth, semi-sticky, semi-grainy, semi-slippery feel
S67-F1.0	.67	.33	99	45.41	1.0	22	Thick but smooth, semi-sticky, semi-grainy, semi-slippery feel
S67-F1.5	.67	.33	98.5	45.19	1.5	22	Thick but smooth, semi-sticky, semi-grainy, semi-slippery feel

S67-F2.0	.67	.33	98	44.95	2.0	22.5	Thick but smooth, semi-sticky, semi- grainy, semi-slippery feel
----------	-----	-----	----	-------	-----	------	--

## 5.4.2 Soil Mix Design

This section presents the compressive strength and shrinkage measurements of cast soil samples. The tests aimed to determine the optimal substitution of S with CS in the first set of mixes, followed by identifying the necessary content of natural fibers based on strength and shrinkage characteristics for 3D printing applications in the second set of mixes.

### 5.4.2.1 Optimizing Soil Mix Design: Substituting Local Soil with Concrete Sand

Figure 5-18 illustrates the compressive strength of the first set of soil mixes with varying replacements of S by CS. Mix S100, which had the highest (traditional consistency) water content at 36%, exhibited the overall highest 28-day compressive strength at 939.50 psi. As evident, increasing the replacement of S with CS led to a reduction in strength at both time points and water demand, with the lowest strength observed, in 28 days, in the S25 mix (75% CS), resulting at 458.3 psi in 28 days, an overall 28-day decrease of 51.2% from the S100 mix. Moreover, decreasing the S content diminished strength gain within each individual mix from 7 to 28 days; S100 showed a significant 94.3% increase, whereas S25 experienced a marginal 2% decrease in compressive strength. This outcome suggests that reducing the high clay local soil content by substituting it with CS may impair soil mixes' strength development and gain over time, as the clay's bonding ability improves with extended drying periods.

Additionally, as noted earlier, each mix's water content was tailored based on the traditional consistency test results to emphasize the significance of water content adjustment. For the S75 mix, the compressive strength was evaluated at both the LL (35.5%) and adjusted traditional

consistency water content (32%). Notably, reducing the water content from 35.5% to 32% within the same S75 mix resulted in improved compressive strength of the material (28% increase at 7 days and 13.3% at 28 days). Therefore, employing the correct technique to determine the appropriate water content for each soil mix is crucial in engineering soil properties.

All the mixes generally achieved the minimum compressive strength requirement of 300 psi. Previous studies [47] indicate that incorporating materials like lime or straw fiber may reduce strength while enhancing shrinkage properties.

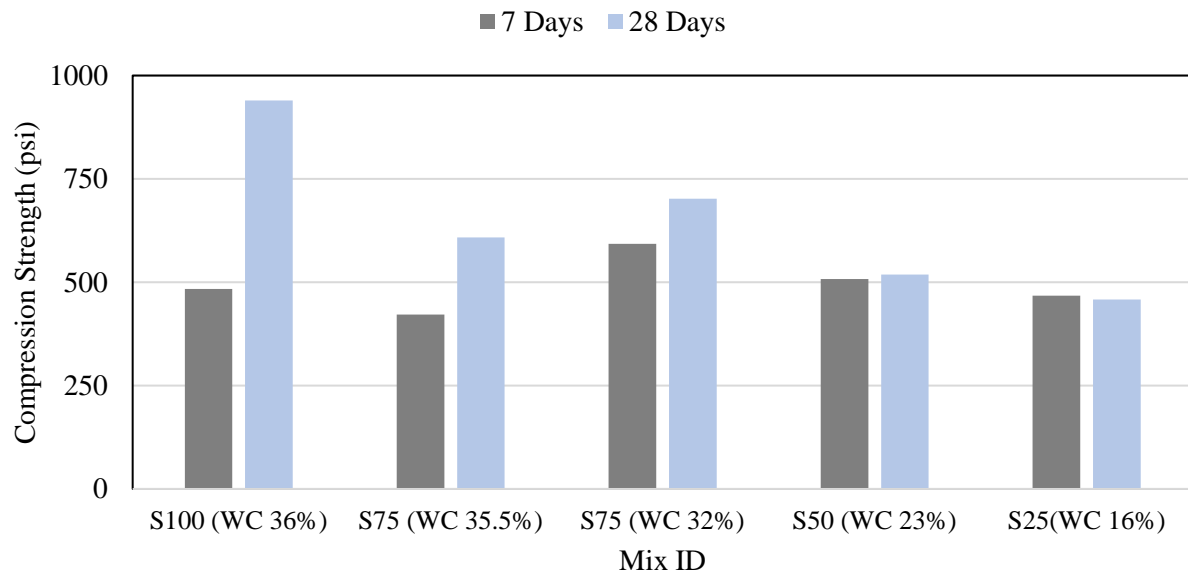


Figure 5-18: Compressive strength results of S & CS mixes (Max aggregate size No. 4)

Figure 5-19 illustrates the linear shrinkage for the first set of mixes with varying substitutions of S by CS (max aggregate size No. 4). As expected, decreasing the amount of S resulted in reduced linear shrinkage. XRD analysis indicated the presence of high swelling clay, i.e., montmorillonite is a contributing factor to volume instability in soil mixes, as evidenced by the 12.33% shrinkage observed for S100, and is also consistent with the high compressive strength findings. As CS content increased from S100 to S25, linear shrinkage decreased from 12.33% to 1.12% at 7 days, a difference in reduction of 11.23%. However, the 28-day strength of the soil

mixes decreased by 51.2% from S100 to S25, underscoring the need for careful optimization of soil replacement to maintain strength while reducing shrinkage. It's important to note that although S25 showed the least amount of shrinkage (1.12%), it was prone to slumping, as observed in the traditional consistency test, and will more than likely lack the strength to maintain its shape under the pressure exerted by the upper layer filaments in 3D printing applications. Therefore, achieving lower shrinkage or acceptable strength alone won't render this mix suitable for 3D printing.

Linear shrinkage of all soil mixes plateaued after 7 days of drying,**Error! Reference source not found.** with Figure 5-20 illustrating crack growth on day 3 across the different sample mixes. As anticipated, S100 showed the most extensive cracking with wider widths, while S25 exhibited finer and thinner cracks, consistent with the measured shrinkage.

Additionally, shrinkage results for S75 were collected at two different water contents (LL of 35.5% and traditional consistency test of 32%). After 7 days of measurement, the linear shrinkage results for both mixes intersected at 11.36%. Although reducing the water content from 35.5% to 32%, within the same S75 mix resulted in improved compressive strength of the material (28% increase at 7 days and 13.3% at 28 days), it did not improve the linear shrinkage results; they remained the same.

In conclusion, the mechanical and dimensional stability results indicate that replacing S with CS requires careful optimization. However, these tests alone are insufficient for assessing printability. While higher CS content reduced shrinkage, it could also compromise strength, stability, and interlayer bonding in 3D printed structures. Although shrinkage values remain high, additional strategies, such as incorporating shrinkage mitigation additives like fiber, may be necessary to control large shrinkage. This is the case with Adobe and may also be correlated to producing a balanced 3DSP mixture.

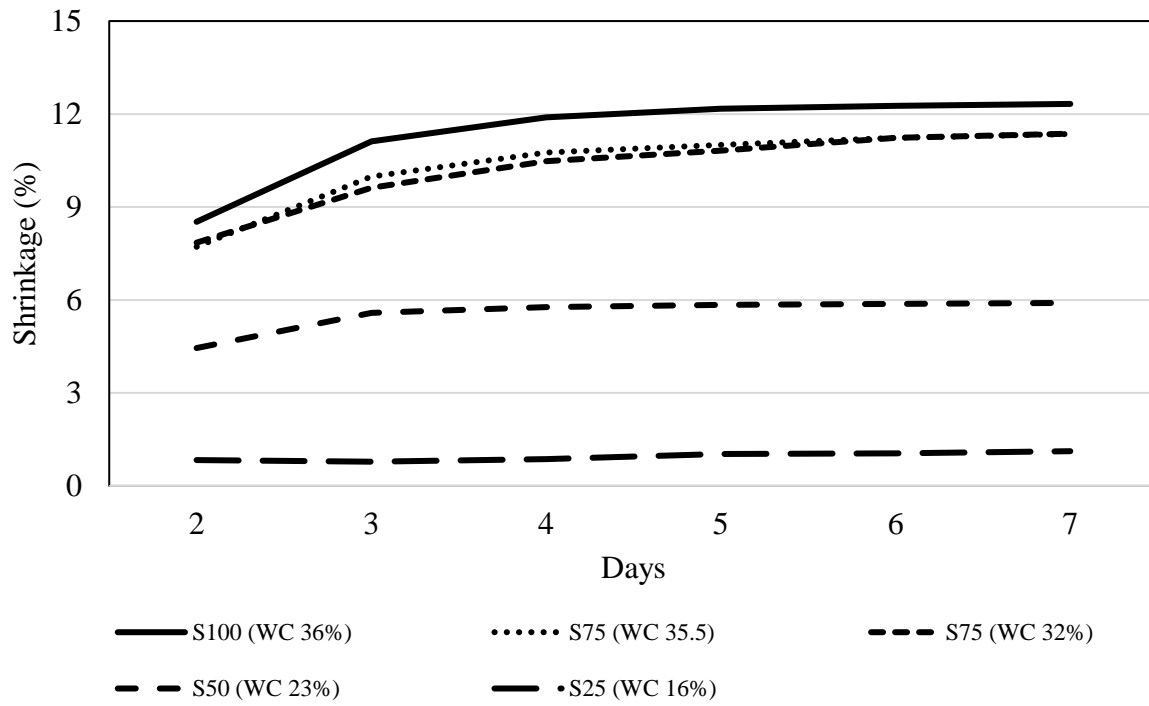


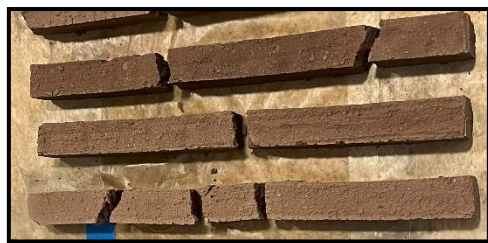
Figure 5-19. Linear shrinkage results of the first set of soil mix to optimize the S replacement by CS



S100 (WC 36%) at Day 3 age



S75 (WC 35.5%) at Day 3 age



S75 (WC 32%) at Day 3 age



S50 (WC 23%) at Day 3 age



S25 (WC 16%) at Day 3 age

Figure 5-20. Crack pattern formation in various soil mixes after 3 days of drying

#### 5.4.3 Optimizing Soil Mix Design: Including Natural Rice Hull Fibers

Based on the findings from the previous section and various trial 3D printability tests, it was determined that the optimal substitution of CS is a 2:1 ratio of S to CS (67% S, 33% CS with max aggregate size No.16) and will be referred to as mix ID S67F0 as the baseline mix with no fiber added for this set of mixes.) With the second set of mixes, this section further supports reducing shrinkage as sustainably as possible by adding rice hull fibers without compromising strength requirements of 300 psi, similar to S25 or flexure (MoR) requirements of 50 psi.

Figure 5-21 illustrates the compressive strength results of the second set of mixes with soil mix ID S67F0 as the baseline and shows how increasing percentages of fiber (.5-2%) are added. The results indicate that mix ID S67F0 had the highest overall 28-day compressive strength of 881.67 psi, and S67F2 showed the lowest overall 28-day compressive strength at 663.0 psi. Increasing the fiber from .5% to 2% resulted in a 24.8% decrease in strength over 28 days, but it still meets the minimum required compressive strength of 300 psi. by almost double. The addition of fiber also indicates that the increase in strength over 28 days is closer to the strength gained at 7 days. Mix ID S67F0 showed a 19.35% increase in strength from 7 to 28 days, whereas mix ID S67F2 exhibited a 7.5% increase. This may indicate that adding fiber may reduce the overall

strength but also assists in stabilizing the mix sooner. This can aid in the buildability aspect of printing. All mixes in the second set with added fiber generally met the minimum requirements of 300 psi.

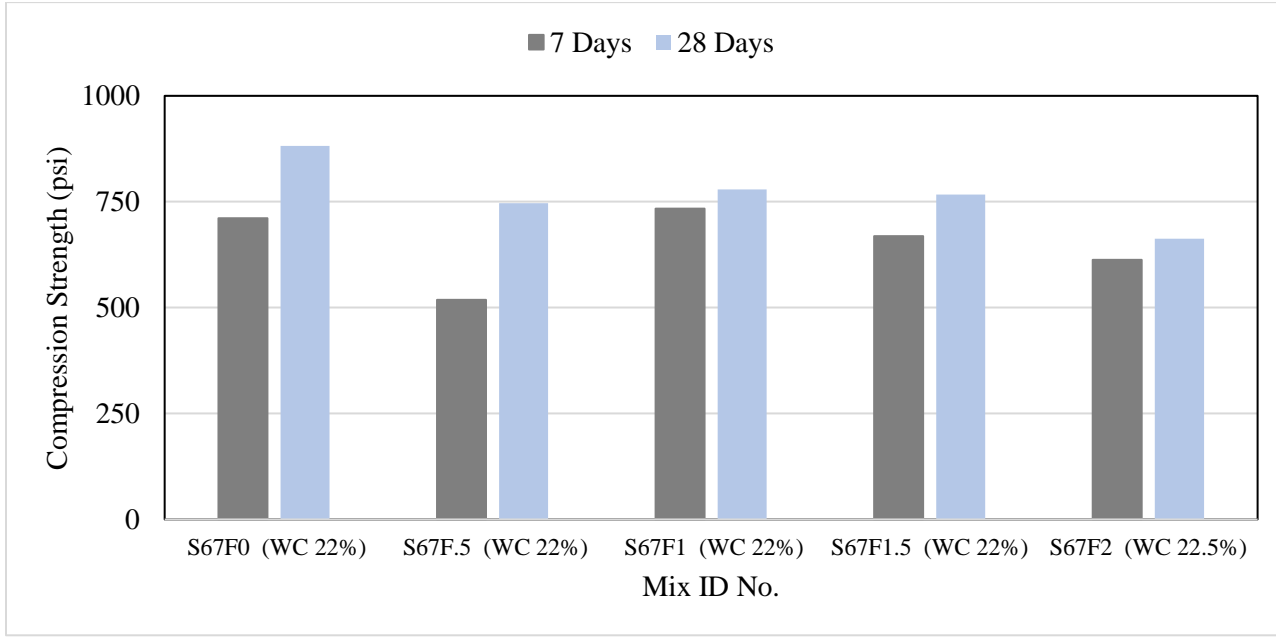


Figure 5-21: Compressive strength results of the second set of mixes with S, CS, F

Figure 5-22 illustrates the linear shrinkage of the second set of mixes with the fiber added over a 7-day period. Mix ID S67F0, which had no rice hull fiber, showed the greatest linear shrinkage after 7 days at 6.23%. Mix ID S67F2, which had the highest amount of fiber in this test, showed the least linear shrinkage after 7 days at 3.48%. These findings indicate that a 2% increase of rice hull fiber added to the S67 mix decreased the linear shrinkage by an overall 44% while still maintaining the required 300 psi compressive strength by almost double (663 psi). Figure 5-23 illustrates the reduced cracking and shrinkage observed in the shrinkage sample prisms on day 3.

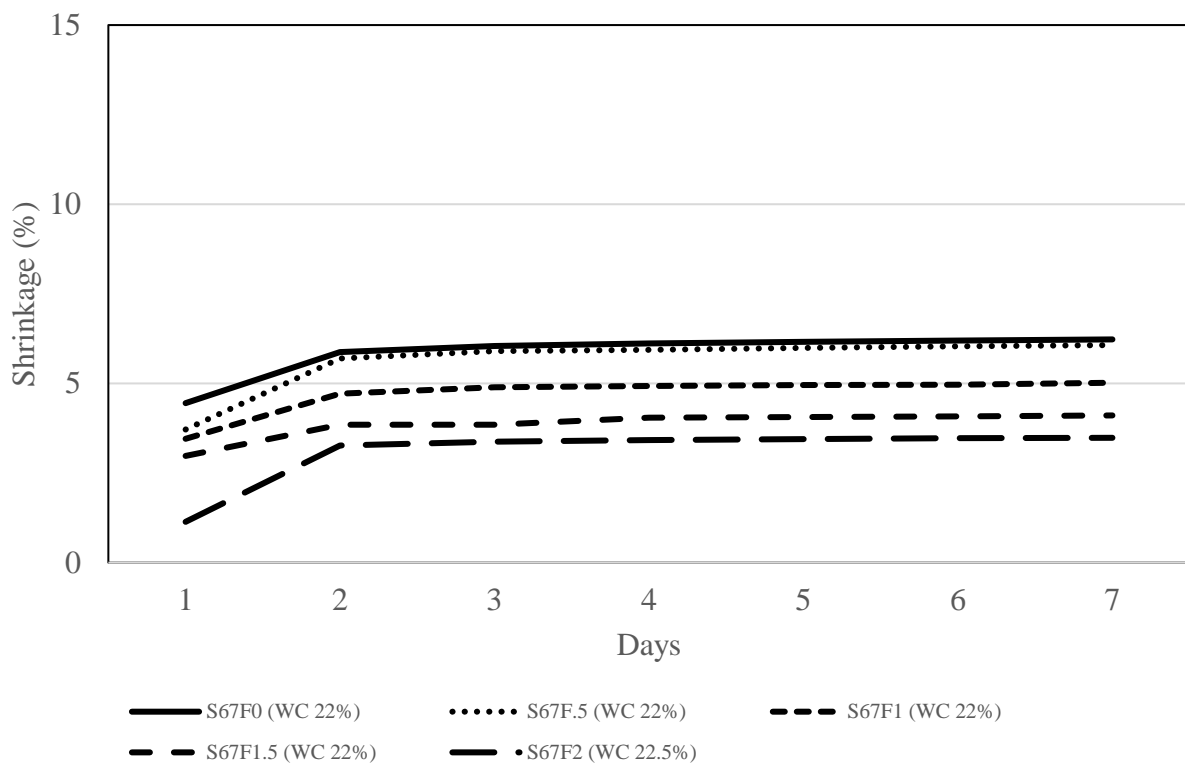
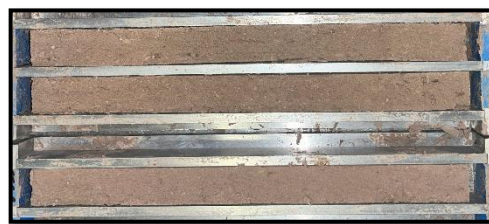


Figure 5-22: Linear shrinkage results of the second set of soil mixes to optimize the S67 with the addition of rice hull fiber



S67F0 (WC 22%) at Day 3 age



S67F.5 (WC 22%) at Day 3 age



S67F1 (WC 22%) at Day 3 age



S67F1.5 (WC 22%) at Day 3 age



S67F2 (WC 22.5%) at Day 3 age

Figure 5-23: Shrinkage samples of the second set of mixes with fiber added showing less cracks and shrinkage after 3 days of drying

In conclusion, the addition of fiber has been confirmed to decrease the linear shrinkage of the S67 soil mix from 6.23% to 3.48% without jeopardizing the compression strength below the required 300 psi. Mix S67F2 was chosen to proceed to the next set of mechanical 3D printing tests towards printing a 2-foot diameter dome.

#### **5.4.4 Printability Test Results**

Printability tests were conducted on mix ID S67F2, indicating the least shrinkage, acceptable compressive strength, and acceptable textural consistency. The following test results will indicate the material's ability to be 3D printed by testing the extrudability, buildability, and flexural strength.

##### **5.4.4.1 Extrudability**

Figure 5-24a illustrates the extrudability zigzag test results where the S67F2 soil mix was extruded through a 20 mm nozzle, with a printing width of 20 mm, constant extrusion speed of 0.15 rounds/second and variable printing speeds. This test indicates at what printing speed the material can be printed without skipping, over-extruding, or under-extruding the desired width. The widths of the zigzags were visually inspected for consistency and measured based on which printing speed produced the most precise intended width of 20 mm. The 10 mm/s path showed over-extrusion, indicating that the printing speed was too slow. The skipping on the 30 mm/s and

35 mm/s paths indicates the printing speed is too fast. The 20 mm/s and 25 mm/s indicate slight under-extrusion. From visual inspection and measurements, and based on the author's experience, the printing speed of 15 mm/s was the most suitable for smooth extrudability and the closest printed path to the projected 20 mm width. Figure 5-24b shows the zigzag test results with the best indicated extrudability printing speed of 15 m/s throughout the entire print, showing constant width and extrudability. This test shows us that the S67F2 soil mix can be extruded consistently through the nozzle without clogging, breaking the flow, or causing cracks, and it can maintain dimensional accuracy for 3DSP.

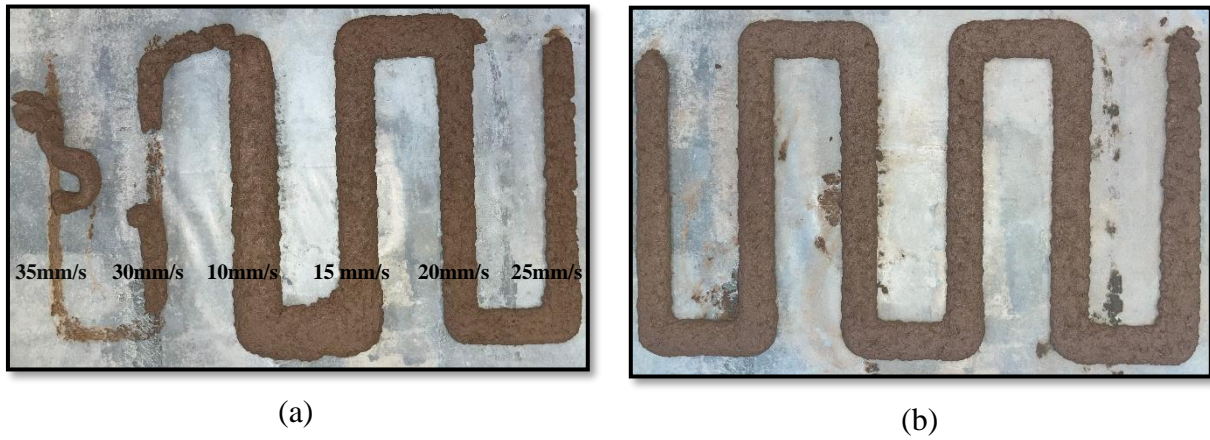


Figure 5-24: (a) Extrudability zigzag test with variable printing speeds; (b) Extrudability zigzag test with constant printing speed of 15 m/s

#### 5.4.4.2 Buildability

The buildability test results are illustrated in Figure 5-25 where the S67F2 mix was printed until failure at the 25<sup>th</sup> layer, indicating that the soil mix can sustain its weight and the subsequent layers without collapsing or deforming up to the 24th layer. Previous studies [49] had a maximum stacking layer of 18. Mix S67F2 has a maximum stacking layer of 24. These results are a good prediction that the mix will be a decent selection for 3D printing a 2-foot diameter dome.



Figure 5-25: (a) Buildability test prior to collapse; (b) Collapse of material at 25<sup>th</sup> layer

#### 5.4.4.3 Mechanical Properties

Figure 5-26 illustrates the flexure samples being printed from the S67F2 soil mix. The 5 samples were dried for 28 days, and the MoR test was conducted ASTM C293 [103]. Figure 5-27 shows that the average flexure strength for the soil mix is 189.24 psi (1.30MPa), which is almost 3 times the minimum requirement of 50 psi detailed by the NM Earthen building code [86]. This test verifies that the S67F2 soil mix can withstand flex (bending) forces up to 189.24 psi once dried.



Figure 5-26: 3DSP of mix ID S67F2 flexure samples

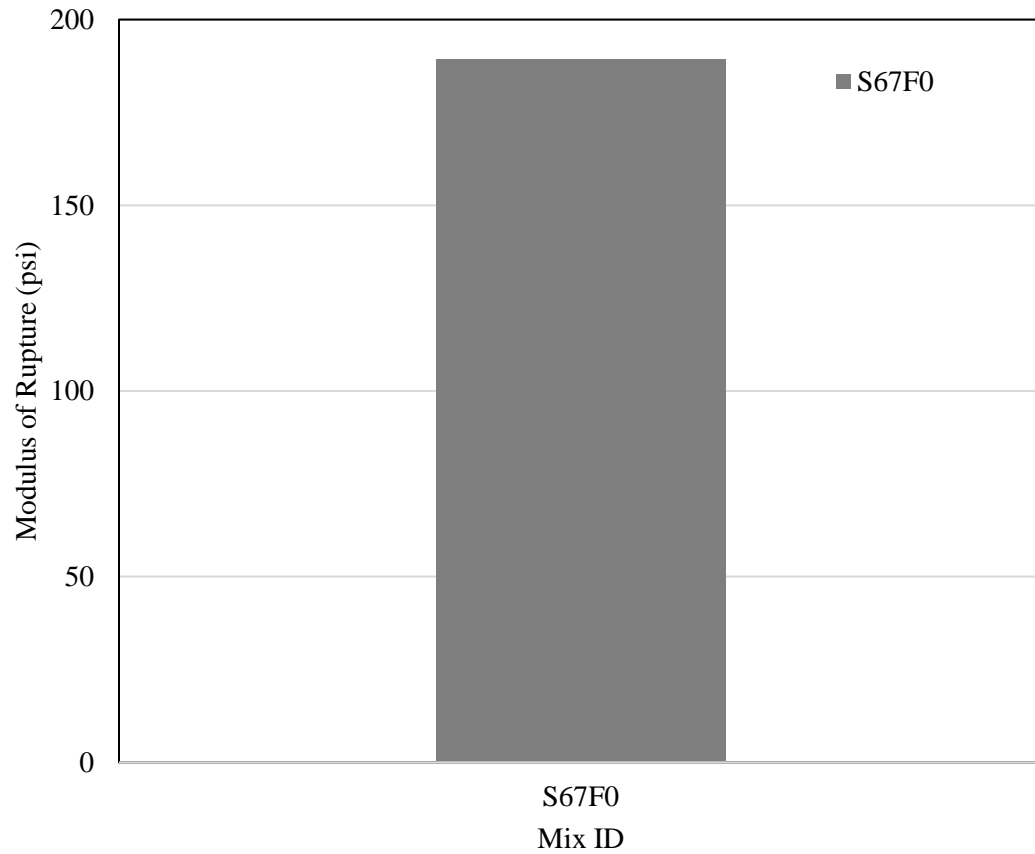


Figure 5-27: Modulus of rupture results for mix ID S67F2

## 5.4.5 Large Scale 3D printing

### 5.4.5.1 Results of Preliminary 3DSP (1-foot diameter dome)

After the 1-foot diameter dome was printed it was not covered and was allowed to dry in the ambient conditions of the laboratory, which had an average temperature of  $73^{\circ}\text{F}$  ( $23^{\circ}\text{C}$ )  $\pm 2^{\circ}$  and an average indoor humidity of  $16\% \pm 2\%$ . The 3DSP dome was visually inspected for 7 days to monitor the drying rate and if shrinkage cracks would occur. Day one showed minor cracks surfacing at the top of the dome, and the sample was still wet, as seen in Figure 5-28. On day two, a large crack up the side of the dome in between one of the periods was noticed; the sample was still wet, as seen in Figure 5-29. On day three, a large crack was still observed, and the sample looked partially dry, as seen in Figure 5-30. On day 5, a second crack on the opposite side of the dome was observed; the sample was approximately 80% dry, as seen in Figure 5-31. On day 7, no new cracks were observed, and the sample was approximately 90% dry, as seen in Figure 5-32. On day 10 the sample looked completely dry, and it was flipped over to examine if the cracks had penetrated all the way through the wall thickness. As seen in Figure 5-33, the two large cracks are seen to penetrate the wall thickness.



Figure 5-28: Day 1 results (Mix S67, WC 20%)



Figure 5-29: Day 2 results (Mix S67, WC 20%)

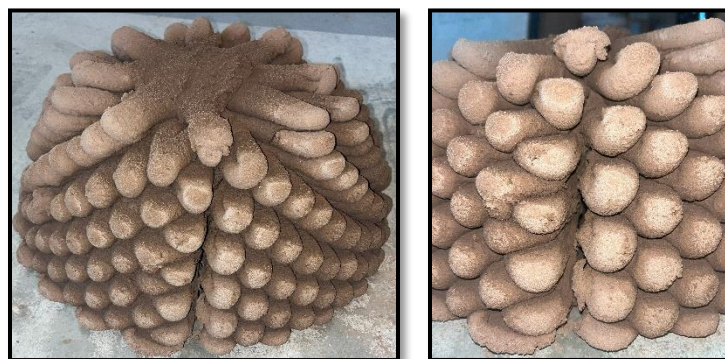


Figure 5-30: Day 3 results (Mix S67, WC 20%)



Figure 5-31: Day 5 (Mix S67, WC 20%)



Figure 5-32: Day 7 (Mix S67, WC 20%)

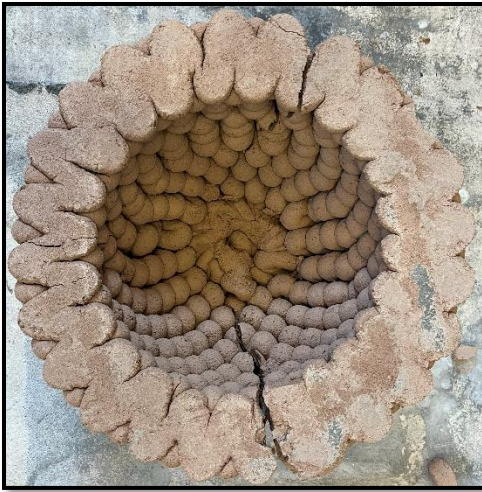


Figure 5-33: Day 10 (Mix S67, WC 20%)

#### **5.4.5.2 Discussion of Preliminary 3DSP (1-foot diameter dome)**

During the first printing session, one of the major notes that needed to be addressed was the material getting stuck in the auger and not flowing through the system. This could be due to the max aggregate size of No. 4 in the CS being too large, the printing hopper not having a pressurized pump to push the material though instead of the material being hand fed and gravity pushing it downwards, the nozzle being too small, and the consistency of the material being too thick. It was decided that these issues would be addressed by re-evaluating the changing of the g-code parameters by reducing the period and amplitude, improving the soil mixture by reducing the max aggregate size in the CS to No. 16, and adding fiber to the mix.

#### **5.4.5.3 Results of Secondary 3DSP (2-foot diameter dome)**

After the 2-foot diameter dome was printed, it was covered with plastic to ensure that the dome dried slowly to minimize the chance of cracks occurring. Attempts were made to observe the shrinkage by measuring the circumference at the base of the dome and over the middle top arc of the dome with a string after it was printed, as seen in Figure 5-34b. Still, it was difficult to know exactly where the string was placed each time due to the irregularities of the surface. After printing, the circumference at the base of the dome was measured at 2044.7 mm. The vertical arc over the

top of the dome, as shown in Figure 5-34b, was measured at 1022.35 mm after printing. The dome was visually inspected and observed for cracks for 10 days. On day 3 of drying, the arc over the top of the dome shrunk 15.86 mm and was measured at 1006.49 mm, a 1.5% reduction, as seen in Figure 5-35c. The base circumference did not appear to shrink, as seen in Figure 5-35d. On day 7 a crack was noticed along the side of the dome, as seen in Figure 5-36b. The measurement over the top of the dome remained at 1006.49 mm, and the base circumference did not appear to shrink either; it remained at 2044.7 mm. On day 10, an additional crack was noticed. The widths of the cracks were noted as 3.78 mm wide and 11.31 mm wide, as seen in Figure 5-36c. The arc over the top of the dome shrunk 32.55 mm and was now measuring at 989.94 mm, a 3.2% reduction. The dome remained covered with plastic until it seemed 90% dry on the 13<sup>th</sup> day when it was removed. On the 13th day, the widths of the cracks were noted. The first crack observed was measured at 4.37mm wide and 147 mm long. The second crack observed measured 11.74 mm wide and 238 mm long. The measurements for the arc over the dome were randomly taken on day 33 and measured at 939.8 mm, an overall reduction of 8%.



(a)



(b)

Figure 5-34: (a) Photo of mix S67F2 2-foot dia. dome after printing; (b) measuring arc over the top of the dome after printing



(a)



(b)



(c)



(d)

Figure 5-35: Mix ID S67F2 day 3 results (a) side of dome; (b) top of dome; (c) over the top arc string measurement; (d) base of dome circumference string measurement



(a)



(b)

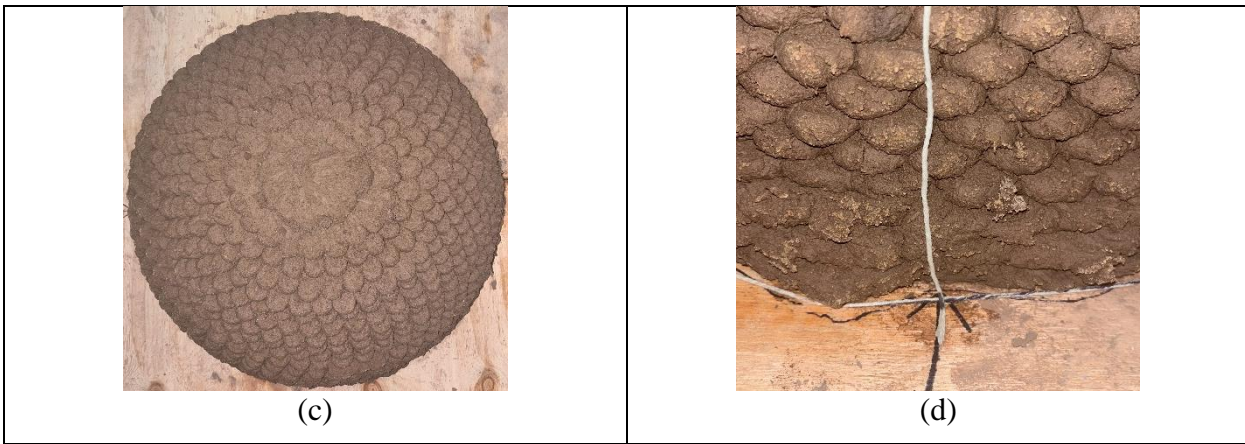


Figure 5-36: Mix ID S67F2 day 7 results (a) side of dome; (b) crack in the side of dome noticed; (c) top of dome; (d) over the top string measurement

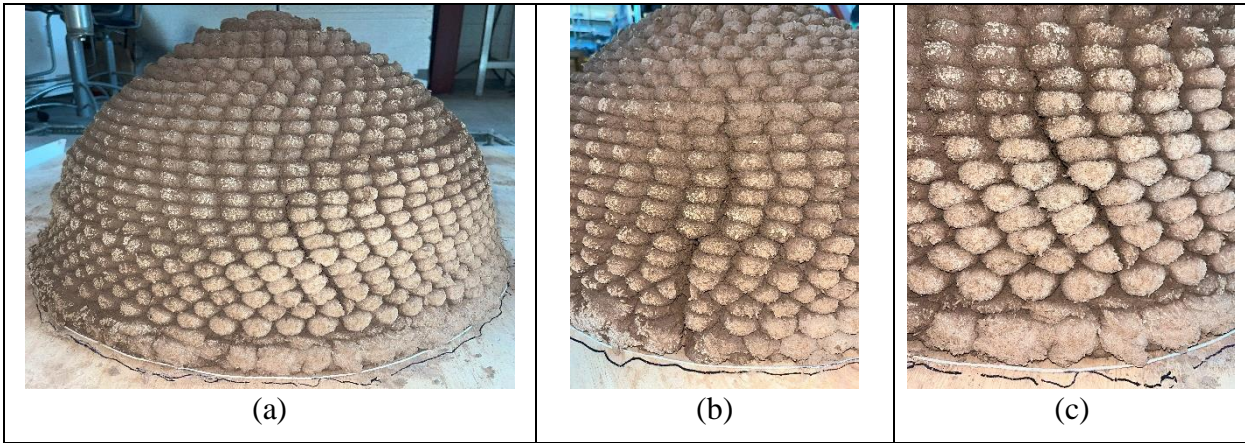


Figure 5-37: Mix ID: S67F2 day 10 results (a) side of the dome; (b) additional crack observed; (c) first crack observed

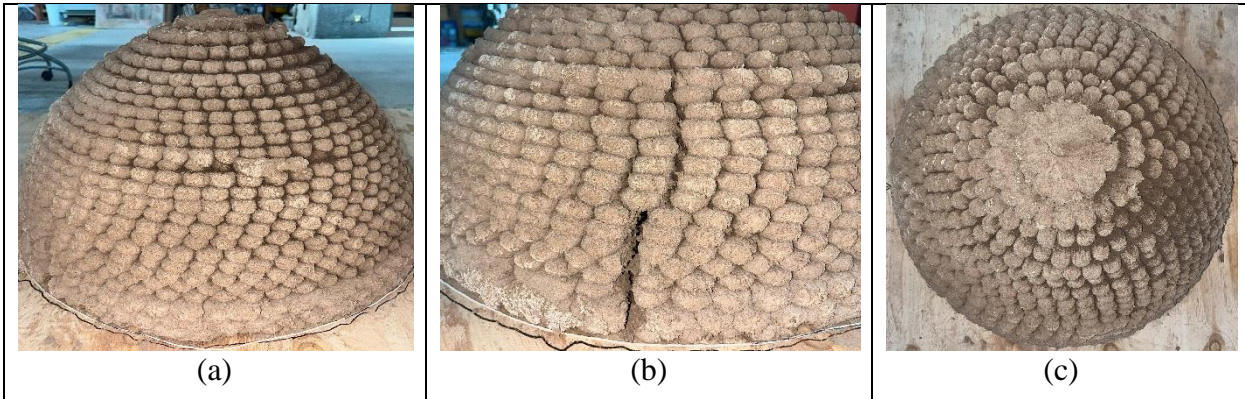


Figure 5-38: Mix ID S67F2 day 13 results (a) side of the dome; (b) second large crack observed; (c) top of the dome

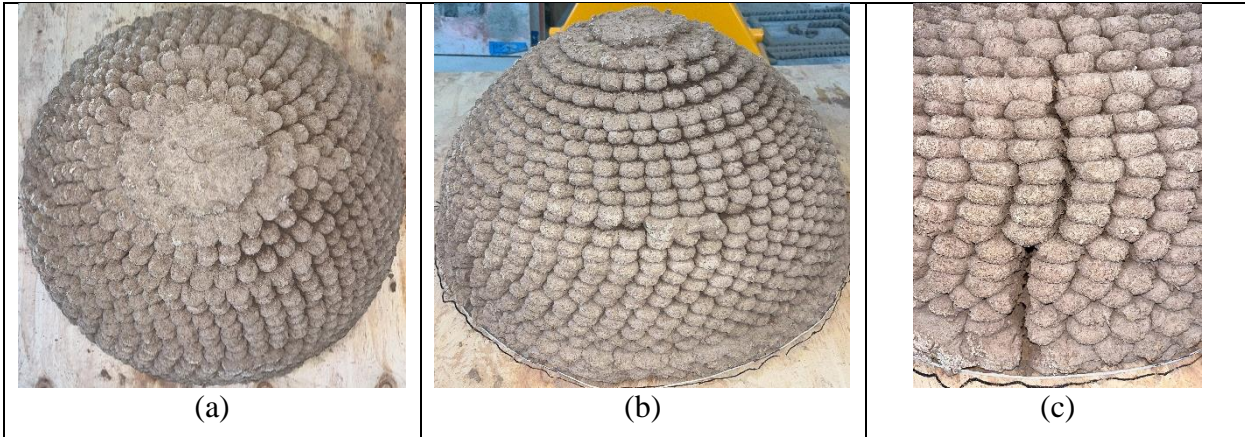


Figure 5-39: Mix ID S67F2 day 14 (a) top view of the dome; (b) side view of the dome; (c) second large crack observed

#### 5.4.5.4 Discussion of secondary 3DSP (2-foot diameter dome)

During the secondary printing process of the 2-foot diameter dome, one of the major notes that needs to be addressed is the mixing process for large-scale batches. Preparing and crushing plain soil, sifting concrete sand, and mixing 3 batches in a wheelbarrow to have enough material to print a 2-foot diameter dome was extremely labor intensive. The issue with the material getting stuck in the auger is still a problem and could potentially be resolved if we had a pressurized pump to feed the material into the hopper instead of relying on gravity to feed the material. Another way to facilitate this issue is to create a softer material without jeopardizing the minimum required compressive strength.

In conclusion, the 3DSP of the 2-foot diameter dome was successful except for two cracks that can most likely be mitigated by modifying the g-code design. An opening in the dome, similar to a traditional horno can assist in the dome drying evenly from the inside and the outside more consistently. The bottom of the dome is in tension while the top of the dome is in compression so an opening might alleviate some of those stress forces. Another option is to increase the fiber content and see if that will assist in reducing the shrinkage or add water reducers to help increase the plasticity, but additional shrinkage and compression tests would need to be conducted to verify.

# **Chapter 6**

## **6. Conclusions and Future Work**

This chapter's objective is to:

- i. Summarize this thesis
- ii. Draw conclusions
- iii. Suggest future research in this area

### **6.1 Summary**

This thesis investigates the use of a local earthen material mix, similar to adobe mixes used in NM, for 3DSP towards a community-based project of building a traditional horno. This study emphasizes reducing the linear shrinkage characteristics while maintaining the required compressive strength of 300 psi. Soil was gathered from Belén, NM and was characterized utilizing conventional and alternative traditional testing methods which provides a framework for future research detailing material collection, testing procedures, and printing parameters. The soil mixes' grain size distribution was improved with the addition of concrete sand which reduced the linear shrinkage from initial tests and was further improved by adding rice hull fibers and reducing the maximum aggregate size to a smaller size.

Chapter 3 examines the significance of soil particle size distribution and the appropriate tests necessary to conduct them. This study emphasized the need to conduct a wet sieve analysis on materials that show a high clay content that can be determined quickly from an alternative traditional shake jar test. Additionally, XRD analysis showed that the clay mineralogy present in the soil material contained swelling characteristics which can have an affect on additives. This is

issue is highlighted in chapter 4 where xanthan gum was added to the soil mix in an effort to improve the material compressive strength but due to the high clay content that possessed high swelling characteristics the study resulted in failed results, most likely due to a biner-to-binder problem. Chapter 5 highlights the addition of concrete sand to the soil mix, where linear shrinkage was decreased but when the material was tested on a 1-foot diameter dome, the structure cracked significantly. Modifications were made in lowering the max aggregate size in the concrete sand, adding rice hull fiber to the mix, and improving the g-code printing parameters. The results further decreased the linear shrinkage while maintaining the required compressive and flexure strengths. Although the printed 2-foot diameter structure proved to be pumpable, extrudable, and buildable there were still concerning shrinkage cracks that will need further investigation to mitigate.

Overall, this thesis not only advanced academic understanding but also raised consciousness, self-reflection, personal growth, and a local community bond. It nurtured connection to heritage, storytelling, and interdisciplinary and transdisciplinary relationships.

## **6.2 Major Findings**

Previous studies on 3D printing of local soil materials did not adequately measure the amount of finer particles (clay and silt) in the material resulting in higher shrinkage results and lower than required compressive strength, which could be due to the soil particle size distribution not being accurate. This study found that conducting a shake jar test followed by a wet sieve analysis of the soil material was an acceptable way to determine a more precise method to conduct for preparation of soil material for 3DSP. In addition, this study found that once an accurate measurement of fines was determined, a ratio of 2:1 of plain soil to concrete sand proved to be an acceptable proportion that proved to be printable. This study further discovered that utilizing this proportion and reducing the max aggregate size to sieve No.16 and adding 2%, by weight, of rice hull fiber improved the

mix further without affecting minimum compression and flexure requirements or printability, extrudability and buildability printing characteristics. A total reduction in 71.7% from the plain Belén soil was achieved.

### **6.3 Future Research**

The focus of this thesis was to produce a 3D printed traditional horno for the NACA community, although the 2-foot diameter dome fell slightly short of producing a functional horno, by not being able to print a 3-foot diameter structure with an opening, it did leave plenty of room for future development and research:

- This thesis leaves room for improvement in several aspects which include reanalyzing the soil mix to include a higher percentage of fiber and test how much fiber can be added before it affects the minimum required compression and flexure strengths.
- Deeper research on the quality properties of rice hull fiber
- Different fibers such as hemp and straw can be evaluated to determine if the shrinkage and compressive strengths are improved.
- Conducting a life cycle analysis can assess the sustainability aspects associated with using earthen material over cement for 3D printing or 3DSP over conventional home building with lumber.
- Additional traditional tests that are conducted on adobe such as water absorption and compression tests utilizing cast and printed samples, similar to adobe sizes, can assist in improving the 3DSP material.
- Different g-code geometries can be studied and tested to enhance the tension and compression forces that the printed structure experiences.

- Further mineralogy tests on the clay properties and more in-depth accounts of the amounts of swelling vs. non-swelling clay present can assist in determining parallels to shrinkage and compression results
- Print 3-foot diameter horno and gift to NACA for their outdoor Cook Shack

## Chapter 7

### 7. References

- [1] D. E. Williams, “Sustainable Design Ecology, Architecture, and Planning.” Accessed: Aug. 28, 2023. [Online]. Available: <https://acrobat.adobe.com/link/review?uri=urn%3Aaaid%3Ascds%3AUS%3A5a8f9647-a12b-4fe9-ba68-3133908d3c76>
- [2] T. Jojola, M. Shirly, and C. Begay, “Place Knowing - Introduction to Place Knowing.”
- [3] NACA Land Fam, A. Stone, M. Stone, and V. Gonzales, “Native American Community Academy (NACA) Partnership Guiding Principles.” Sep. 2023.
- [4] “Who We Are.” Accessed: May 02, 2024. [Online]. Available: [https://www.nacaschool.org/apps/pages/index.jsp?uREC\\_ID=1663943&type=d&pREC\\_ID=1813044](https://www.nacaschool.org/apps/pages/index.jsp?uREC_ID=1663943&type=d&pREC_ID=1813044)
- [5] “Land-Based Healing & Learning.” Accessed: May 02, 2024. [Online]. Available: [https://www.nacaschool.org/apps/pages/index.jsp?uREC\\_ID=1663962&type=d&pREC\\_ID=2166924](https://www.nacaschool.org/apps/pages/index.jsp?uREC_ID=1663962&type=d&pREC_ID=2166924)
- [6] “Our Educational Philosophy.” Accessed: May 02, 2024. [Online]. Available: [https://www.nacaschool.org/apps/pages/index.jsp?uREC\\_ID=1664046&type=d&pREC\\_ID=1813147](https://www.nacaschool.org/apps/pages/index.jsp?uREC_ID=1664046&type=d&pREC_ID=1813147)
- [7] NACA, “NACA Foundation Turnkey - Edible Garden Narrative Proposal.” Jan. 24, 2023.
- [8] A. Murphy, “The Wondrous Bread of the Pueblo Nations,” Eater. Accessed: May 26, 2024. [Online]. Available: <https://www.eater.com/2019/1/23/18183970/zuni-bread-pueblos-new-mexico>
- [9] L. C. Zeiher, *The Ecology of Architecture: A Complete Guide to Creating the Environmentally Conscious Building*. Whitney Library of Design, 1996. [Online]. Available: <https://books.google.com/books?id=c4ruAAAAMAAJ>
- [10] E. W. Smith and G. S. Austin, “Adobe, pressed-earth, and rammed-earth industries in New México,” *New México Bureau of Mines & Mineral Resources*, vol. Bulletin 127, 1989.
- [11] M. Moquin, “Ancient Solutions for Future Sustainability: Building With Adobe, Rammed Earth, and Mud,” *CIB TG 16, Sustainable Construction, Tampa, Florida, USA, November 6-9, 1994*, [Online]. Available: [https://www.irbnet.de/daten/iconda/CIB\\_DC24848.pdf](https://www.irbnet.de/daten/iconda/CIB_DC24848.pdf)
- [12] B. Fletcher and D. Cruickshank, *Sir Banister Fletcher's a History of Architecture*. Architectural Press, 1996. [Online]. Available: <https://books.google.com/books?id=Gt1jTpXATHwC>
- [13] F. U. C. Cornerstones Community Partnership, *Adobe Conservation: A Preservation Handbook*. Sunstone Press, 2006. [Online]. Available: <https://www.cstones.org/books-and-manual/adobe-conservation-a-preservation-handbook-media-mail-shipping-lmm24>
- [14] L.-P. Dana and R. Anderson, “Taos Pueblo: an indigenous community holding on to Promethean values,” *Journal of Enterprising Communities: People and Places in the Global Economy*, vol. 1, Oct. 2007, doi: 10.1108/17506200710833827.
- [15] B. Oswald, “Pueblo Bonito, Chaco Canyon,” World History Encyclopedia. [Online]. Available: <https://www.worldhistory.org/image/8964/pueblo-bonito-chaco-canyon/>
- [16] P. Doat, C. Norton, A. Hays, H. Houben, S. Matuk, and F. Vitoux, *Building with Earth. Mud Village Society*, 1991. [Online]. Available:

[https://ia801806.us.archive.org/31/items/4172-building-with-earth/4172\\_Building\\_with\\_earth.pdf](https://ia801806.us.archive.org/31/items/4172-building-with-earth/4172_Building_with_earth.pdf)

- [17] Zunkir, English: *Bricks from Jericho (Tell es-Sultan), some of the earliest house bricks known, ca 9000 BC, Pre-Pottery Neolithic A period. Come from a circular house built into a pit.* Ashmolean Museum <https://collections.ashmolean.org/object/464934> <https://collections.ashmolean.org/object/469082>. 2022. Accessed: Mar. 26, 2024. [Online]. Available: [https://commons.wikimedia.org/wiki/File:Bricks\\_Jericho\\_PPNA\\_Ashmolean.jpg](https://commons.wikimedia.org/wiki/File:Bricks_Jericho_PPNA_Ashmolean.jpg)
- [18] E. W. Smith, “Adobe bricks in New México,” New México Bureau of Mines & Mineral Resources, Socorro, NM, 188, 1982.
- [19] H. Scoggins, *The Portalab Manual: Low-Cost Soil-Engineering Tests for Construction Earthen Buildings*. New México Appropriate Technology Program, 1981.
- [20] T. Dominguez, “ABCs of Making Adobe Bricks.” NM State University, Mar. 2011.
- [21] B. Sidibe, “Understanding Adobe,” *Volunteer in technical assistance (VITA)*, p. 30, 1985.
- [22] E. Hubbell, *Earth Brick Construction*. in Home improvement pamphlets. Education Division, U.S. Office of Indian Affairs, 1943. [Online]. Available: <https://books.google.com/books?id=KsnlF-f4ZtAC>
- [23] E. Mazria, *The Passive Solar Energy Book*. Emmaus, Pennsylvania: Rodale Press, 1979. [Online]. Available: <https://books.google.com/books?id=ftBSAAAAMAAJ>
- [24] Chayet, Anne, Corneille Jest, and John Sanday, “Earth used for Building in the Himalayas, the Karakoram, and Central Asia,” presented at the 6th International Conference on Earthen Architecture, 1990, pp. 29–34. [Online]. Available: [https://www.getty.edu/conservation/publications\\_resources/pdf\\_publications/pdf/adobe90\\_1.pdf](https://www.getty.edu/conservation/publications_resources/pdf_publications/pdf/adobe90_1.pdf)
- [25] Y. Cao, M. A. Bowker, M. Delgado-Baquerizo, and B. Xiao, “Biocrusts protect the Great Wall of China from erosion,” *Science Advances*, vol. 9, no. 49, p. eadk5892, Dec. 2023, doi: 10.1126/sciadv.adk5892.
- [26] J. Eyeson, “Rammed Earth: A Timeless Solution for Sustainable Architecture,” Hive Earth. Accessed: Apr. 01, 2024. [Online]. Available: <https://www.hiveearth.com/post/rammed-earth-a-timeless-solution-for-sustainable-architecture>
- [27] G. Botti, “A geopolitics of mud construction: Self-help and the CINVA-Ram machine in Ghana and South Vietnam during the Cold War,” *Frontiers of Architectural Research*, vol. 12, no. 6, pp. 1180–1194, Dec. 2023, doi: 10.1016/j foar.2023.07.002.
- [28] L. Wolfskill, W. Dunlap, and B. Gallaway, *Handbook For Building Homes of Earth*, R-34., vol. Bulletin No. 21. Texas Transportation Institute, 1981. [Online]. Available: <https://files.eric.ed.gov/fulltext/ED242877.pdf>
- [29] D. Zozaya, “Mayan hut construction and translation,” Apr. 03, 2024.
- [30] E. Barnard, “Living in mud houses: exploring the materiality of Formative Mesoamerican domestic structures,” *Research Gate*, vol. 38, Apr. 2016, [Online]. Available: [https://www.researchgate.net/publication/304461517\\_Living\\_in\\_mud\\_houses\\_exploring\\_the\\_materiality\\_of\\_Formative\\_Mesoamerican Domestic\\_structures](https://www.researchgate.net/publication/304461517_Living_in_mud_houses_exploring_the_materiality_of_Formative_Mesoamerican Domestic_structures)
- [31] K. Seligson, T. Gallareta Negrón, R. May Ciau, and G. J. Bey, “Burnt lime production and the Pre-Columbian Maya socio-economy: A case study from the northern Yucatán,” *Journal of Anthropological Archaeology*, vol. 48, pp. 281–294, Dec. 2017, doi: 10.1016/j.jaa.2017.09.003.
- [32] T. Y.-O. A. & J. Dominguez, “La Casa Tradicional Maya.” Accessed: Mar. 29, 2024. [Online]. Available: <https://en-yucatan.com.mx/mundo-maya/casa-tipica-maya/>

- [33] P. G. McHenry, *Adobe: Build it Yourself*. University of Arizona Press, 1985. [Online]. Available: <https://books.google.com/books?id=APP5CBFeLvoC>
- [34] “New México Earthen Buiding Materials Code 2021.” Construction Industries Division of the Regulation and Licensing Department, 2021.
- [35] “2018 INTERNATIONAL BUILDING CODE (IBC) | ICC DIGITAL CODES.” Accessed: May 15, 2024. [Online]. Available: [https://codes.iccsafe.org/content/IBC2018P5/chapter-21-masonry#IBC2018P5\\_Ch21\\_Sec2109](https://codes.iccsafe.org/content/IBC2018P5/chapter-21-masonry#IBC2018P5_Ch21_Sec2109)
- [36] T. Watari, Z. Cao, A. C. Serrenho, and J. Cullen, “Growing role of concrete in sand and climate crises,” *iScience*, vol. 26, no. 5, p. 106782, May 2023, doi: 10.1016/j.isci.2023.106782.
- [37] J. H. Potgieter, “An Overview of Cement production: How ‘green’ and sustainable is the industry?,” *Environmental Management and Sustainable Development*, vol. 1, pp. 14–37, Aug. 2012, doi: 10.5296/emsd.v1i2.1872.
- [38] F. Althoey, W. S. Ansari, M. Sufian, and A. F. Deifalla, “Advancements in low-carbon concrete as a construction material for the sustainable built environment,” *Developments in the Built Environment*, vol. 16, p. 100284, Dec. 2023, doi: 10.1016/j.dibe.2023.100284.
- [39] R. M. Andrew, “Global CO<sub>2</sub> emissions from cement production, 1928–2018,” *Earth System Science Data*, vol. 11, no. 4, pp. 1675–1710, Nov. 2019, doi: 10.5194/essd-11-1675-2019.
- [40] I. Agustí-Juan and G. Habert, “Environmental design guidelines for digital fabrication,” *Journal of Cleaner Production*, vol. 142, pp. 2780–2791, Jan. 2017, doi: 10.1016/j.jclepro.2016.10.190.
- [41] M. Weißberger, W. Jensch, and W. Lang, “The convergence of life cycle assessment and nearly zero-energy buildings: The case of Germany,” *Energy and Buildings*, vol. 76, pp. 551–557, Jun. 2014, doi: 10.1016/j.enbuild.2014.03.028.
- [42] M. Xu, J. David, and S. Kim, “The Fourth Industrial Revolution: Opportunities and Challenges,” *International Journal of Financial Research*, vol. 9, p. 90, Feb. 2018, doi: 10.5430/ijfr.v9n2p90.
- [43] iED Team, “A Brief History of The 4 Industrial Revolutions that Shaped the World,” Institute of Entrepreneurship Development. [Online]. Available: <https://ied.eu/project-updates/the-4-industrial-revolutions/>
- [44] M. Gomaa, W. Jabi, V. Soebarto, and Y. M. Xie, “Digital manufacturing for earth construction: A critical review,” *Journal of Cleaner Production*, vol. 338, p. 130630, Mar. 2022, doi: 10.1016/j.jclepro.2022.130630.
- [45] A. Chiusoli, “The first 3D printed House with earth | Gaia,” 3D Printers | WASP. Accessed: May 25, 2024. [Online]. Available: <https://www.3dwasp.com/en/3d-printed-house-gaia/>
- [46] D. H. Murcia, “3D PRINTED CONCRETE & POLYMER CONCRETE FOR INFRASTRUCTURE APPLICATIONS”.
- [47] S. Bhusal, “3D PRINTING OF EARTHEN MATERIALS: TOWARD THE CARBON-ZERO CONSTRUCTION”.
- [48] S. Bhusal, F. Uviña Contreras, and M. Hojati, “PRELIMINARY STUDY ON 3D PRINTING OF LOCALLY AVAILABLE EARTHEN MATERIALS IN NEW MÉXICO,” Oct. 2022.
- [49] S. Bhusal, R. Sedghi, and M. Hojati, *Evaluating the Printability and Rheological and Mechanical Properties of 3D-Printed Earthen Mixes for Carbon-Neutral Buildings*, vol. 15. 2023. doi: 10.3390/su152115617.

- [50] H. Dickinson, “The Next Industrial Revolution? The Role of Public Administration in Supporting Government to Oversee 3D Printing Technologies,” *Wiley Periodicals, Inc on behalf of The American Society for Public Administration*, vol. 76, no. 6, pp. 922–925, 2018, doi: <https://doi.org/10.1111/puar.12988>.
- [51] H.-J. Steenhuis, X. Fang, and T. Ulusemre, “Global Diffusion of Innovation during the Fourth Industrial Revolution: The Case of Additive Manufacturing or 3D Printing,” *Int. J. Innovation Technol. Management*, vol. 17, no. 01, p. 2050005, Feb. 2020, doi: 10.1142/S0219877020500054.
- [52] S. Nazarian *et al.*, “Additive Manufacturing of Architectural Structures: An Interplay Between Materials, Systems, and Design,” in *Sustainability and Automation in Smart Constructions*, H. Rodrigues, F. Gaspar, P. Fernandes, and A. Mateus, Eds., Cham: Springer International Publishing, 2021, pp. 111–119. doi: 10.1007/978-3-030-35533-3\_15.
- [53] H. Hassan, E. Rodriguez-Ubinas, A. Al Tamimi, E. Trepči, A. Mansouri, and K. Almehairbi, “Towards innovative and sustainable buildings: A comprehensive review of 3D printing in construction,” *Automation in Construction*, vol. 163, p. 105417, Jul. 2024, doi: 10.1016/j.autcon.2024.105417.
- [54] M. Hojati *et al.*, *3D Printing of Concrete: a Continuous Exploration of Mix Design and Printing Process*. 2018.
- [55] Z. Li *et al.*, “Fresh and Hardened Properties of Extrusion-Based 3D-Printed Cementitious Materials: A Review,” *Sustainability*, vol. 12, no. 14, Art. no. 14, Jan. 2020, doi: 10.3390/su12145628.
- [56] A. A. Rashid, S. alim Khan, F. Ali, and J. Muhammad, “3D Printing Technology for Rapid Response to Climate Change: Challenges and Emergency Needs,” Feb. 2024, doi: DOI:10.35534/ism.2024.10004.
- [57] R. Sedghi, K. Rashidi, and M. Hojati, “Large-scale 3D wall printing: From concept to reality,” *Automation in Construction*, vol. 159, p. 105255, Mar. 2024, doi: 10.1016/j.autcon.2023.105255.
- [58] Z. Bryson, W. III, S. Kawashima, and L. Ben-Alon, “Towards 3D Printed Earth- and Bio-Based Insulation Materials: A Case Study on Light Straw Clay,” Jun. 2022. doi: 10.5281/zenodo.6611395.
- [59] J. A. Arrieta-Escobar *et al.*, “3D printing: An emerging opportunity for soil science,” *Geoderma*, vol. 378, p. 114588, Nov. 2020, doi: 10.1016/j.geoderma.2020.114588.
- [60] A. Y. Alqenae, A. M. Memari, and M. Hojati, “TRANSITION FROM TRADITIONAL COB CONSTRUCTION TO 3D PRINTING OF CLAY HOMES,” *Journal of Green Building*, vol. 16, no. 4, pp. 3–28, Jan. 2022, doi: 10.3992/jgb.16.4.3.
- [61] J. Daher, J. Kleib, M. Benzerzour, N.-E. Abriak, and G. Aouad, “The Development of Soil-Based 3D-Printable Mixtures: A Mix-Design Methodology and a Case Study,” *Buildings*, vol. 13, no. 7, Art. no. 7, Jul. 2023, doi: 10.3390/buildings13071618.
- [62] M. Buson, H. Varum, and M. A. Rezende, “First Impressions on Three-Dimensional Printing with Earth-Based Mortar at the Faculty of Engineering of the University of Porto,” *Buildings*, vol. 14, no. 2, Art. no. 2, Feb. 2024, doi: 10.3390/buildings14020312.
- [63] E. A. de Souza, P. H. R. Borges, T. Stengel, B. Nematollahi, and F. P. Bos, “3D printed sustainable low-cost materials for construction of affordable social housing in Brazil: Potential, challenges, and research needs,” *Journal of Building Engineering*, vol. 87, p. 108985, Jun. 2024, doi: 10.1016/j.jobe.2024.108985.

- [64] Y. Maierdan *et al.*, “Rheology and 3D printing of alginate bio-stabilized earth concrete,” *Cement and Concrete Research*, vol. 175, p. 107380, Jan. 2024, doi: 10.1016/j.cemconres.2023.107380.
- [65] I. Chang, J. Im, and G.-C. Cho, “Introduction of Microbial Biopolymers in Soil Treatment for Future Environmentally-Friendly and Sustainable Geotechnical Engineering,” *Sustainability*, vol. 8, no. 3, Art. no. 3, Mar. 2016, doi: 10.3390/su8030251.
- [66] M. A. Kumar, A. A. B. Moghal, K. V. Vydehi, and A. Almajed, “Embodied Energy in the Production of Guar and Xanthan Biopolymers and Their Cross-Linking Effect in Enhancing the Geotechnical Properties of Cohesive Soil,” *Buildings (2075-5309)*, vol. 13, no. 9, p. 2304, Sep. 2023, doi: 10.3390/buildings13092304.
- [67] B. Kelechava, “ASTM D2487 Unified Soil Classification System,” The ANSI Blog. Accessed: May 08, 2024. [Online]. Available: <https://blog.ansi.org/2018/03/unified-soil-classification-astm-d2487-17/>
- [68] *ASTM C136/C136M-14 Standard Test Method For Sieve Analysis of Fine and Coarse Aggregates*. ASTM International.
- [69] “ASTM D4318 - Standard Test Methods for Liquid Limit, Plastic Limit, and Plasticity Index of Soils.” ASTM International, 2010. Accessed: Apr. 13, 2024. [Online]. Available: <https://www.astm.org/d4318-17e01.html>
- [70] *ASTM D-2487 Standard Practice for Classification of Soils for Engineering Purposes (Unified Soil Classification System)*, vol. 04. ASTM international, 2000.
- [71] “ASTM C117-23 Standard Test Method for Materials Finer than 75- $\mu\text{m}$  (No. 200) Sieve in Mineral Aggregates by Washing.” ASTM International, Nov. 2023. [Online]. Available: <https://www.astm.org/c0117-23.html>
- [72] Soil Survey Staff, “USDA Soil Textural Classification Chart.” Natural Resources Conservation Service, 1993.
- [73] R. Pandian and M. Nasir, “Characterization of nanomaterial used in nanobioremediation,” *Science Direct*, 2021, [Online]. Available: <https://www.sciencedirect.com.libproxy.unm.edu/topics/materials-science/x-ray-diffraction-analysis>
- [74] “USGS OFR01-041: Clay Mineral Identification Flow Diagram.” Accessed: May 10, 2024. [Online]. Available: <https://pubs.usgs.gov/of/2001/of01-041/htmldocs/flow/index.htm>
- [75] A. Soldo, M. Miletic, and M. L. Auad, “Biopolymers as a sustainable solution for the enhancement of soil mechanical properties,” *Sci Rep*, vol. 10, no. 1, Art. no. 1, Jan. 2020, doi: 10.1038/s41598-019-57135-x.
- [76] J. Baranwal, B. Barse, A. Fais, G. L. Delogu, and A. Kumar, “Biopolymer: A Sustainable Material for Food and Medical Applications,” *Polymers (Basel)*, vol. 14, no. 5, p. 983, Feb. 2022, doi: 10.3390/polym14050983.
- [77] *ASTM C305-20 Standard Practice for Mechanical Mixing of Hydraulic Cement Pastes and Mortars of Plastic Consistency*. ASTM International, 2020. [Online]. Available: <https://www.astm.org/c0305-20.html>
- [78] “ASTM C109/C109M-02 Standard Test Method for Compressive Strength of Hydraulic Cement Mortars.” ASTM International, 2020. [Online]. Available: [https://www.astm.org/c0109\\_c0109m-02.html](https://www.astm.org/c0109_c0109m-02.html)
- [79] I. Ibrahim, F. Eltarabishi, H. Abdalla, and M. Abdallah, “3D Printing in Sustainable Buildings: Systematic Review and Applications in the United Arab Emirates,” *Buildings*, vol. 12, no. 10, Art. no. 10, Oct. 2022, doi: 10.3390/buildings12101703.

- [80] A. Perrot, D. Rangeard, and E. Courteille, “3D printing of earth-based materials: Processing aspects,” *Construction and Building Materials*, vol. 172, pp. 670–676, May 2018, doi: 10.1016/j.conbuildmat.2018.04.017.
- [81] J. Assunção *et al.*, “Contribution of production processes in environmental impact of low carbon materials made by additive manufacturing,” *Automation in Construction*, vol. 165, p. 105545, Sep. 2024, doi: 10.1016/j.autcon.2024.105545.
- [82] A. Curth, N. Pearl, A. Castro-Salazar, C. Mueller, and L. Sass, “3D printing earth: Local, circular material processing, fabrication methods, and Life Cycle Assessment,” *Construction and Building Materials*, vol. 421, p. 135714, Mar. 2024, doi: 10.1016/j.conbuildmat.2024.135714.
- [83] T. T. Le, S. A. Austin, S. Lim, R. A. Buswell, A. G. F. Gibb, and T. Thorpe, “Mix design and fresh properties for high-performance printing concrete,” *Mater Struct*, vol. 45, no. 8, pp. 1221–1232, Aug. 2012, doi: 10.1617/s11527-012-9828-z.
- [84] O. J. Adebowale and J. N. Agumba, “Sustainable building materials utilization in the construction sector and the implications on labour productivity,” *Journal of Engineering, Design and Technology*, vol. ahead-of-print, no. ahead-of-print, Jan. 2023, doi: 10.1108/JEDT-04-2023-0164.
- [85] C. J. Kibert, “The next generation of sustainable construction,” *Building Research & Information*, vol. 35, no. 6, pp. 595–601, Nov. 2007, doi: 10.1080/09613210701467040.
- [86] “2021 New México Earthen Building Materials Code.” 2021. Accessed: Apr. 08, 2024. [Online]. Available: <https://www.srca.nm.gov/parts/title14/14.007.0004.html>
- [87] T. T. Wilson, P. T. Mativenga, and A. L. Marnewick, “Sustainability of 3D Printing in Infrastructure Development,” *Procedia CIRP*, vol. 120, pp. 195–200, Jan. 2023, doi: 10.1016/j.procir.2023.08.035.
- [88] M. Gomaa, S. Schade, D. W. Bao, and Y. M. Xie, “Automation in rammed earth construction for industry 4.0: Precedent work, current progress and future prospect,” *Journal of Cleaner Production*, vol. 398, p. 136569, Apr. 2023, doi: 10.1016/j.jclepro.2023.136569.
- [89] “Rael San Fratello 3D prints mud structures as prototypes for low-cost construction,” Dezeen. Accessed: Jun. 19, 2024. [Online]. Available: <https://www.dezeen.com/2019/10/03/mud-frontiers-rael-san-fratello-3d-printed-low-cost-construction/>
- [90] V. S. Fratello and R. Rael, “Innovating materials for large scale additive manufacturing: Salt, soil, cement and chardonnay,” *Cement and Concrete Research*, vol. 134, p. 106097, Aug. 2020, doi: 10.1016/j.cemconres.2020.106097.
- [91] M. Gomaa, J. Vaculik, V. Soebarto, M. Griffith, and W. Jabi, “Feasibility of 3DP cob walls under compression loads in low-rise construction,” *Construction and Building Materials*, vol. 301, p. 124079, Sep. 2021, doi: 10.1016/j.conbuildmat.2021.124079.
- [92] “The Transformation Network | the University of New México.” Accessed: May 06, 2024. [Online]. Available: <https://transformimw.unm.edu/>
- [93] “Land-Based Healing & Learning.” Accessed: May 02, 2024. [Online]. Available: [https://www.nacaschool.org/apps/pages/index.jsp?uREC\\_ID=1663962&type=d&pREC\\_ID=2166924](https://www.nacaschool.org/apps/pages/index.jsp?uREC_ID=1663962&type=d&pREC_ID=2166924)
- [94] D. Zozaya, S. Bhusal, F. Uviña Contreras, and M. Hojati, “EVALUATING GRAIN SIZE DISTRIBUTION OF LOCAL SOILS FOR 3D PRINTING IN CONSTRUCTION,” presented at the Earth USA 2024, 2024.

- [95] “ASTM C-33 - Standard Specification for Concrete Aggregates.” ASTM International. [Online]. Available: <https://www.astm.org/c0033-07.html>
- [96] N. C. Brady and R. Weil, *Soil architecture and physical properties in.* 2007.
- [97] “VTSYIQI Digital Fruit Penetrometer Hardness Tester Fruit Firmness Tester Sclerometer with Range 0.2 to 15 kgf/cm<sup>2</sup> Diameter 11.1mm: Amazon.com: Industrial & Scientific.” Accessed: May 31, 2024. [Online]. Available: <https://www.amazon.com/VTSYIQI-Penetrometer-Hardness-Firmness-Sclerometer/dp/B082W86M8B>
- [98] I. Glushankova, A. Ketov, M. Krasnovskikh, L. Rudakova, and I. Vaisman, “Rice Hulls as a Renewable Complex Material Resource,” *Resources*, vol. 7, p. 31, May 2018, doi: 10.3390/resources7020031.
- [99] B. S. Luh, “Rice Hulls,” in *Rice: Volume I. Production/Volume II. Utilization*, B. S. Luh, Ed., Boston, MA: Springer US, 1991, pp. 688–713. doi: 10.1007/978-1-4899-3754-4\_23.
- [100] K. Haddad, S. Lannon, and E. Latif, “Investigation of Cob construction: Review of mix designs, structural characteristics, and hygrothermal behaviour,” *Journal of Building Engineering*, vol. 87, p. 108959, Jun. 2024, doi: 10.1016/j.jobe.2024.108959.
- [101] M. Gomaa, W. Jabi, A. Veliz Reyes, and V. Soebarto, “3D printing system for earth-based construction: Case study of cob,” *Automation in Construction*, vol. 124, p. 103577, Apr. 2021, doi: 10.1016/j.autcon.2021.103577.
- [102] R. Sedghi, M. S. Zafar, and M. Hojati, “Exploring Fresh and Hardened Properties of Sustainable 3D-Printed Lightweight Cementitious Mixtures,” *Sustainability*, vol. 15, no. 19, Art. no. 19, Jan. 2023, doi: 10.3390/su151914425.
- [103] C01 Committee, “ASTM C293 - Standard Test Method for Flexural Strength of Concrete (Using Simple Beam With Center-Point Loading).” ASTM International. Accessed: Jun. 28, 2024. [Online]. Available: <https://www.astm.org/c0293-08.html>
- [104] C. Friedman-Gerlicz, D. Gelosi, F. Bell, and L. Buechley, “WeaveSlicer: Expanding the Range of Printable Geometries in Clay,” in *Proceedings of the CHI Conference on Human Factors in Computing Systems*, Honolulu HI USA: ACM, May 2024, pp. 1–16. doi: 10.1145/3613904.3642622.
- [105] “Rhinocerous 3D.” Rhinocerous 3D, 2023. [Online]. Available: <https://www.rhino3d.com/>